



**AL-TAHADI UNIVERSITY
FACULTY OF SCIENCE
DEPARTMENT OF CHEMISTRY**

**STUDY ON SOME AZOPYRAZOLONE
DERIVATIVES AND THEIR COMPLEXES
WITH SOME TRANSITION METAL IONS**

**For Partial Fulfillment for the Requirement of the Master
Degree of Science (Chemistry)**

**Submitted by
AWATIF ABDEL-SALAM MASOUD**

Supervised By

**Dr. Samir Abou El-Kassem Abdel-Latif
Assist. Prof. of Inorganic Chemistry
Chemistry Department
Faculty of Science
Omar Al-Mukhtar University**

**Dr. Hassan Amroun Ewais
Assist. Prof. of Physical Chemistry
Chemistry Department
Faculty of Science
Al-Tahadi University**

SERET-LIBYA

2008-2007

إن الدراسة ليست غاية في حد ذاتها
ولذا التلميح من خلق الإنسان للتوابع المتجدد



الجمهورية العربية السورية الشعبية الاشتراكية العظمى
جامعة التحدي
سرت

التاريخ: 2008/7/22
الموافق: 2/11/52
الرقم الإداري: 10

Faculty of Science
Department of Chemistry

Title of Thesis

**Study on some Azo Pyrazolone Derivatives and Their Complexes
with some Transition Metal Ions**



Awatif Abdel - Salam Masoud

Approved by:

Dr. Samir Abou El-Kassem Abdel-Latif
(Supervisor)

Dr. Hassan Amroun Ewais
(Co-Supervisor)

Dr. Salem Kalefa Elfared
(External examiner)

Dr. Ziadan Jassim Khalaf
(Internal examiner)

[Signatures]
H. A. Ewais
14. Z. J. Khalaf

Countersigned by:

Dr. Ahmed Farag Mhgoub
(Dean of faculty of science)



بِسْمِ اللَّهِ الرَّحْمَنِ الرَّحِيمِ

قَالَ لَوْلَا تُسَبِّحُونَ لِلَّهِ الَّذِي خَلَقَ لَنَا الْجَنَّةَ إِنَّا كُنَّا فِيهَا كَانُوا فِيهَا سَاهِبِينَ

بِسْمِ اللَّهِ الرَّحْمَنِ الرَّحِيمِ

سورة البقرة الآية (21)

Dedication

To My Father,

My Mother,

My Husband (Walid)

Dr. Khaial

And

To all of my brothers & sisters,

I dedicate this work with high happiness and great pleasure

Acknowledgments

Praise is to Allah, the cherisher and the sustainer of the world.

I wish to record my sincere appreciation and gratitude to supervisor; *Dr. Samir Abou El-Kassem Abdel-Latif*, for supervising this work and his objective criticism, continuous encouragements, support and valuable comments.

Thanks a lot for *Dr. Hassan A. Ewais*, for his kind notes and for his continuous concern and support.

Great thanks to *Mr. Goma'a El-Ghannai* for helping me to transfer the research into Omar Al-Mukhtar University, and for following the related issues during my absence interval.

I wish to express my great thanks to *Mrs. Anad Fhemah* the coordinator of the post graduate affairs of the Faculty of Science, Al-Tahadi University .

I wish to express my thanks to Administration of Al-Tahadi University, Administration of Omar Al-Mukhtar University and *Prof. Dr. Hosny Ibrahim Mohamed*, Professor of Analytical Chemistry, Department of Chemistry, Cairo University, Egypt, for kind help and for

the facilities for perform this study, and to ***Dr. Fahim Abdel-Karim Ben Khaial*** manger of the staff members affairs at Omar Al-Moukhtar University for his kind help.

Deep thanks to all individuals who offered help at any stage of the preparation of this study.

Finally; I wish to record my respectful thanks and gratitude to ***Mr. Adel-Rahman Abdel-Fattah Fatouh***, for his help during the preparation of the compounds and his kind help during the preparation of the Thesis and during my stay in the Chemistry Department, Omar Al-Mukhtar University.

List of Contents

Chapter I : Introduction

I.1. Introduction	1
I.2. Literature survey	3
I.3. Aim of the work	22

Chapter II : Experimental

II.1. Chemicals	24
II.2. Synthesis	24
<i>II.2.1 . Synthesis of 1,3-diphenyl-5-pyrazolone</i>	<i>24</i>
<i>II.2.2. Synthesis of 1,3-diphenyl-4-phenylazo-5-pyrazolone ..</i>	<i>25</i>
<i>II.2.3. Synthesis of 1,3-diphenyl-4-(p-chlorophenylazo)-5-pyrazolone.....</i>	<i>26</i>
<i>II.2.4. Synthesis of 1,3-diphenyl-4-(p-methylphenylazo)-5-pyrazolone.....</i>	<i>26</i>
<i>II.2.5. Synthesis of 1,3-diphenyl-4-(p-methoxyphenylazo)-5-pyrazolone.....</i>	<i>26</i>
<i>II.2.6. Synthesis of 1,3-diphenyl-4-(o-carboxyphenylazo)-5-pyrazolone.....</i>	<i>27</i>
<i>II.2.7. Synthesis of solid complexes</i>	<i>28</i>
<i>II.2.8. Determination of metal-content in the complexes</i>	<i>28</i>

<i>II.2.9. Molar conductivity Measurements</i>	29
II.3. Physical Measurements	30
<i>II.3.1. Magnetic susceptibility measurements</i>	30
<i>II.3.2. Elemental analysis of the ligands and complexes</i>	32
<i>II.3.3. Infrared spectral measurements</i>	32
<i>II.3.4. The nuclear magnetic resonance</i>	32
<i>II.3.5. Mass spectral measurements</i>	32
<i>II.3.6. Thermal analysis</i>	32
II.4. Reactions, Mechanisms and Structures	34
<i>II.4.1. Preparation of 1,3-diphenyl -5- pyrazolone</i>	34
<i>II.4.2. Preparation of azo compounds</i>	35
<i>II.4.3. The structures of the investigated ligands</i>	36
 Chapter III : Results and Discussion.	
III.1. Spectral studies on the free ligands	38
<i>III.1.1. Infrared spectral analysis</i>	38
<i>III.1.2. ¹H NMR spectral studies</i>	45
<i>III.1.3. Mass spectral studies</i>	49

<i>III.1.4. Elemental analysis for the investigated ligands</i>	57
<i>III.1.5. The absorption of ligand V in organic solvents of different polarities</i>	58
III.2. Stoichiometries and structures of the solid complexes	61
<i>III.2.1. Infrared spectra of the solid complexes</i>	62
<i>III.2.2. ¹H NMR spectra of the complexes</i>	76
<i>III.2.3. Elemental analysis for the complexes</i>	83
<i>III.2.4. Thermogravimetric analysis (TG)</i>	88
<i>III.2.5. Differential thermal analysis (DTA)</i>	94
<i>III.2.6. Molar conductivity measurements</i>	101
<i>III.2.7. Magnetic susceptibility measurements</i>	101
<i>III.2.8. Electron spin resonance (ESR)</i>	104
<i>III.2.9. General structure of the complexes</i>	109
Summery	112
References	115

List of Figures

Figure No.	Title of figure	page
Figure (1)	Schematic diagram illustrates the method of preparation of 1,3-diphenyl-5-pyrazolone starting with ethyl benzoylacetate and phenyl hydrazine.	34
Figure (2)	Schematic diagram illustrates the reactions occurred during preparation of azopyrazolone derivatives.	35
Figure (3)	Structures and names of the investigated ligands.	36
Figure (4)	Infrared spectra of the investigated ligands.	43
Figure (5)	¹ H NMR spectra of the investigated ligands (I-V).	46
Figure (6)	The mass fragmentation pattern of ligand I.	49
Figure (7)	Schematic diagram illustrates the general mechanism of fragmentation of ligand I.	50
Figure (8)	The mass fragmentation pattern of ligand II.	51
Figure (9)	Schematic diagram illustrates the general mechanism of fragmentation of ligand II.	52
Figure (10)	The mass fragmentation pattern of ligand III.	53
Figure (11)	Schematic diagram illustrates the general mechanism of fragmentation of ligand III.	53
Figure (12)	The mass fragmentation pattern of ligand IV.	54

Figure (12)	The mass fragmentation pattern of ligand IV.	54
Figure (13)	Schematic diagram illustrates the general mechanism of fragmentation of ligand IV.	54
Figure (14)	The mass fragmentation pattern of ligand V.	55
Figure (15)	Schematic diagram illustrates the general mechanism of fragmentation of ligand V.	55
Figure (16)	Relation between the maximum absorption of C.T. band of ligand V and $(D-1)/(D+1)$ of solvents of different polarities (ethanol, methanol, isopropanol, dioxane, cyclohexane and chloroform).	59
Figure (17)	Relation between the maximum absorption of C.T. band of ligand V and $f(D)$ of solvents of different polarities (ethanol, methanol, isopropanol, dioxane, cyclohexane and chloroform).	60
Figure (18)	Relation between the maximum absorption of C.T. band of the investigated ligand V and $\phi(D)$ of solvents of different polarities (ethanol, methanol, isopropanol, dioxane, cyclohexane and chloroform).	60
Figure (19)	Infrared spectra of the complexes of ligand I with the metal ions Mn^{2+} and Co^{2+} .	63
Figure (20)	Infrared spectra of the complexes of ligand I with the metal ions Ni^{2+} , Cu^{2+} and Zn^{2+} .	64
Figure (21)	Infrared spectra of the complexes of ligand II with the metal ions Mn^{2+} , Co^{2+} and Ni^{2+} .	65
Figure (22)	Infrared spectra of the complexes of ligand II with	66

	the metal ions Ni^{2+} , Cu^{2+} and Zn^{2+} .	
Figure (23)	Infrared spectra of the complexes of ligand III with the metal ions Mn^{2+} , Co^{2+} and Ni^{2+} .	67
Figure (24)	Infrared spectra of the complexes of ligand III with the metal ions Ni^{2+} , Cu^{2+} and Zn^{2+} .	68
Figure (25)	Infrared spectra of the complexes of ligand IV with the metal ions Mn^{2+} , Co^{2+} and Ni^{2+} .	69
Figure (26)	Infrared spectra of the complexes of ligand IV with the metal ions Ni^{2+} , Cu^{2+} and Zn^{2+} .	70
Figure (27)	Infrared spectra of the complexes of ligand V with the metal ions Mn^{2+} , Co^{2+} and Ni^{2+} .	71
Figure (28)	Infrared spectra of the complexes of ligand V with the metal ions Ni^{2+} , Cu^{2+} and Zn^{2+} .	72
Figure (29)	^1H NMR spectra of the complexes of Zn with ligands I, II and III.	78
Figure (30)	^1H NMR spectra of the complexes of Zn with ligands IV and V.	79
Figure (31)	TG of the complex [Mn-I (2:2)]	95
Figure (32)	TG of the complex [Mn-I (2:3)].	95
Figure (33)	TG of the complex [Ni-II (2:2)].	96
Figure (34)	TG of the complex [Ni-II (2:3)].	96
Figure (35)	TG of the complex [Co-III (2:2)].	97
Figure (36)	TG of the complex [Co-III (2:3)].	97
Figure (37)	TG of the complex [Cu-IV (2:2)].	98

Figure (38)	TG of the complex [Cu-IV (2:3)].	98
Figure (39)	TG of the complex [Zn-V (1:1)].	99
Figure (40)	TG of the complex [Zn-V (1:2)].	99
Figure (41)	ESR spectrum of the complex [Cu-I (2:2)].	105
Figure (42)	ESR spectrum of the complex [Cu-I (2:3)].	105
Figure (43)	ESR spectrum of the complex [Cu-IV (2:2)].	106
Figure (44)	ESR spectrum of the complex [Cu-IV (2:3)].	106
Figure (45)	ESR spectrum of the complex [Cu-V (1:1)].	107
Figure (46)	ESR spectrum of the complex [Cu-V (1:2)].	107
Figure (47)	Structures of 1:1 and 1:2 complexes of ligand V.	110
Figure (48)	structures of 2:2 and 2:3 complexes of ligands (I-IV).	111

List of Tables

Table No.	Title of table	Page
Table (1)	The most significant bands in IR spectra of the investigated ligands (I-V).	44
Table (2)	¹ H NMR spectral data of the azopyrazolones.	47
Table (3)	Elemental analysis data of the investigated ligands (I-V).	57
Table (4)	Some solvent parameters.	59
Table (5)	The most significant bands in IR spectra of the complexes of ligand I with the metal ions (Mn ²⁺ , Co ²⁺ , Ni ²⁺ , Cu ²⁺ and Zn ²⁺).	73
Table (6)	The most significant bands in IR spectra of the complexes of ligand II with the metal ions (Mn ²⁺ , Co ²⁺ , Ni ²⁺ , Cu ²⁺ and Zn ²⁺).	73
Table (7)	The most significant bands in IR spectra of the complexes of ligand III with the metals (Mn ²⁺ , Co ²⁺ , Ni ²⁺ , Cu ²⁺ and Zn ²⁺).	74
Table (8)	The most significant bands in IR spectra of the complexes of ligand IV with the metal ions (Mn ²⁺ , Co ²⁺ , Ni ²⁺ , Cu ²⁺ and Zn ²⁺).	74
Table (9)	The most significant bands in IR spectra of the complexes of ligand V with the metal ions (Mn ²⁺ , Co ²⁺ , Ni ²⁺ , Cu ²⁺ and Zn ²⁺).	75

Table (10)	¹ H NMR spectral data of Zn complexes with the investigated ligands (I-III).	80
Table (11)	¹ H NMR spectral data of Zn complexes with the investigated ligands (IV and V).	81
Table (12)	Elemental analysis, (Λ_m) and μ_{eff} for the complexes of the divalent metal ions (Mn^{2+} , Co^{2+} , Ni^{2+} , Cu^{2+} and Zn^{2+}) with ligand I.	83
Table (13)	Elemental analysis, (Λ_m) and μ_{eff} for the complexes of the divalent metal ions (Mn^{2+} , Co^{2+} , Ni^{2+} , Cu^{2+} and Zn^{2+}) with ligand II.	84
Table (14)	Elemental analysis, (Λ_m) and μ_{eff} for the complexes of the divalent metal ions (Mn^{2+} , Co^{2+} , Ni^{2+} , Cu^{2+} and Zn^{2+}) with ligand III.	85
Table (15)	Elemental analysis, (Λ_m) and μ_{eff} for the complexes of the divalent metal ions (Mn^{2+} , Co^{2+} , Ni^{2+} , Cu^{2+} and Zn^{2+}) with ligand IV.	86
Table (16)	Elemental analysis, (Λ_m) and μ_{eff} for the complexes of the divalent metal ions (Mn^{2+} , Co^{2+} , Ni^{2+} , Cu^{2+} and Zn^{2+}) with ligand V.	85
Table (17)	Molecular weight, temperatures of decomposition, loss percent and the corresponding groups in thermogravimetry (TG).	100
Table (18)	ESR spectral data of Cu^{2+} complexes with ligands I, IV and V.	108

CHAPTER I
INTRODUCTION

1.1. INTRODUCTION

The importance of the pyrazolone azo dyes in the industry as well as their analytical applications and excellent ability to act as ligand attracted the attention of coordination chemists to study their reactions with transition metal ions.

Azo compounds containing a heterocyclic moiety drew the attention of many workers. The importance of pyrazolone azo-dyes in industry as well as their analytical applications and excellent ability to act as potential ligands attracted the attention of coordination chemists to study their reactions with transition metal ions.

Pyrazolone and pyrazole derivatives such as 5-pyrazolones are formed by the reaction between hydrazines and β -ketonic esters e.g. 3-methyl-1-phenyl-5-pyrazolone was prepared from phenyl hydrazine and ethyl acetoacetate, this on methylation gives antipyrine which is used in medicine as an antipyretic.

Pyrazolone-5-ones have attracted much attention as ligands for a large number of metal ions. The metal chelates produced are well known for their analytical and biological uses. The azo derivatives of 5-pyrazolones, as well as their metal complexes have wide application in the dye industry and as analytical reagents for micro determination of metals. Various methods were reported for the synthesis of 4-arylaazo-5-pyrazolone. The electronic and infrared (IR) spectra of a large number of arylazo-5-pyrazolones were investigated for structure elucidation, nuclear magnetic resonance was used as a tool to determine the tautomeric forms of arylazo-3-, -4-, and -5-pyrazolones and several related azo heterocycles in chloroform. Mass spectral fragmentation patterns of arylazo pyrazolones were found to be largely dependent on structure.

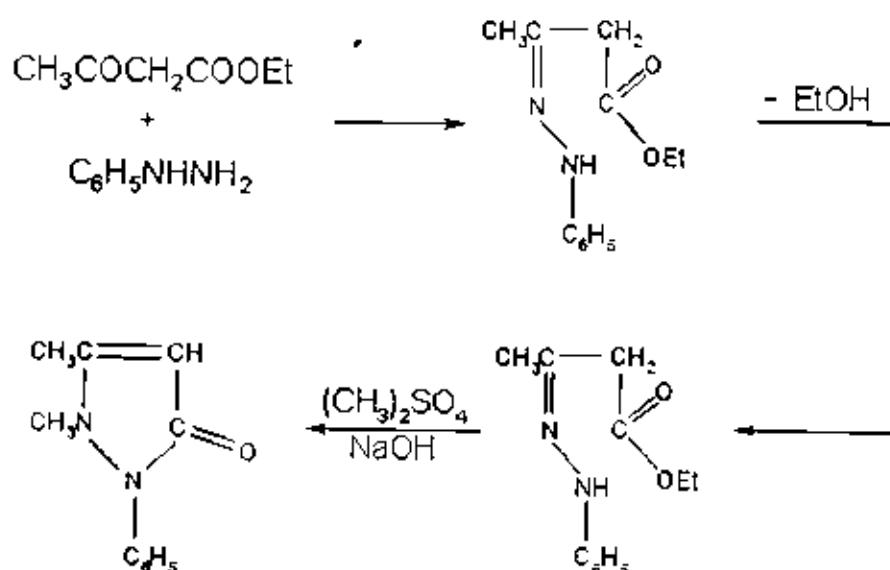
The metal complexes of the arylazo pyrazolones were prepared and their structures were determined by electronic absorption spectra, IR, ^1H NMR spectra, electron spin resonance (ESR) and thermogravimetric (TG) analysis.

In this research some azopyrazolone derivatives were prepared and used as ligands in this investigation, and the complexes of the transition metal ions (Mn^{2+} , Co^{2+} , Ni^{2+} , Cu^{2+} and Zn^{2+}) with the ligands (I-V) were prepared.

In order to make sure about the structures of the prepared ligands, some spectral analysis (IR, ^1H NMR, elemental analysis, mass spectra and UV-Visible absorption in different solvents) were done. For the prepared complexes the analysis [IR, ^1H NMR, Elemental analysis, Thermogravimetric analysis (TG), Differential thermal analysis (DTA), Molar conductivity, Magnetic susceptibility and Electron spin resonance (ESR)] were studied.

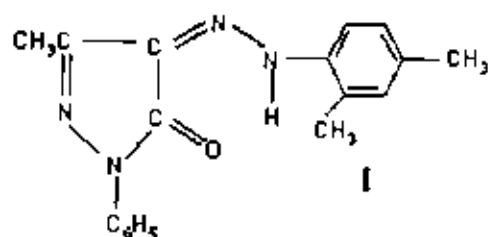
I.2. literature survey

Azole is the suffix used for five-membered ring containing two or more hetero-atoms, at least one of which is nitrogen for example pyrazoles and pyrazole derivatives such as 5-pyrazolones which were formed by reaction between hydrazines and β -Ketonic esters, e.g 3-methyl-1-phenylpyrazolone from phenylhydrazine and ethyleacetoacetate. This, on methylation gives antipyrine (phenazone, 2,3-dimethyl-1-phenylpyrazol-5-one), which is used in medicine as a febrifuge^[1,2].



The coordination chemistry of pyrazolin-5-ones has attracted much attention by virtue of their applicability as potential ligands for a large number of metal ions^[3-13]. The metal chelates thus produced are well known for their analytical and biological uses. The 4-position of pyrazolin-5-one system is highly reactive and undergoes coupling reactions with diazonium salts to give 4-arylazo derivatives^[14-16]. These azo-derivatives of 5-pyrazolones as well as their metal complexes have wide applications in the dye industry as well as analytical reagents for micro determination of metals^[17]

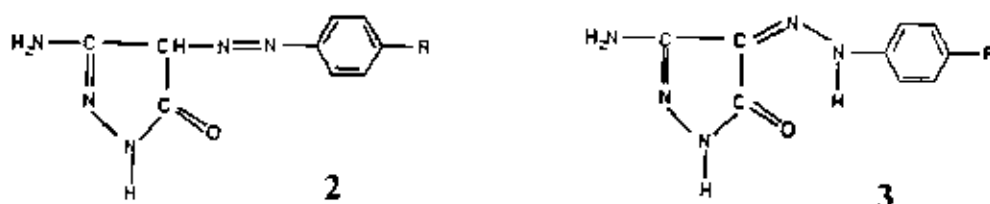
Different methods were reported for the syntheses of 4-arylaazo-5-pyrazolones^[18-25]. The electronic; IR and ¹H NMR spectra of some arylazopyrazolones were obtained^[26] in pure organic solvents and buffer solutions and absorption bands in the UV and visible spectra were assigned. The IR and ¹H NMR spectra confirmed that the investigated compounds exist mainly as hydrazo-keto tautomers. The pK_a values were obtained using spectrophotometric and potentiometric methods, X-ray diffraction and spectral studies of 1-phenyl-3-methyl-4-(2,4-dimethylphenylazo)-5-pyrazolone indicated that it exists as tautomer I in its crystals^[27]. The pyrazole ring and its substituents are nearly coplanar, and an intramolecular NH-O bond forms a 6-membered ring.



The infrared spectra of thirteen substituted 4-benzenehydrazo-5-pyrazolones were investigated^[28]. The N-H vibration of the arylhydrazo pyrazolones was undetectable as the NH absorption was broad and weak due to hydrogen bonding. A strong absorption band at 1525-1550 cm⁻¹ was assigned to NH—N vibration coupled with the C=C vibration. It was found that the ν_{N-NH} frequencies correlate with σ -Hammett function of the substituents of the phenylhydrazo moiety. The C=O, C=N were located at 1635-1650 and 1570-1585cm⁻¹, respectively.

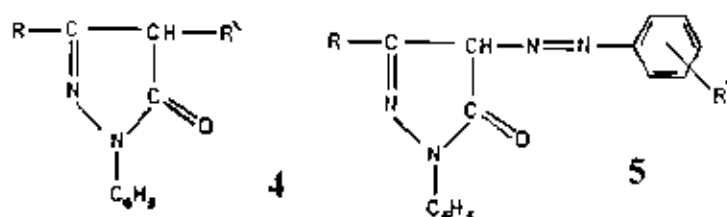
The electronic spectra of some 3-amino-4-arylaazo-2-pyrazolin-5-ones 2 were investigated in pure organic solvents of varying polarities^[29]. In terms of the molecular structures of azo compounds and the solvents characteristics, the different absorption bands observed in the UV-visible

spectra of the studied compounds were assigned to locally or to predominantly intra-and inter-molecular charge transfer electronic transitions. It was confirmed that these compounds exist mainly as a chelated hydrazo-keto structure 3. Furthermore, it was concluded that, under the influence of high electron accepting substituents (NO_2) and in high polar solvents (DMF), the azopyrazolone compound was liable to exist in hydrazone-azo tautomeric equilibrium.



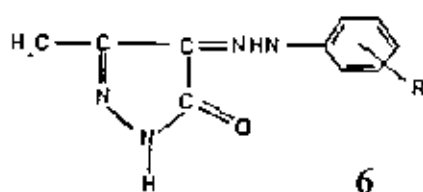
Nuclear magnetic resonance was used to determine the tautomeric forms of arylazo -3-, -4- and -5-pyrazolones and several related azo heterocycles in chloroform^[30]. The assignment of the hydrazone structure to the 5-pyrazolones was supported by infrared data. Several conclusions emerged from the NMR spectra: (a) in the heterocyclic system studied the hydrazone NH resonance comes from 3-5 ppm lower than the azohydroxy OH resonance and (b) the hydrazone NH resonance of structurally similar azo heterocycles falls within a 2-ppm range.

Mass spectral fragmentation of the phenylazopyrazolones 4 and 5



(for 4, $R=Me$, $R^1=H$, $p-CH_3$, $p-OH$, $o-OH$) was found^[31] to occur primarily via rupture of the phenyl N-bond and less readily via rupture of the pyrazole-oxocyclic N bond. Compound 5 where $R=AcNH$; $R^1=H$, $p-CH_3$, $p-NO_2$, $p-CF_3$, fragmented primarily via loss of ketene and secondarily via rupture of the ring-azo group bonds, while for $R=H$, NH_2 , CH_3 ; $R^1=H$, NH_2 , fragmentation occurred in the ring or by loss of CH_3 .

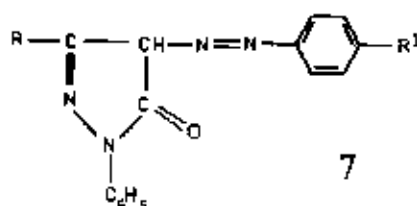
The mass spectra of the compounds having the general formula 6



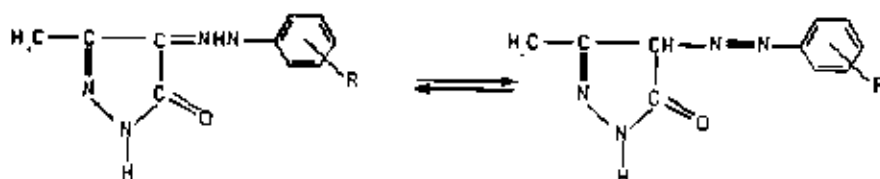
($R = H$, $o-CH_3$, $p-CH_3$, $-OCH_3$, $-NO_2$, $-COOH$, $-Cl$)

were determined and the fragmentation rationalized from high resolution and metastable mass measurements^[32]. Intense molecular ions and ions formed by consecutive decomposition of the N-containing part of the molecule were observed. In addition, ions with aniline-type structures and their decomposition products were also observed.

The mass spectra of 7 ($R=CH_3$, $AcNH$; $R^1=H$, $(CH_3)_2N$, OH , OCH_3 , Cl , NO_2 , etc) were given^[33]. Compound 7 cleaved on either side of the azo group. Rearrangement processes leading to arylamine radical ions were also described.



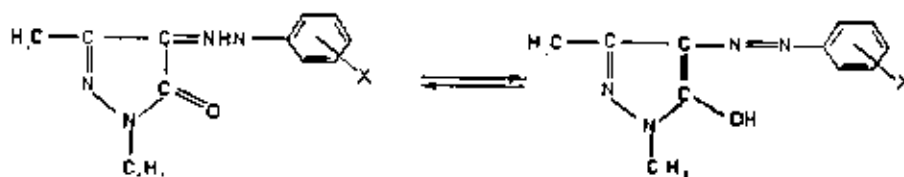
The electronic absorption and IR spectra of some 4-arylhydrazone-3-methyl-5-pyrazolones were assigned and correlated to its molecular structure^[34]. The electronic spectra in ethanol comprise four absorption bands. The first three bands located near 253-260 and 335 nm, being characterized by high molar absorptivities, were assigned to $\pi\text{-}\pi^*$ type transition. The first two bands were assigned to (${}^1L_a \rightarrow 1A$) and (${}^1L_b \leftarrow 1A$) transition, respectively. The third band was assigned to a $\pi\text{-}\pi^*$ transition involving the whole molecule influenced by C.T. interaction of the band on the longer wavelength side (400-438 nm) is broad, solvent sensitive and corresponds to a charge transfer (C.T.) transition. The C.T. originates from the phenyl ring to the carbonyl group by resonance and from the hetero ring by induction. The authors noticed that this band was highly influenced by the nature and position of the substituent on the phenyl ring, donor group cause a red shift while acceptor groups cause a counter-shift relative to the non-substituted compound. These compounds display azo-hydrazo tautomerism.



The keto form is enhanced by the electron acceptor groups while electron donor groups favor the enol form due to increased polarization of the carbonyl group. The latter assumption was further proved from IR spectra. A broad band was observed within the $3338\text{-}3500\text{ cm}^{-1}$ region which corresponds to the stretching vibration of the OH- group. The appearance, broadness and low frequency of that band supported the occurrence of keto-enol tautomerism within these compounds. The

spectra show bands in the range 1670-1640 cm^{-1} assigned to $\nu_{\text{C=O}}$, $\nu_{\text{C=N}}$ and $\nu_{\text{N=N}}$.

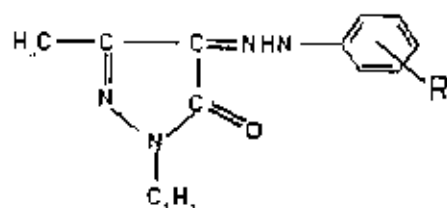
El -Inany et al^[35] investigated the UV-visible electronic spectra of some 1-phenyl-3-methyl-4-arylhydrazone-5-pyrazolones. In ethanol the spectra comprise 4 bands in the region 200-500 nm. The band observed in the range 240-260 nm (A) was ascribed to the $\pi-\pi^*$ transition in the 1-phenyl ring. The second band, observed at 275-280 nm (B), was ascribed to the $\pi-\pi^*$ transition of pyrazolone ring involving carbonyl and azomethine groups in addition to electron migration along the heterocyclic system. The bands observed in the ranges 343-352 nm (c) and 380-410 nm (D) were assigned to $n-\pi^*$ transition due to their observed weak absorbances. In cyclohexane, the absorbance and shape of band (B) changed compared to ethanol, thus denoting changes in the structure of the pyrazolone moiety by changing the polarity of the solvent. This was explained on the basis of a shift in the tautomeric equilibrium:



The authors prepared the complexes of Cu, Co, Ni, Mn, Zn and Pd with the mentioned ligands and determined their structures by electronic absorption spectral studies. A bathochromic shift of band (D) of the ligand was observed with the complex formation which was ascribed to the polarity of M-O bond (M=divalent ion and O=pyrazolone oxygen) and by the perturbation of the π electron system by the $d\pi-\pi\pi$ interaction between the hydrazone group and the metal ion. Band (B) was related to this change in polarity and a slight shift was noticed indicating a covalent

character of the M-O bond. Bands (B) and (C) are parallel to the shifts observed for band (D) but appear as shoulders. Band (A) was observed in its position but displaying some increase in its molar absorptivity.

The absorption and fluorescence spectra of some arylazopyrazolone dyes were investigated^[30]. The emission was assigned to their hydrazone form.



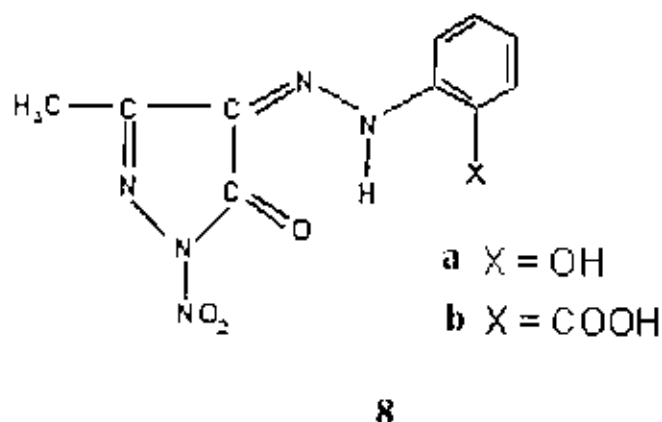
(R = H₂N, Me₂N, OH, H, OMe, Cl, CN, NO₂, COOH)

A very good linear correlation was obtained between the σ -Hammett constant and the differences between the absorption maxima of the hydrazone and the anion forms. Quantum chemical calculation indicated a charge migration upon excitation. The electron donor substituents caused bathochromic and hypsochromic shifts in the absorption and fluorescence maxima, respectively, while the acceptor substituents shifted both maxima bathochromically.

The proton ligand stability constant of 3-methyl-4-(2¹-hydroxy phenylazo)-2-pyrazoline-5-one and the stability constants of its complexes with Ni, Co, Zn and Mn were determined potentiometrically^[37], at 50% aqueous ethanol and at ionic strength 0.8 (KNO₃). The stability constants are Zn < Ni > Co > Mn.

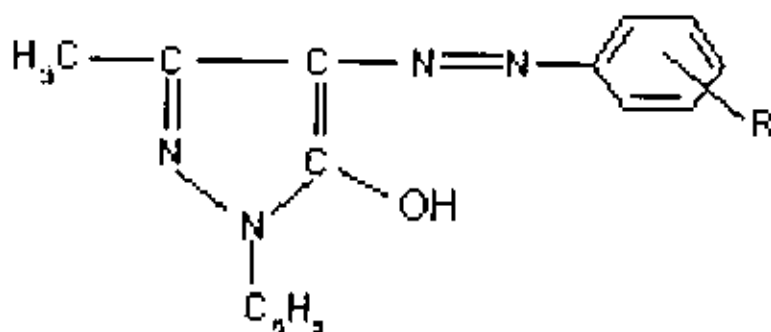
The use of 3-methyl-4-(p-ethoxyphenylazo)-2-pyrazoline-5-one as a ligand with some divalent metal ions^[38], resulted in an order of stability having the sequence Zn < Cu > Ni > Co > Mn.

The stability of chelates of 1-(p-nitrophenyl)-3-methyl-4-arylhyazone-5-pyrazolones with divalent iron, cobalt, nickel, copper and zinc ions in 70% ethanol were determined potentiometrically^[39]. The observed order of stability ($\log\beta_1$) follows the sequence $\text{Fe} > \text{Co} > \text{Ni} > \text{Zn}$ for pyrazolone **8-a** and $\text{Fe} > \text{Co} > \text{Ni} < \text{Cu} > \text{Zn}$ for pyrazolone **8-b**.



A theoretical explanation of this order was given considering the ionic radii of the metal ions regardless of their respective coordination numbers or geometry. The abnormal high stability of the Fe^{2+} pyrazolone complex is attributed to the known orbital stabilization which occurs in Fe^{2+} ion during complex formation.

The relative stabilities of the metal complexes (Cu, Ni, Co and Zn) of simple arylazo pyrazolones having the formula:



(R = p-Br, p-I, m-CH₃, m-Br, m-Cl and NO₂)

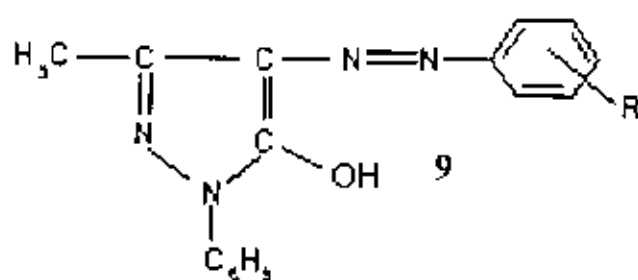
were measured potentiometrically in 75% by volume dioxane^[40]. For a given substituent X, the order of decreasing stability was found to be Cu > Ni > Co > Zn. The $\log\beta_2$ values were greater than $\log\beta_1$ values.

Stability constants of the copper complexes with investigated dyes was found, to depend on the substituent and increase in the order, NO < (Cl, Br) < I < OCH₃ < CH₃ < H, with the exception of the methoxy derivative the order followed the electron attracting power of the substituent group. In case of the methoxy group the inductive effect prevailed over the resonance effect.

Dissociation constants of 4-(3-pyridylazo)-3-amino-2-pyrazolin-5-one (PAP) and 4-(2-pyridyl-3-hydroxyazo)-1-phenyl-3-methyl-2-pyrazolin-5-one (PMP) and stability constants of their chelates with Th(IV), Zr(IV), Ce(III), Y(III), La(III) and UO₂(II) were determined potentiometrically in 20% (v/v) EtOH-H₂O at an ionic strength of 0.1 mol dm⁻³ (NaClO₄)^[41]. The order of the stabilities is: Zr(IV) > Th(IV) > UO₂(VI) > Y(III) > Ce(III) > La(III).

The reaction of La(III), Ce(III), Th(IV) and UO₂(II) with some heterocyclic azopyrazolones was studied by the spectrophotometric molar ratio and continuous variation methods and IR spectra^[42]. The solid complexes were prepared and studied by elemental analysis and conductance measurements. The azopyrazolones studied act as neutral or monobasic bidentate ligands and bonded to the metal ions through the O atom of the carbonyl group and the α -N of the arylazo group. All solid chelates prepared behave as non electrolytes in DMF solutions.

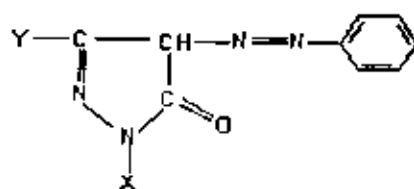
Kinetic studies of the thermal decomposition of metal chelates of substituted hydrazopyrazolone **9** were done^[43] by TG, DTG and DTA.



(R = OH, COOH, OCH₃)

Complexation was strongest with the hydroxy derivative and the relative order of thermal stability was $\text{UO}_2^{2+} > \text{Fe}^{3+} > \text{Cu}^{2+} > \text{Hg}^{2+}$. The results were used to explain the stabilization of such chelates by dative π -bonding between M^{n+} and the ligand.

Metal chelates of pyridine azopyrazolin-5-one derivatives with



(X = H (L₁, L₂), C₆H₅ (L₃), Y = NH₂ (L₁), CH₃ (L₂, L₃))

Zr(IV), La(III), Y(III) and UO₂(VI) have been prepared and characterized by electronic, IR, ¹H NMR spectra and thermogravimetric analyses^[17]. Electronic absorption spectra of the free ligands exhibit mainly two bands in the ranges 234-250 and 350-380 nm. The former one may be attributed to π - π^* electronic transition in the conjugated system of the ligands, while the latter one corresponding to n - π^* transition in the azo (L₁, L₃) or hydrazo (L₂) bond involving C.T. However, the broad band at 405 nm for (L₂) was assigned to Keto-hydrazone intramolecular hydrogen bonding confirming thus its hydrazone structure. The above two bands were red shifted in the presence of the metal ions studied. The visible band shifts decreased in the order Zr(IV) > UO₂(VI) > Y(III) >

La(III). The stoichiometry of the different metal complexes was determined by applying conventional spectrophotometric methods. The results revealed the possibility of both 1:1 and 1:2 metal ion to ligand adducts. These results were confirmed by conductimetric titrations of each metal ion using the ligands as titrants. Definite evidence for the structure and coordination sites of the ligands was obtained from infrared data. The keto structure of the free ligands and their complexes was confirmed by ^1H NMR data which revealed that there is no signal for the OH proton. Broad band at ~ 5.8 and 4.4 ppm for L_1 and L_2 was ascribed to the NH proton of the pyrazolone ring. The pyridyl (L_1 , L_2) and phenyl (L_3) protons resonate downfield in the δ 7.1-9.1 ppm range. The δ NH_2 (L_1) and δ CH_3 (L_2 , L_3) signals appearing at 4.03 and 2.5 ppm were up field shifted, indicating that the shielding was increased as a result of complex formation. The signal around 3.4 ppm in the NMR of all complexes was assigned to the associated water molecules. This assumption was supported by thermogravimetric analysis which indicated loss of water molecules in the range 120-230 $^\circ\text{C}$ confirming that water molecules are coordinated. It was concluded that L_1 and L_3 act as neutral bidentate ligands while ligand L_2 can act as monobasic bidentate.

Structural studies of transition metal complexes of Co(II), Ni(II), Cu(II), and Pd(II) with 3-amino-4-(substituted-aryazo)-5-(1H) pyrazolone compounds were discussed^[44]. The stoichiometries of the complexes reported are 1:1, 2:3 Co(II), 1:1 Ni(II), 1:1, 2:1 Cu(II) and 1:2 Pd(II). The investigators suggested rhombic symmetry with 4- or -5-coordinate Co(II), square planar and tetrahedral configuration for Ni(II), tetrahedral Cu(II) and square planar for Pd(II) Complexes. The complexes contained no anions.

$M(HL)_2$ ($M=Cu, Cr, Mn$; $HL=1$ -phenyl-3-methyl-4-(2-hydroxy-4-nitrophenylazo)-5-pyrazolone, ML ($M=Cu, Ni$), CuL ($H_2L=1$ -phenyl-3-methyl-4-(2-hydroxy-5-nitrophenylazo)-5-pyrazolone, and $Ni(HL)_2$ were prepared^[45]. The complexes were characterized by IR and UV spectra stability constants were determined for Ni, Co, and Cu complexes with H_2L and H_2L , both ligands coordinate through the azomethine N and deprotonated phenol O atom in the 1:2 complexes. The 1:1 complexes are polymeric and the ligands are tetradentate, bridging and coordinating through the two azo N atoms and the O atoms.

The syntheses and temperature-dependent magnetic properties of Cu(II) and Ni(II) complexes of 2-hydroxybenzeneazo derivatives of 1-phenyl-3-methyl-5-pyrazolone and 2,4-pentanedione were reported^[46]. The Cu(II) complexes exhibit antiferromagnetic behavior. It was suggested that these compounds form sheet like polymers with the Cu ions acting as the bonding agent between the azo groups and the antiferromagnetism was due primarily to direct Cu-Cu interaction between these sheets. The Ni(II) complexes, however, are diamagnetic, which is consistent with the suggested polymer structure.

Mixed ligand complexes were obtained by the replacement of coordinated water in some Cu(II) and Ni(II) complexes derived from 3-methyl-4-(p-methylphenylazo)-pyrazol-5-ones^[47]. The Cu(II) and Ni(II) complexes were assigned planar and distorted octahedral structures, respectively, on the basis of IR, magnetic moment and electronic spectral data. The authors made an attempt to correlate the replacement of the ligands in the parent complexes with the crystal field strength of the incoming N donors, as well as the geometry of the products so obtained. Complexes of cobalt(II) with 3-methyl-4-(p-methyl (a), p-methoxy (b), o-methoxy (c), phenylazo) pyrazol-5-one and 1-phenyl-3-methyl-4-(o-

carboxyphenylazo) pyrazol-5-one (d) have been prepared and studied through elemental analysis, magnetic measurements and spectral studies^[48]. In the electronic spectra of the complexes (a), (b), and (c) three principal bands were observed in the ranges 5320-7200, 9790-10380 and 16490-26000 cm^{-1} . In case of complex (d), the bands were observed at 7000, 18600 and 21000 cm^{-1} and assigned to ${}^4T_{1g}(F) \rightarrow {}^4T_{2g}(F)$, ${}^4T_{1g}(F) \rightarrow {}^4A_{2g}(F)$ and ${}^4T_{1g}(F) \rightarrow {}^4T_{1g}(P)$ respectively assuming octahedral symmetry.

Some planar and octahedral complexes of Cu(II) and Ni(II) with different 3-methyl-4-arylazopyrazol-5-ones have been prepared^[49] and their structures established using analytical, conductance, magnetic, infrared and electronic spectral data. The complexes have been prepared by refluxing Cu(II) or Ni(II) sulphate suspended in toluene with the corresponding ligand in toluene for 6-10 hrs. Toluene was then distilled off and the reaction mixture was allowed to cool. When the complex separated out it was recrystallised from toluene. The complexes contain only one molecule of the ligand which functions as bidentate donor, coordinating through the carbonyl and azo groups while the rest of the positions in the coordination geometry of the metal are occupied by water molecules. The magnetic and electronic data of the complexes were discussed in the light of the structures assigned.

Chelates of Mn(II), Fe(III), Zr(IV), Pd(II) and Ag(I) with 4-[(4-R- NO_2)] were prepared and characterized by IR and UV-visible spectra and conductance measurements^[50]. In the chelates L-exists in the hydrazone-keto form L-are coordinated through the carbonyl O and arylazo N atom.

Mathur et al^[51] prepared complexes of some platinum metal ions with 4-arylazopyrazol-5-one. Square planar Pd(II) and octahedral Pt(IV) and Rh(III) were proposed from IR, magnetic and electronic spectral data. All

complexes are diamagnetic. Ligand field parameters were reported and discussed. The higher stability of Pt(IV) complexes and its position in spectrochemical series was discussed. The IR spectra of the complexes indicated the bonding of carbonyl, N:N and COOH group to the metal.

La(III), Ce(III), Th(IV), and UO₂(VI) chelates with 3-phenyl-4-arylo-5-pyrazolones have been synthesized and were characterized by several analytical tools such as elemental analyses, IR, NMR, TG, and molar conductance techniques. The data obtained show that all of the prepared complexes contain water and/or alcohol in their coordination sphere and the ligands form 1:1 and 1:2 complexes which are in good agreement with the proposed formula. The NMR data of the prepared ligands show the existence of the ketonic structure rather than the enolic form. The TG data revealed no crystal water outside the coordination sphere. The azopyrazolone ligands act as neutral bidentate ligands bonded to the metal ions through the oxygen atom of the carbonyl group and the α nitrogen of the arylazo group. All solid chelates prepared behave as non-electrolytes in DMF solution^[52].

3-phenyl-4-arylo-5-pyrazolones have been synthesized and characterized by elemental, infrared (IR), ultraviolet and visible spectra (UV-Vis), proton nuclear magnetic resonance (¹H NMR) and mass spectra. It has been proved that these compounds exhibit a keto-enol tautomerism in solution. The donor character of the substituent increase the enol form. The ionization constants of the investigated ligands have been determined potentiometrically and they found to decrease in the order OCH₃(IV) > CH₃(III) > H(I) > Cl(II). The Co(II) complexes of the investigated 3-phenyl-4-arylo-5-pyrazolones have been prepared and characterized by elemental and thermal analyses as well as by IR, UV-Vis, electronic transition, potentiometric, conductimetric and magnetic

measurements. The data suggest octahedral geometry for Co(II) (1:1) complexes and tetrahedral for Co(II) (2:3) complexes^[53].

Mn(II), Co(II), Ni(II) and Cu(II) chelates with 3-phenyl-4-(*p*-methoxyphenylazo)-5-pyrazolone have been synthesized^[54] and were characterized by elemental, thermal analyses, IR, UV-VIS, ¹H NMR, conductometric and magnetic measurements. The first stage in the thermal decomposition process of these complexes shows the presence of water of hydration, the second denotes the removal of the coordinated water molecules. The final decomposition products were found to be the respective metal oxides. The data of the investigated complexes suggest octahedral geometry with respect to Co(II) 1:1, tetrahedral for Ni(II) 1:1 and 2:3 square planar for Cu(II) 1:1 and 2:3 complexes with no coordinated water molecules (2:3) Co(II) and Mn(II) complexes are tetrahedral.

Six kinds of 4-acylpyrazolone were synthesized from 1-phenyl-3-methyl-5-pyrazolone (PMP) and 1,3-diphenyl-5-pyrazolone (DPP), and then six new compounds of semicarbazone containing pyrazolone: 1-phenyl-3-methyl-4-acetyl-5-pyrazolone semicarbazone (PMAP-SC) (1a), 1-phenyl-3-methyl-4-chloroacetyl-5-pyrazolone semicarbazone (PMCP-SC) (1b), 1-phenyl-3-methyl-4-propionyl-5-pyrazolone semicarbazone (PMPP-SC) (1c), 1,3-diphenyl-4-acetyl-5-pyrazolone semicarbazone (DPAP-SC) (2a), 1,3-diphenyl-4-chloroacetyl-5-pyrazolone semicarbazone (DPCP-SC) (2b), and 1,3-diphenyl-4-propionyl-5-pyrazolone semicarbazone (DPPP-SC) (2c), were synthesized by direct condensation of the pyrazolone with semicarbazide (SC). The products were characterized by elemental analysis, IR, ¹H NMR and ¹³C NMR spectra. The crystal structure of compound 1c was determined by X-ray diffraction analysis. 1c belongs to the monoclinic system with space

group C2/c and cell dimensions: $a = 2.3590$ nm, $b = 0.9456$ nm, $c = 1.3319$ nm, $\beta = 101.65(2)^\circ$, $V = 2.9098(8)$ nm³, $Z=8$, $D[c] = 1.312$ g/cm³, $F(000) = 1216$, $R[1] = 0.0348$, $wR[2] = 0.0913$ ^[55].

According to the importance of the pyrazolone derivatives and their Antifungal and Antimicrobial activities as well as their azo compounds in dying. The thesis presented the synthesis of some new pyrazolone derivatives and elucidating their structures by using different tools viz, Elemental analysis, IR and UV-visible. The binary solid complexes of the prepared ligands with UO₂(II), La(III) and Ce(III) are separated and investigated and discussed using the previous tools and TGA. Furthermore, the ionization constants of the synthesized ligands as well as of their chelates with Cu(II), Co(II), Ni(II), UO₂(II), La(III) and Ce(III) are evaluated by using potentiometric and spectrophotometric techniques. The results obtained on the basis of the nature of the metal ions under investigation and the nature of the prepared ligands^[56].

4-(4-ethoxy-phenylhydrazono)-1-phenyl-3-methyl-1H-pyrazolin-5(4H)-one (H-EMPhP) as ligand and its Cu(II), Co(II) and Ni(II) complexes were synthesized and characterized by their thermal and spectral properties. The azocoupling product (H-EMPhP), able of azo-hydrazone tautomerism act as a bidentate ligand involving in coordination the azogroup nitrogen of its common anion, and the oxygen atom that is bound to the pyrazole ring of the mentioned anion^[57].

New compounds, structurally related to the potent protein kinase C inhibitor staurosporine, with a bisindolylpyrazolone framework and substituted on the pyrazolone nitrogens with N,N-dialkylaminoalkyl side chain, were synthesized and evaluated for growth-inhibitory properties in several human cell lines. Many showed inhibition of TNF- α production in response to the tumor promotor TPA on HL-60 cells. The apoptotic

activity on HeLa cells has been examined for several of these compounds^[58].

The known NMR spectroscopy data on different types of synthetic azo and polyazo dyes, including metal complexes, are correlated. The fundamentally new opportunities in the NMR spectroscopy of ^1H , ^{13}C , and ^{15}N nuclei in solving problems of structural chemistry in this field of industrial chemistry are demonstrated^[59].

The new azopyrazolone dye has been synthesized and its crystal structure has been investigated. The structure has been solved by direct methods and refined by full-matrix least-squares techniques to $R=0.050$ for 2622 unique reflections. The tautomeric form of the molecules has been determined as a hydrazo form. Delocalization of the $\text{C5}=\text{O3}$ and $\text{C4}=\text{N3}$ π -electrons and delocalization of the lone-pair electrons of N1 , N3 , and N4 atoms has been observed. The intramolecular $\text{N-H}\dots\text{O}$ hydrogen bond forms the six-membered ring $\text{C}_2\text{N}_2\text{H}\dots\text{O}$ condensed with the pyrazolone ring. The molecules are connected by intramolecular $\text{C-H}\dots\text{O}$ hydrogen bonds^[60].

The dissociation constants of 4-(4-chlorophenylazo)-3-methyl-1-[2-hydroxy-3-morpholinopropane-1-yl]-2-pyrazolin-5-one (CAMP) has been determined potentiometrically in 0.1 M KCl and 40% (v/v) ethanol-water mixture^[28]. The stepwise stability constants of the formed complexes of Mn^{2+} , Co^{2+} , Ni^{2+} , Cu^{2+} , Zn^{2+} , La^{3+} , Ce^{3+} and UO_2^{2+} with CAMP have been determined. The stability of the formed complexes were found as follows: $\text{UO}_2^{2+} > \text{Ce}^{3+} > \text{La}^{3+} > \text{Mn}^{2+} < \text{Co}^{2+} < \text{Ni}^{2+} < \text{Zn}^{2+}$. The thermodynamic parameters (ΔG , ΔH and ΔS) for CAMP and its complexes were evaluated and discussed. The dissociation process is non-spontaneous, endothermic and entropically unfavourable. The formation of the complexes has been found to be spontaneous, exothermic or endothermic

(depending on the metal) and entropically favourable. The stoichiometries of these complexes were determined spectrophotometrically and conductometrically and indicated the formation of 1:1 and 1:2 (metal:ligand) complexes^[61].

The dissociation constants of 3-methyl-1-phenyl-{p-[N-(pyrimidin-2-yl)sulfamoyl]phenylazo}-2-pyrazolin-5-one and metal-ligand stability constants of its complexes with some transition metal ions have been determined potentiometrically in 0.1 M KCl and ethanol-water mixture (30 vol. %)^[62]. The order of stability constants of the formed complexes increases in the sequence Mn^{2+} , Co^{2+} , Ni^{2+} , Cu^{2+} , La^{3+} , Hf^{3+} , UO_2^{2+} , Zr^{4+} . The effect of temperature was studied and the corresponding thermodynamic parameters (ΔG , ΔH , and ΔS) were derived and discussed. The dissociation process is nonspontaneous, endothermic, and entropically unfavourable. The formation of the metal complexes was found to be spontaneous, exothermic, and entropically favourable.

Proton-ligand dissociation constants of 4-sulfamethazineazo-3-methyl-1-phenyl-2-pyrazolin-5-one (SMP) and metal-ligand stability constants of its complexes with bivalent metal ions (Mn^{2+} , Co^{2+} , Ni^{2+} , Cu^{2+} , and Zn^{2+}) have been determined potentiometrically in 0.1 M KCl, and a 40% (v/v) ethanol-water mixture^[63]. The order of the stability constants of the complexes was found to be $Mn^{2+} < Co < Ni < Cu < Zn$. The dissociation constants, pK^{11} , of SMP and the stability constants, $\log K$, of its complexes at different temperatures and the corresponding thermodynamic parameters were determined.

The ligand 2-(2'-thienyl)-8-hydroxyquinoline has been synthesized and the solution stability of some of its metal chelates were determined^[64]. It was found that $\log K_1 < \log K_2$ is attributed to strong steric interaction between the 2-substituent and coordinated water on

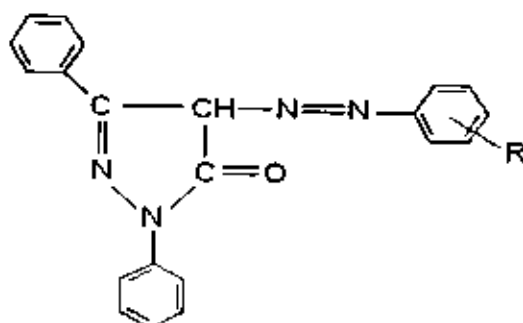
addition of the first ligand. This interaction results in distortion toward tetrahedral geometry. Previously unexplained data for other 2-substituted 8-hydroxyquinolines have been interpreted in terms of this effect.

Potentiometric studies on the free ligands and the metal complexes of indium (III) with thiomalic, malic and aspartic acid have yield step wise protonation constants of the ligands and the formation constant of the complexes^[65]. Thermodynamic constants have been obtained by extrapolation the values at various ionic concentrations. The values of overall changes in ΔG , ΔH , and ΔS accompanying the reaction have been evaluated at 35°C, the trend in the stability constant values of indium (III) complexes has been found to be thiomalic > malic > aspartic.

Infrared (IR), nuclear magnetic resonance (NMR), thermogravimetric analysis (TG), derivative thermogravimetric analysis (DTG), differential thermal analysis (DTA) and molar conductivity studies have been carried out on the chelates of (Mn(II), Co(II), Ni(II), Cu(II) and Zn(II) with 3-methyl and 3-phenyl-4-nitroso-5-pyrazolones^[66]. The solid chelates were synthesized, separated, analyzed and their structures were elucidated.

I.3. Aim of Work

The present investigation is concerned with the use of azo pyrazolone dyes having the general formula



(where R = H, p-Cl, p-CH₃, p-OCH₃ or o-COOH)

as chelating agents for divalent Mn, Co, Ni, Cu and Zn. The ligands will thus be synthesized and subjected to elemental analysis and spectral studies (IR, ¹H NMR, Mass spectra and UV-visible) for the purpose of structure elucidation.

The reactions of the above ligands with the metal cations will be prepared in suitable media (ethanol). The solid chelates of the azopyrazolone dyes with divalent Mn, Co, Ni, Cu and Zn will be prepared and subjected to several analytical studies [Elemental analyses, ¹H NMR, IR, TG, DTA, Molar conductivity, Magnetic susceptibility and Electron spin resonance (ESR)] to elucidate their structures. In the light of the previous studies, the metal ligand bond characters will be discussed.

CHAPTER II

EXPERIMENTAL

II. Experimental

II.1. Chemicals

All chemicals used were of the highest purity available. These included manganese (II) chloride ($\text{MnCl}_2 \cdot 4\text{H}_2\text{O}$), cobalt (II) chloride ($\text{CoCl}_2 \cdot 6\text{H}_2\text{O}$), nickel (II) chloride ($\text{NiCl}_2 \cdot 6\text{H}_2\text{O}$), copper (II) chloride ($\text{CuCl}_2 \cdot 2\text{H}_2\text{O}$), zinc chloride (ZnCl_2), aniline, p-chloroaniline, p-toluidine (p-methylaniline), p-ansidine (p-methoxyaniline), o-carboxyaniline (o-aminocarboxylic acid), sodium hydroxide, ammonium hydroxide (30% NH_3), ammonium chloride, disodium salt of ethylenediamine tetraacetic acid dihydrate, sodium chloride, silver nitrate (AgNO_3), sulphuric acid (H_2SO_4), hydrogen peroxide (H_2O_2) and hydrochloric acid (37% HCl). The solvents used were ethanol, methanol, dioxane, isopropanol, cyclohexane, chloroform, Dimethylsulphoxide (DMSO) and dimethyl formamide (DMF) derived from Merck and BDH. These solvents were purified by distillation^[67]. The water used doubly distilled.

II.2. Synthesis.

II.2.1. Synthesis of 1,3-diphenyl-5-pyrazolone^[68].

A mixture of ethyl benzoylacetate (9.6g; 0.05mol) and phenyl hydrazine (5.4g; 0.05mol) was heated at 100°C in water bath for one hr. the resulting oil was cooled and stirred with ether (50 ml) until solidification occurred. The crude product was then filtered off. The final product was crystallized from 50% aqueous ethanol and collected as white powder.

The mechanism and the occurred reactions are illustrated in figure (1) (p 32).

II.2.2. Synthesis of 1,3-diphenyl-4-phenylazo-5-pyrazolone^[67].

A well-stirred solution of aniline 0.01 mole in 40 ml ethanol and 20 ml of 2M HCl was cooled in an ice salt bath and diazotized with aqueous sodium nitrite solution (20 ml, 0.01mol). The cooled (0-5° C) diazonium solution was added slowly to a well-stirred solution of (0.01 mole) 1,3-diphenyl-5-pyrazolone in (100 ml) ethanol containing sodium hydroxide (10 g). The reaction mixture was stirred for one hour at room temperature, then acidified with diluted HCl (100 ml, 2.5M) to neutralize the reaction mixture and precipitate the azopyrazolone derivative. The product was recrystallized from ethanol to give the azopyrazolone derivative *1,3-diphenyl-4-phenylazo-5-pyrazolone*, Figure (3).

II.2.3. Synthesis of 1,3-diphenyl-4-(p-chlorophenylazo)-5-pyrazolone^[67].

A well-stirred solution of p-chloroaniline (0.01mole in 40 ml ethanol) and 20 ml of 2M HCl was cooled in an ice salt bath and diazotized with aqueous sodium nitrite solution (20 ml, 0.01mol). The cooled (0-5° C) diazonium solution was added slowly to a well-stirred solution of (0.01 mole) 1,3-diphenyl-5-pyrazolone in (100 ml) ethanol containing sodium hydroxide (10 g). The reaction mixture was stirred for one hour at room temperature, then acidified with diluted HCl (100 ml, 2.5M) to neutralize the reaction mixture and precipitate the azopyrazolone derivative. The products was recrystallized from ethanol to give the azopyrazolone derivative *1,3-diphenyl-4-(p-chlorophenylazo)-5-pyrazolone*, Figure(3).

II.2.4. Synthesis of 1,3-diphenyl-4-(p-methylphenylazo)-5-pyrazolone^[67].

A well-stirred solution of p-toluidine (p-methylaniline) (0.01mole in 40 ml ethanol) and 20 ml of 2M HCl was cooled in an ice salt bath and diazotized with aqueous sodium nitrite solution (20 ml, 0.01mol). The cooled (0-5° C) diazonium solution was added slowly to a well-stirred solution of (0.01 mole) 1,3-diphenyl-5-pyrazolone in (100 ml) ethanol containing sodium hydroxide (10 g). The reaction mixture was stirred for one hour at room temperature, then acidified with diluted HCl (100 ml, 2.5M) to neutralize the reaction mixture and precipitate the azopyrazolone derivative. The product was recrystallized from ethanol to give the azopyrazolone derivative *1,3-diphenyl-4-(p-methylphenylazo)-5-pyrazolone*, Figure (3).

II.2.5. Synthesis of 1,3-diphenyl-4-(p-methoxyphenylazo)-5-pyrazolone^[67].

A well-stirred solution of p-ansidine (p-methoxyaniline) (0.01mole in 40 ml ethanol) and 20 ml of 2M HCl was cooled in an ice salt bath and diazotized with aqueous sodium nitrite solution (20 ml, 0.01mol). The cooled (0-5° C) diazonium solution was added slowly to a well-stirred solution of (0.01 mole) 1,3-diphenyl-5-pyrazolone in (100 ml) ethanol containing sodium hydroxide (10 g). The reaction mixture was stirred for one hour at room temperature, then acidified with diluted HCl (100 ml, 2.5M) to neutralize the reaction mixture and precipitate the azopyrazolone derivative. The product was recrystallized from ethanol to give the azopyrazolone derivative *1,3-diphenyl-4-(p-methoxyphenylazo)-5-pyrazolone*, Figure(3).

II.2.6. Synthesis of 1,3-diphenyl-4-(*o*-carboxyphenylazo)-5-pyrazolone¹⁶⁷.

A well-stirred solution of 2-carboxyaniline acid (*o*-aminoenzoic acid) (0.01 mole in 40 ml ethanol) and 20 ml of 2M HCl was cooled in an ice salt bath and diazotized with aqueous sodium nitrite solution (20 ml, 0.01 mol). The cooled (0-5° C) diazonium solution was added slowly to a well-stirred solution of (0.01 mole) 1,3-diphenyl-5-pyrazolone in (100 ml) ethanol containing sodium hydroxide (10 g). The reaction mixture was stirred for one hour at room temperature, then acidified with diluted HCl (100 ml, 2.5M) to neutralize the reaction mixture and precipitate the azopyrazolone derivative. The product was recrystallized from ethanol to give the azopyrazolone derivative 1,3-diphenyl-4-(*o*-carboxyphenylazo)-5-pyrazolone, Figure (3).

Azopyrazolone derivatives were used as ligands in this investigation, these derivatives are :

1,3-diphenyl-4-phenylazo-5-pyrazolone (**ligand I**)

1,3-diphenyl-4-(*p*-chlorophenylazo)-5-pyrazolone (**ligand II**)

1,3-diphenyl-4-(*p*-methylphenylazo)-5-pyrazolone (**ligand III**)

1,3-diphenyl-4-(*p*-methoxyphenylazo)-5-pyrazolone (**ligand IV**)

1,3-diphenyl-4-(*o*-carboxyphenylazo)-5-pyrazolone (**ligand V**)

Figure (2) illustrates a general reaction which explain the occurring reactions upon ligand preparation process. From this figure, the produced azopyrazolone derivatives are: ligand I when R = H, ligand II when R = Cl (*para*), ligand III when R = CH₃ (*para*), ligand IV when R = OCH₃ (*para*), ligand V when R = COOH (*ortho*).

Figure (3) illustrates the structures and names of the investigated ligands.

II.2.7. Synthesis of solid complexes.

The solid chelates were synthesized by mixing a hot alcoholic saturated solution of (0.001 mole of metal ion dissolved in hot ethanol) with the required amount of ligand under investigation sufficient to form 1:1 or 1:2 (M:L) compounds. The pH of the solution was then maintained at a value of 6.5-7.5 by addition of ammonia solution^[52]. The reaction mixture was heated on a steam bath with occasional stirring for 4 hrs, and evaporated till dryness. The produced chelate was then dissolved in ethanol to remove unreacted species. It was then filtered off by suction and rewashed with ethanol till a colorless filtrate was obtained, suction, filtered and then finally kept in a vacuum desiccator.

II.2.8. Determination of metal-content in the complexes.

The metal content of the prepared solid complexes was determined^[69]. In this case, a weight of 25-35 mg of the solid complex was placed into a 50 ml digestion flask to which 3 ml of concentrated sulfuric acid followed by about 2 ml hydrogen peroxide were added. The solution was heated gently to fumes, and then boiled, excess hydrogen peroxide was added when necessary. The solution was heated to dryness. The residue obtained was then dissolved in the least amount of concentrated nitric acid and diluted with distilled water to a volume of 250 ml. For transition metal ions the pH is adjusted to pH 10 using ammoniacal buffer and Eriochrome black T. (E. B. T.) as an indicator for Mn^{2+} and Zn^{2+} which give a red color, then titration of the red color was performed with standard 0.01 M EDTA (ethylenediaminetetraacetic acid) to the pure blue end point.

For Co^{2+} , Ni^{2+} and Cu^{2+} speck of Murexide indicator was added to give yellow color with Co^{2+} and Ni^{2+} at pH 12 and to give orange color with Cu^{2+} using ammonia solution (1:1) until the formation of dark blue $\text{Cu}(\text{NH}_3)_4^{2+}$. Titration of the yellow or orange color was performed with standard 0.01 M EDTA solution to the pure purple end point. All the obtained results are summarized together with those of the elemental analysis of the complexes in the next chapter.

11.2.9. Effect of solvents of different polarities on ligand V

The absorption values in various solvents are influenced by solvation and/or dielectric constants of the solvents.

The maximum absorption of ligands V at the visible region was found in six different solvents with different polarities (ethanol, methanol, dioxane, isopropanol, cyclohexane and chloroform).

The dielectric constant (D) is the factor which has a substantial influence on the transition energy, or more precisely $f(D)$ or $\phi(D)$ ^[88], where:

$$f(D) = 2(D-1)/2D+1 \quad \text{and} \quad \phi(D) = (D-1)/(D+2)$$

The plots of $(D-1)/(D+1)$, $f(D)$ and $\phi(D)$ against the wavenumber ν_{max} (in cm^{-1}) of the charge transfer (C.T.) band were obtained for each ligand. In order to know whether the dielectric constant (D) is the only factor that influence on the transition energy or there are other factors, like hydrogen bond.

The maximum absorption of the investigated ligand V in organic solvents of different polarities are obtained by measuring the absorption

of ligand V at λ_{max} in the following solvents (ethanol, methanol, isopropanol, dioxane, cyclohexane and chloroform). Ligand V was taken as a sample, and it was the only ligand that studied using the absorption in organic solvents of different polarities.

II.2.10. Molar conductivity Measurements.

The molar conductance of the solid complexes in DMF was measured using a conductivity meter type (Philips, PW 9526 digital conductivity meter).

Conductivity measurements in non aqueous solutions have been used in structural studies of the complexes under investigation. The molar conductivities of 1 M solutions in DMF of the given complexes are measured using Philips conductivity meter of 0.82 cell constant. The product of the cell constant and the measured conductance of a solution give the specific conductivity K. The molar conductance (Λ_m) $\text{ohm}^{-1} \text{cm}^2 \text{mol}^{-1}$ was calculated by using the relation:

$$\Lambda_m = K/C$$

where C is the molar concentration of the metal ion solutions.

II.3. Physical measurements

II.3.1. Magnetic susceptibility measurements^[70].

Magnetic susceptibility measurements were determined using SHERWOOD scientific magnetic susceptibility balance.

The magnetic moment is determined by weighing a sample in and out, the mass susceptibility χ is calculated using the equation:

$$\chi_g = \frac{C_{\text{Bal}} L(R - R_0)}{10^9 m}$$

where:

R_0 = Reading of empty tube.

L = Sample length (cm)

m = Sample mass (g)

R = Reading for tube plus sample.

C_{Bal} = Balance calibration constant, equal to 2.086.

For paramagnetic metal ion, it is customary to quote, not χ_g , but the effective magnetic moment, μ_{eff} , of the ion in Bohr magnetons (BM).

μ_{eff} and χ_g are related by the expression:

$$\mu_{\text{eff}} = 2.828 \sqrt{\chi_g \times \text{mol. wt.} \times T} \quad T = 25 + 273 = 298$$

μ_{eff} will be independent of temperature for a substance obeying the Curie Law.

For compounds containing unpaired electrons, both the spin angular momentum and the orbital angular momentum of the electrons can contribute to the observed paramagnetism. However, for complexes of transition metal ions, the orbital contribution is largely quenched by the field due to the surrounding ligands. In this case, we have the simple spin only formula:

$$\mu_{\text{eff}} = \sqrt{n(n+2)} \quad \text{BM}$$

were n is the number of unpaired spins electrons.

11.3.2. Elemental analysis of the ligands and complexes.

Elemental analysis was performed in the micro-analytical center of Cairo University, Giza, Egypt.

11.3.3. Infrared spectral measurements.

The IR spectra were recorded on SHIMADZU FT-IR 8201 PC spectrophotometer applying the KBr disc technique.

11.3.4. The nuclear magnetic resonance.

The NMR spectra were measured by using a VARIAN Gemini 200 MHz spectrophotometer.

11.3.5. Mass spectral measurements.

Mass spectra were done on GC-Mass 2b 1000 Ex mass spectrophotometer.

11.3.6. Thermal analysis.

Thermal analysis (TG and DTA) were done using SHIMADZU, Type TG-50 and DTA-50 thermal analyzer.

The TG curves were obtained by the weight loss percent for the investigated solid complexes from room temperature up to 800°C with a heating rate of 10°C per minute, Figures (31-40)

11.3.7. Electron spin resonance (e.s.r.)

The electron spin resonance (e.s.r.) of some of the Cu(II) complexes were recorded by using EMX ESR spectrometer (Brucker) 1998 Y at Micro-Analytical center – Cairo University, Giza, Egypt.

II.4. Reactions, mechanisms and structures.

II.4.1. Preparation of 1,3-diphenyl-5-pyrazolone

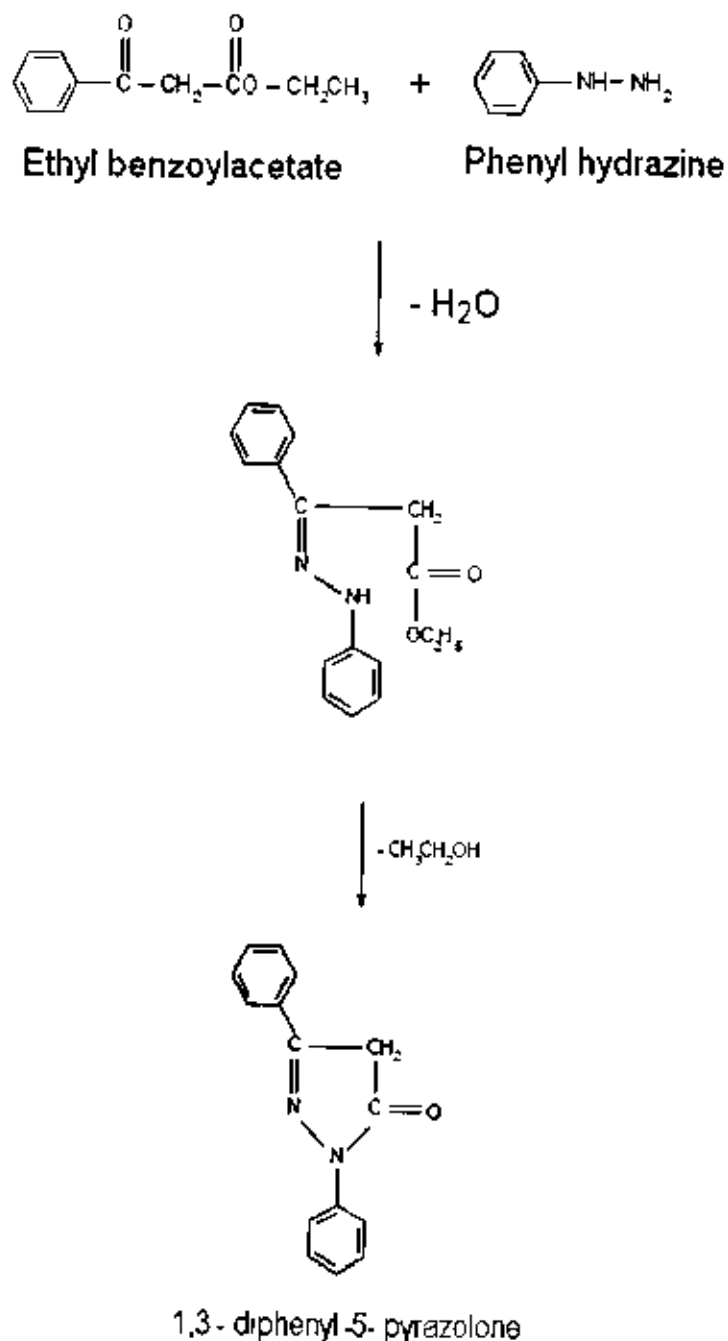


Figure (1): Schematic diagram illustrates the method of preparation of 1,3-diphenyl-5-pyrazolone starting with ethyl benzoylacetate and phenyl hydrazine.

11.4.2. Preparation of azo compounds

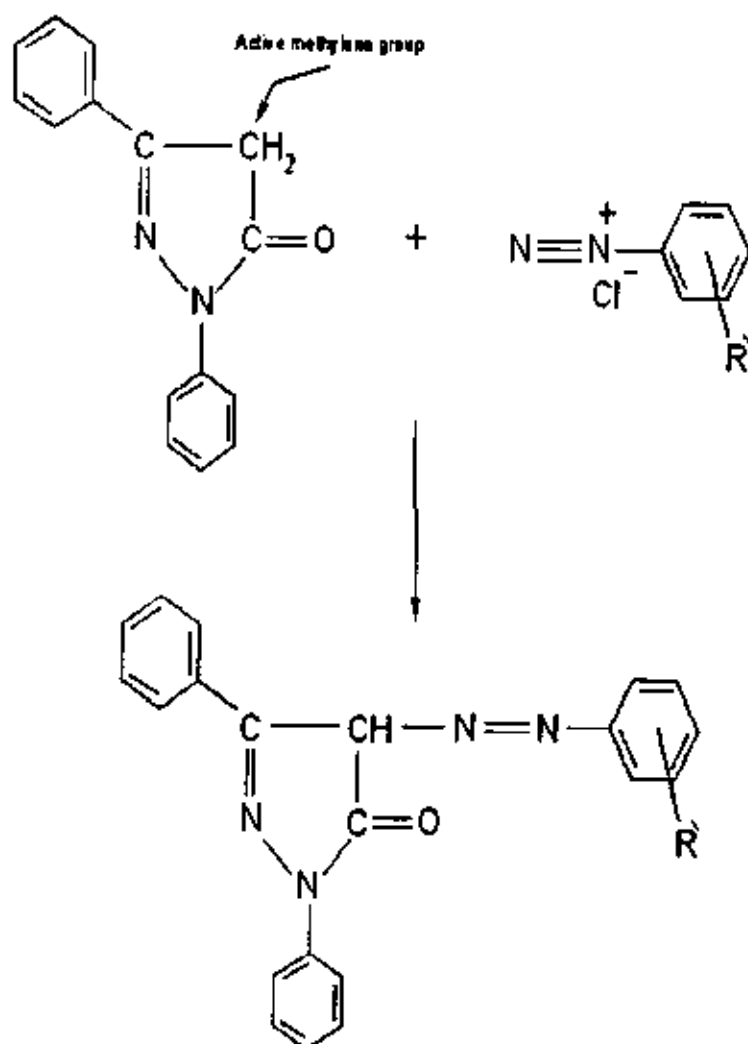
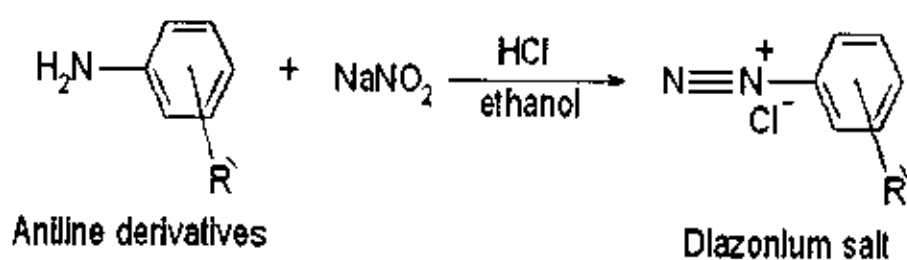


Figure (2): Schematic diagram illustrates the reactions occurred during preparation of azopyrazolone derivatives. $\text{R}' = \text{H}$, $p\text{-Cl}$, $p\text{-CH}_3$, $p\text{-OCH}_3$ or $o\text{-COOH}$.

11.4.3. The structures of the investigated ligands

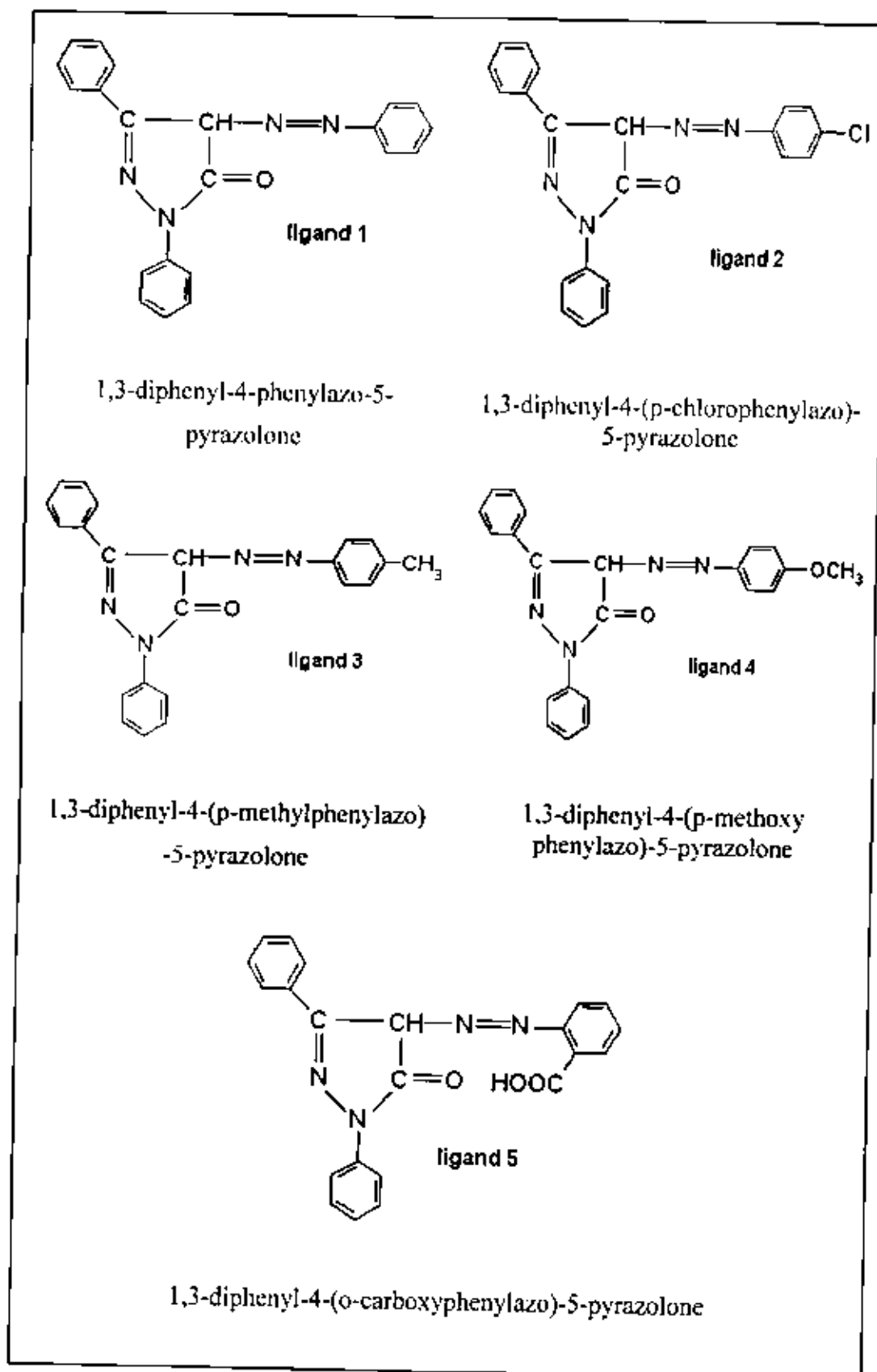


Figure (3) : Structures and names of the investigated ligands.

CHAPTER III
RESULTS
and
DISCUSSION

III. RESULTS and DISCUSSION

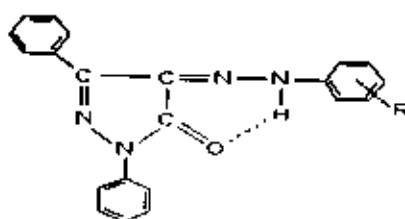
III.1. Spectral studies on the free ligands

The investigated ligands (I-V) were not previously reported in the literature. The syntheses and elemental analyses have been reported in the experimental section. The structures of these ligands was established by the use of elemental analyses, ^1H NMR, mass and IR spectral analysis. In so doing we were guided by published works^[17, 32, 34, 30] on the closely related pyrazolone type compounds.

III.1.1. Infrared spectral analysis.

The infrared absorption spectra of the investigated ligands (I-V) are shown in figure (4). The most significant IR bands that affect the structures are listed in table (1).

Inspection of the IR spectra and the bands frequencies data shows the presence of a broad band at $3406\text{-}3440\text{ cm}^{-1}$ which corresponds to the stretching vibration of the OH group result from the azo-hydrazo tautomerism (CH-N=N to C=N-NH) followed by hydrogen bonding with C=O group of the pyrazolone ring. The appearance as well as the broadness and the low frequency of the band denotes the presence of intramolecular hydrogen bonding^[71].



where R = H (I), p-Cl (II), p-CH₃ (III), p-OCH₃ (IV) or o-COOH (V).

The ν_{NH} band appears as a medium broad one within the range $3031\text{-}3298\text{ cm}^{-1}$ for all compounds studied.

Interpretation of IR spectra of the free ligands

(a) OH bands.

The infrared absorption band arising from the OH valence vibration was first noted as a band near 3440 cm^{-1} appeared to be associated with the hydroxyl group^[72].

However, the absorption range for the O-H stretching vibration of an unbonded hydroxyl group was quoted within the $3700\text{-}3500\text{ cm}^{-1}$ range^[73]. The hydrogen bonds give rise to broad absorption bands in the range $3450\text{-}3200\text{ cm}^{-1}$. The broad shape is usually attributed to the fact that the molecules containing the OH group associate into various polymeric forms in which the molecules are involved in hydrogen bonding to different extents. Accordingly, the broad band observed is a composite one consisting of a number of sharper bands. The IR spectra of the compounds under investigation show a broad band at 3211 cm^{-1} (I), 3171 cm^{-1} (II), 3070 cm^{-1} (III), 3498 cm^{-1} (IV) and 3331 cm^{-1} (V).

The band shows broad appearance and due to its relatively high frequency it can be concluded that the (OH) group of the investigated ligands involved its hydrogen bonding.

Both $\nu_{\text{C-O}}$ stretching and O-H deformation vibrations gives rise to two strong absorption bands in the lower frequency^[74] region characterizing compounds, but there is a good deal of confusion as to which of these is C-O or O-H band. Indeed both may be connected in some way to the O-H deformation modes. The first one absorbs around 1226 cm^{-1} (O-H) while the second band arises in the region $1028\text{-}1055\text{ cm}^{-1}$ C-O. See table (1).

(b) $\text{C}=\text{C}$ - vibration.

It has been pointed out that in mono and disubstituted benzenes, the ring breathing vibrations tends to absorb near 1450, 1500, 1580 and 1600 cm^{-1} [71]. However, in benzene itself, this set of bands is reduced to two bands only because the two half ring stretching vibration have the same frequency and therefore degenerate, this is the reason for the appearance of two bands in the spectrum near 1600 and 1500 cm^{-1} corresponding to the $\text{C}=\text{C}$ vibration.

Colthup^[74] shows that the 1600 cm^{-1} band occurs within the range 1625-1575 cm^{-1} and that one at 1500 cm^{-1} occurs within the range 1525-1475 cm^{-1} . The IR spectra of the present compounds show the first band at 1593 cm^{-1} , the latter at 1550 cm^{-1} for the investigated ligands (I-V), respectively. See table (1).

(C) $\text{C}=\text{C}-\text{H}$ - vibrations.

Aromatic compounds show the $\text{C}-\text{H}$ stretching absorption in the region 3100-3000 cm^{-1} and may thus be differentiated from saturated compounds. The bands due to the ($\text{C}-\text{H}$) stretching modes of alkanes are found in the region 3000-2820 cm^{-1} [75].

Fox and Martin^[76] have noticed the appearance of two strong bands at about 2962 cm^{-1} in hydrocarbons containing methyl group due to asymmetric and symmetric stretching modes of methyl group. The $\text{C}-\text{H}$ stretching bands of methoxy group are found in the region 2832-2815 cm^{-1} [77]. The strong to medium bands lying within the wave number 1490-1440 cm^{-1} and 1340-1310 cm^{-1} may be assigned to CH_3 asymmetric bending vibrations.

Weak absorption bands are observed in the region 1200-900 cm^{-1} which may be assigned to the $\text{C}-\text{H}$ in plane deformation in the benzene

ring (δ_{CH}). Out-of-plane deformation, for aromatic C-H (γ_{CH}) bands are expected within the range 1000-650 cm^{-1} .

Wiffar and Thompson^[78] proposed the range 760-740 cm^{-1} for the absorption of the out-of-plane bending in monosubstituted aromatics. This was slightly extended by Colthup^[74] to 770-730 cm^{-1} . The upper part of range of this band overlaps the range of *o*-disubstituted compounds. On decreasing the number of free adjacent hydrogen atom on the ring, the absorption frequency of the out-of-plane C-H vibrations show a further shift to lower frequencies and strong band appears in the range 860-800 cm^{-1} corresponding to out-of-plane deformation of two adjacent ring hydrogen atoms^[79].

The bands in the 3090-3000 cm^{-1} region in the investigated ligands are due to Ar-H stretching vibration while those appeared in the 2950-2920 cm^{-1} region is due to aliphatic C-H stretching vibration. The bands at 1180-1159 cm^{-1} and 840-780 cm^{-1} arising in the spectra of the investigated ligands may be assigned to C-H in-plane deformation and C-H out-of-plane bending, respectively. The γ_{CH} of the aromatic rings are observed within the wavenumber 899-867 cm^{-1} range. The number and shape of these bands depends on the position and the type of substituents present. The results are listed in table (1).

(d) C-N group.

Assignment for C-N band can be regarded as absorption near 1250 cm^{-1} . Thompson^[73] quoted the range 1325-1280 cm^{-1} when the carbon is unsaturated or aromatic, other bands possible to appear in this region are O-H and C-H in-plane deformation modes, ϕ O-H stretching. The data are listed in table (1). Thus the bands appearing in the IR spectra of the

ligands (I-V) 1230, 1226, 1236, 1230 and 1226 cm^{-1} , respectively are assigned to the stretching vibration of C-N.

(e) $-\text{N}=\text{N}$ band

The $\gamma_{\text{N}=\text{N}}$ bands are observed in the range 1488-1498 cm^{-1} conjugated with the ring skeletal vibrations ($\nu_{\text{C}=\text{C}}$) 1546-1604 cm^{-1} . The strong band observed at 1248 cm^{-1} is assigned to the C-O vibration^[80].

(f) $-\text{C}=\text{O}$ band

The $\nu_{\text{C}=\text{O}}$ band are observed in the range 1635-1650 cm^{-1} ^[81]. The bands at 1660-1630 cm^{-1} are assigned to C=O stretching of the carboxyl group^[82]. Also C=O were found in the range 1674-1650 cm^{-1} ^[83]. The strong band appearing at 1654 cm^{-1} is assigned to the stretching frequency of the C=O group^[54]. Also the band observed with the range 1707-1713 cm^{-1} assigned to $\nu_{\text{C}=\text{O}}$ ^[66]. Thus the bands appearing in the IR spectra of the ligands (I-V) 1654, 1651, 1651, 1654 and 1651 cm^{-1} , respectively are assigned to the stretching vibration of C=O.

%T

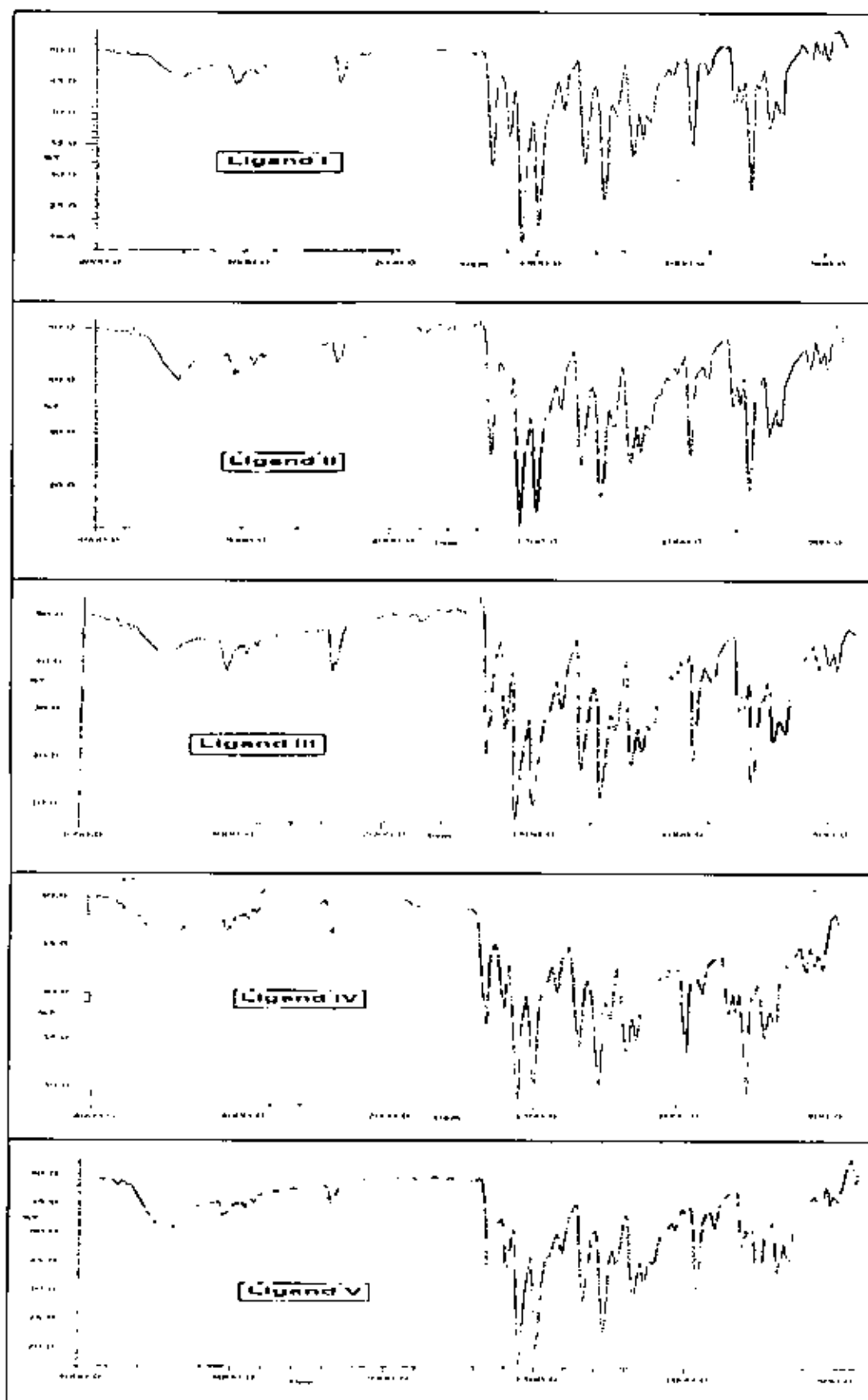


Figure (4): Infrared spectra of the investigated ligands.

Table (1): The most significant bands in IR spectra of the investigated ligands (I-V).

Band Assignment cm ⁻¹	Ligand				
	I	II	III	IV	V
ν_{OH}	3429	3406	3421	3440	3429
ν_{NH}	3294	3058	3298	3031	3058
$\nu_{C=O}$	1654	1651	1651	1654	1651
ν_{C-C}	1593	1593	1593	1593	1593
$\nu_{C=C}$	1550	1550	1550	1550	1550
$\nu_{N=N}$	1496	1492	1492	1496	1497
ν_{C-H}	1338	1338	1338	1338	1338
δ_{OH}	1230	1226	1226	1230	1226

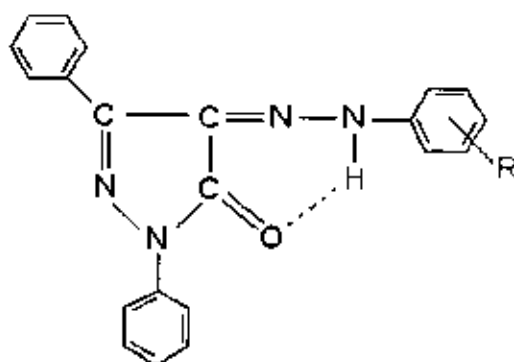
III.1.2. ^1H NMR spectral studies.

Nuclear magnetic resonance (NMR) proved to be powerful tool for structural elucidation, the identification of structural fragments, atoms, connectiveness, relative configuration and conformation, absolute configuration intra- and intermolecular interactions as well as a variety of molecular dynamics.

In this work we invoked the ^1H NMR technique for the purpose of establishing the possible azo-hydrazo^[35] or keto-enol tautomerism.

The ^1H NMR of the investigated ligands (I-V) was recorded in DMSO as a solvent and tetramethylsilane as an internal standard. Figure (5) illustrate ^1H NMR spectra of the investigated ligands (I-V). The chemical shift values of the different types of protons in the investigated ligands (I-V) are reported in table (2).

The ^1H NMR spectra of 1,3-diphenyl-4-phenylazo-5-pyrazolone (ligand I) in DMSO, figure (5), exhibits a sharp signal at (13.7) ppm. This signal is assigned to the proton of NH group. A singlet signal observed downfield at (13.8) ppm, this signal is diagnostic of intramolecular H-bonded proton in the investigated ligand (III)^[71].



where R = H (I), p-Cl (II), p-CH₃ (III), p-OCH₃ (IV) or o-COOH (V).

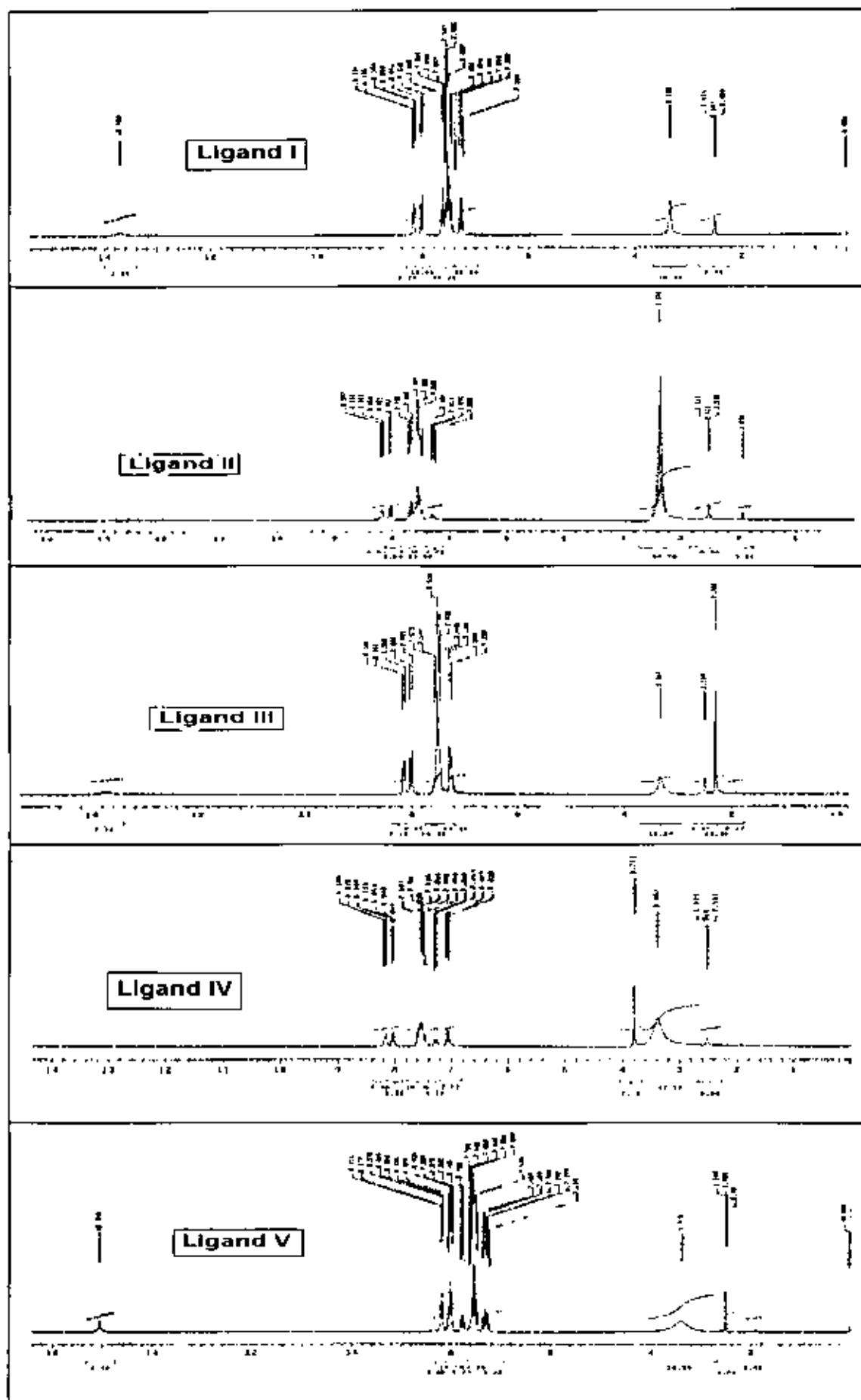


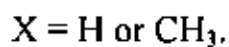
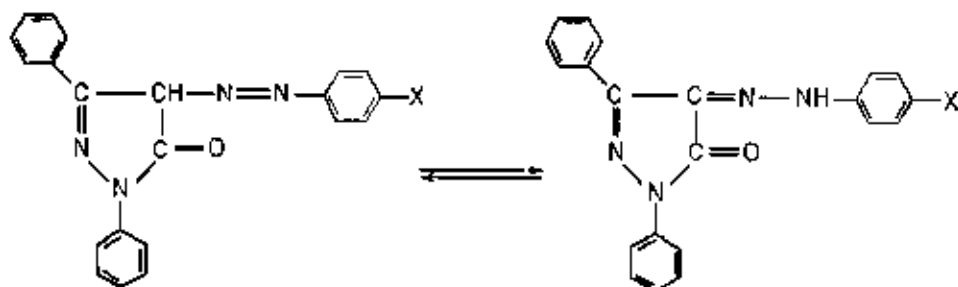
Figure (5): ^1H NMR spectra of the investigated ligands (I-V).

Table (2): ^1H NMR spectral data of the azopyrazolones.

Ligand	Chemical Shift	Assignment
Ligand I	13.7	NH hydrazone
	8.19-7.23	Aromatic C-H protons
	3.33	H ₂ O solvent protons
	2.5	DMSO protons
Ligand II	8.2-7.25	Aromatic C-H protons
	3.35	H ₂ O solvent protons
	2.51	DMSO protons
Ligand III	13.8	NH hydrazone
	8.16-7.23	Aromatic protons
	3.32	H ₂ O solvent protons
	2.5	DMSO protons
	2.30	CH ₃ protons
Ligand IV	8.18-7.03	Aromatic protons
	3.79	OCH ₃ protons
	3.38	H ₂ O solvent protons
	2.52	DMSO protons
Ligand V	15.04	COOH proton
	8.21-7.23	Aromatic protons
	3.37	H ₂ O solvents protons
	2.50	DMSO protons

The ^1H NMR spectra of all ligands exhibit a singlet signal at (2.5-2.52) ppm which is assigned to the CH₃ protons of the solvent, also the aliphatic protons of the methyl groups appeared 2.30 ppm for ligand III. The signals observed at (7.03-8.21) ppm are assigned to the protons of the

aromatic ring^[84]. The signals observed at (13.7-13.8) ppm are assigned to the proton of the NH group for ligands (I) and (III), table (2). The appearance of these signals indicates the involvement of these ligands in azo-hydrazo tautomerism and has the following structure:



The signals observed at 15.04 ppm for ligand (V) are assigned to the proton of the carboxylic group (-COOH).

III.1.3. Mass spectral studies.

Mass spectra is a powerful tool in elucidating and confirming the structure of chemical compounds^[85]. It is known from the standard concept of physical organic chemistry that cyclic structure, double bonds, aromatic and specially heteroaromatic rings stabilize the parent ion, and thus increase the probability of its appearance in the mass spectra.

Fragmentation pattern of ligand I is given in figure (6), figure (7) illustrates the possible pathway for the prominent fragments.

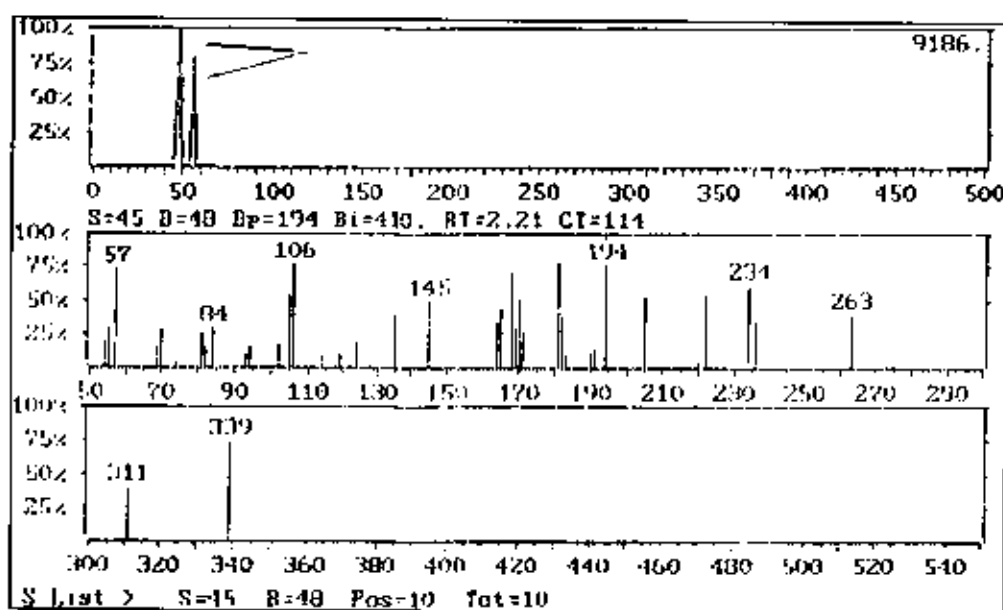


Figure (6): The mass fragmentation pattern of ligand I.

Our attention is restricted only to the general mechanism of fragmentation and thus not all the peaks are going to be interpreted. This is due to the fact that there are usually many possibilities for molecular rearrangements of the produced ionic fragments.

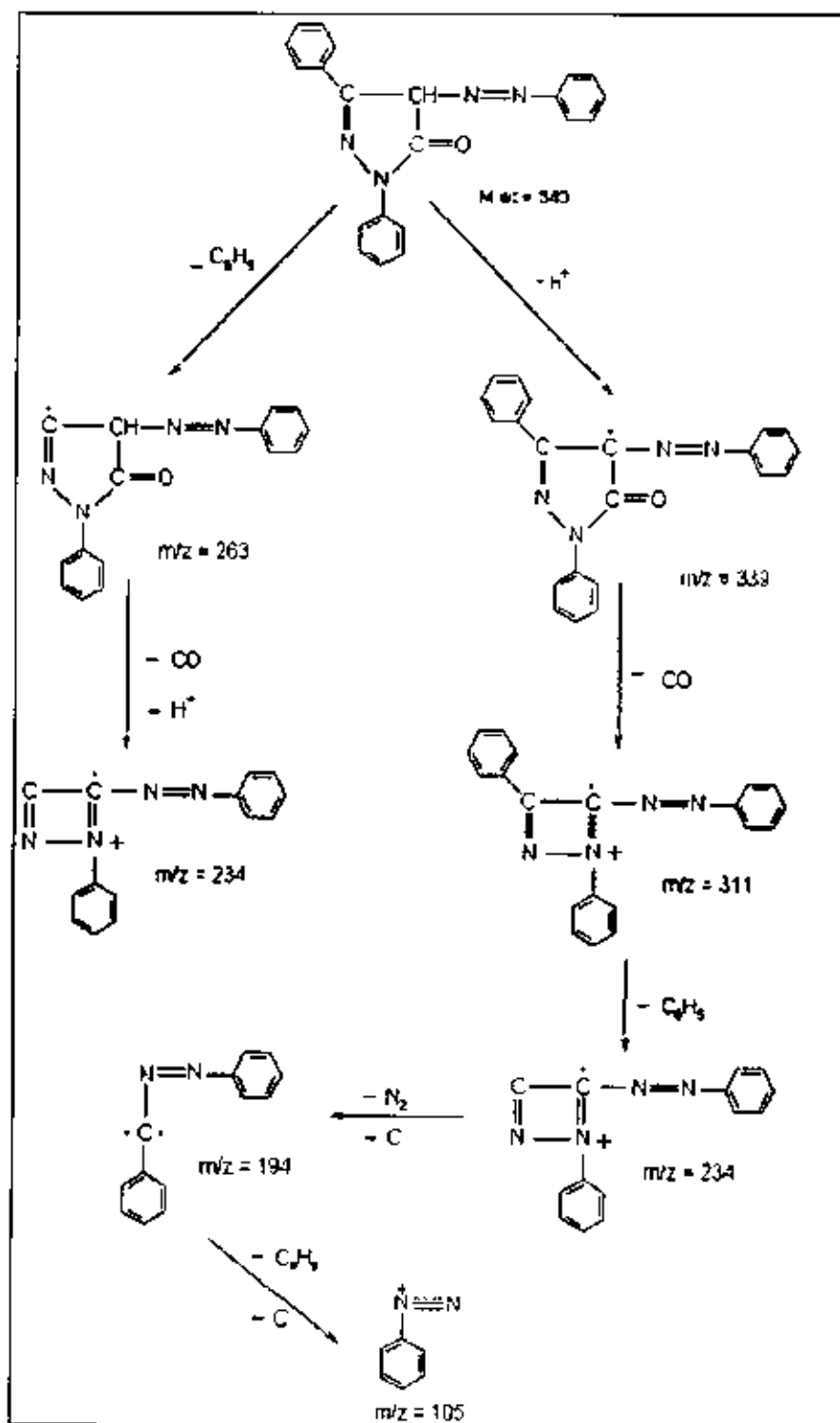


Figure (7): Schematic diagram illustrates the general mechanism of fragmentation of ligand I.

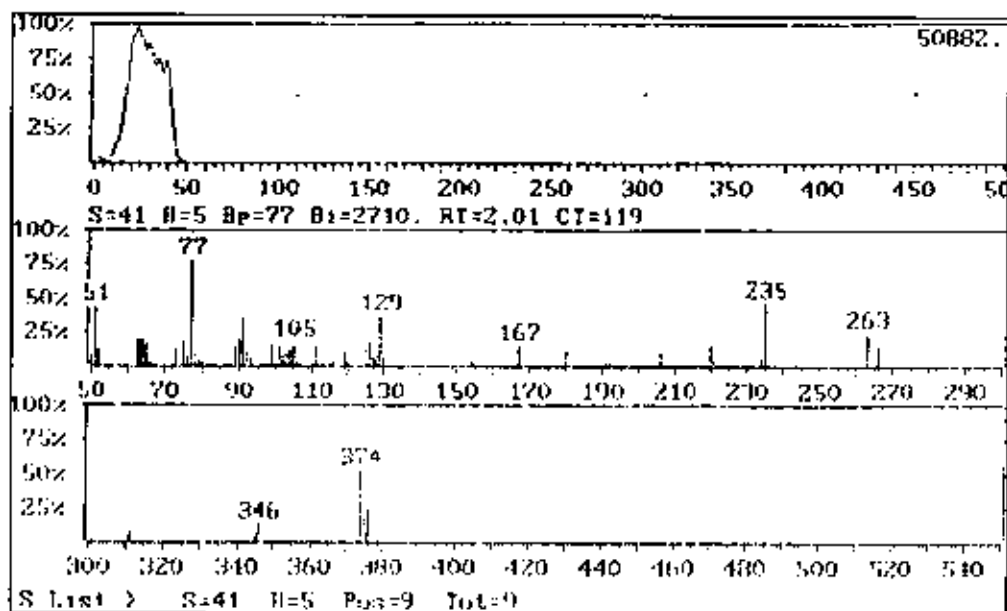


Figure (8): The mass fragmentation pattern of ligand II.

The fragmentation pattern of the unsubstituted 1,3-diphenyl-4-phenylazo-5-pyrazolone (ligand I) can be rearranged as shown in the fragmentation path involved in figure (7).

Differences in the other figures result from the effects of the electronegativities of the substituents attached to the aromatic ring.

For each one of the investigated ligands (I-V), the mass fragmentation pattern and the general mechanism of fragmentation are illustrated in the figures (8-15).

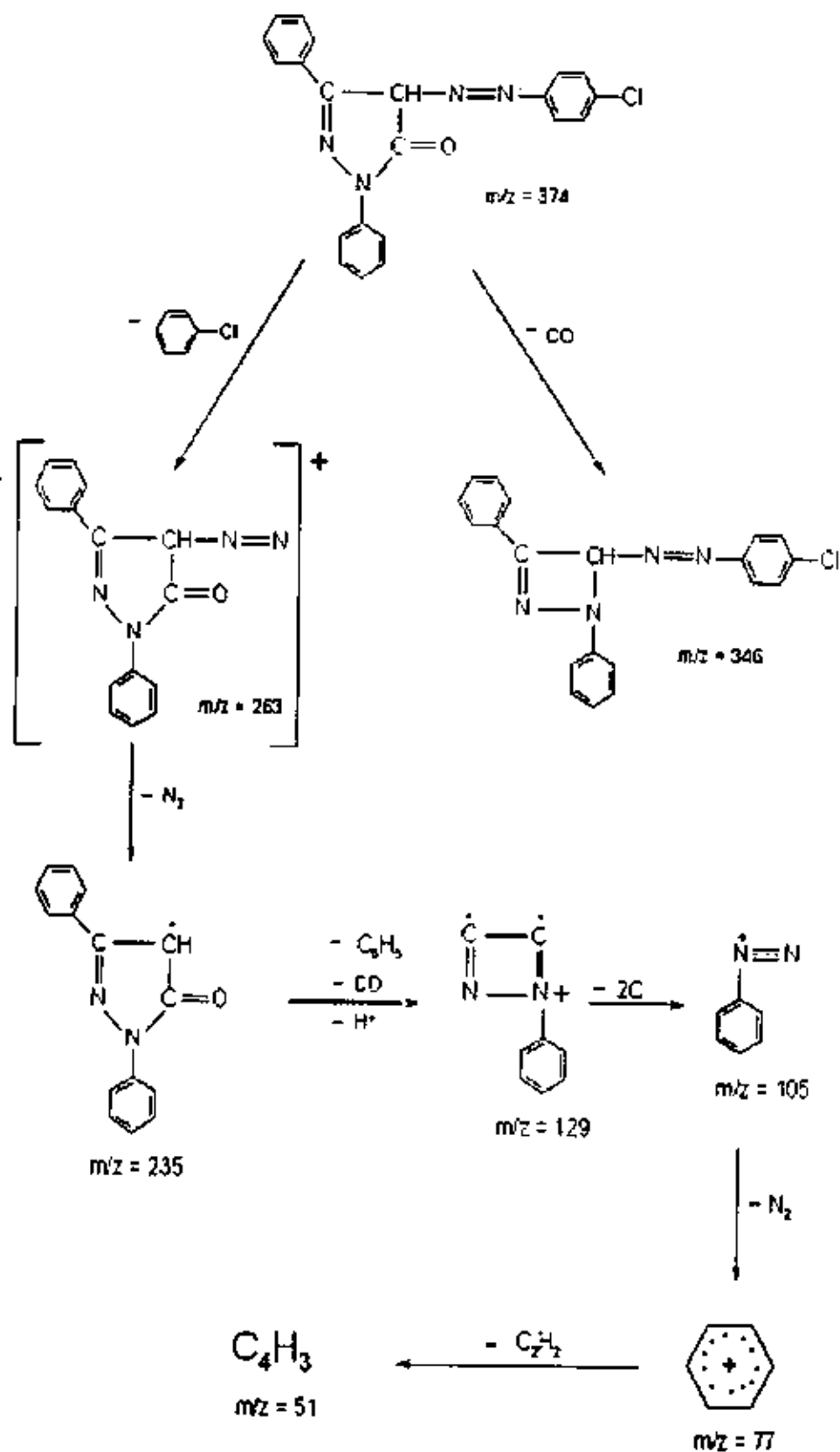


Figure (9): Schematic diagram illustrates the general mechanism of fragmentation of ligand II.

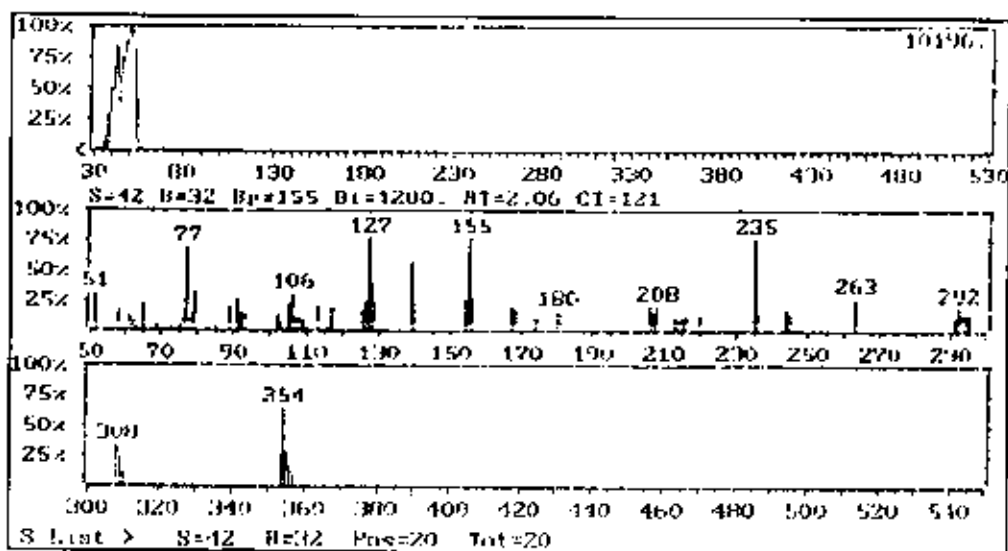


Figure (10): The mass fragmentation pattern of ligand III.

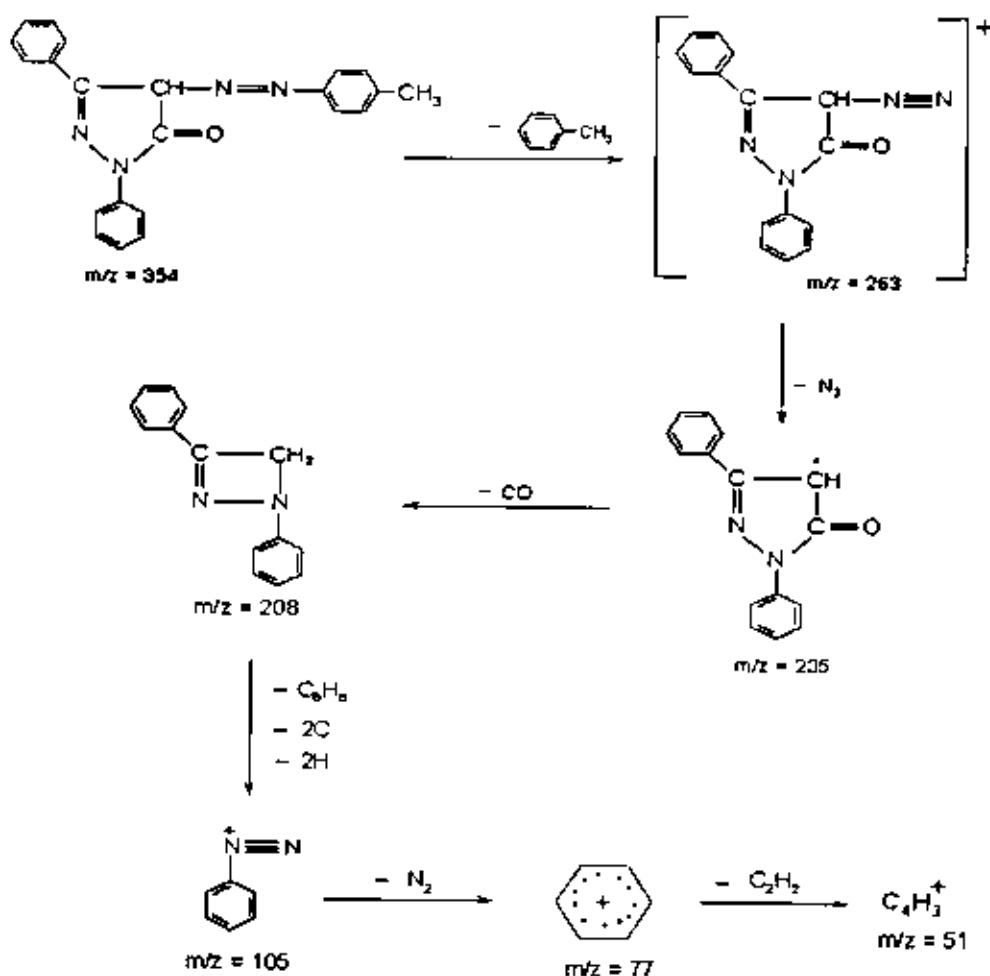


Figure (11): Schematic diagram illustrates the general mechanism of fragmentation of ligand III.

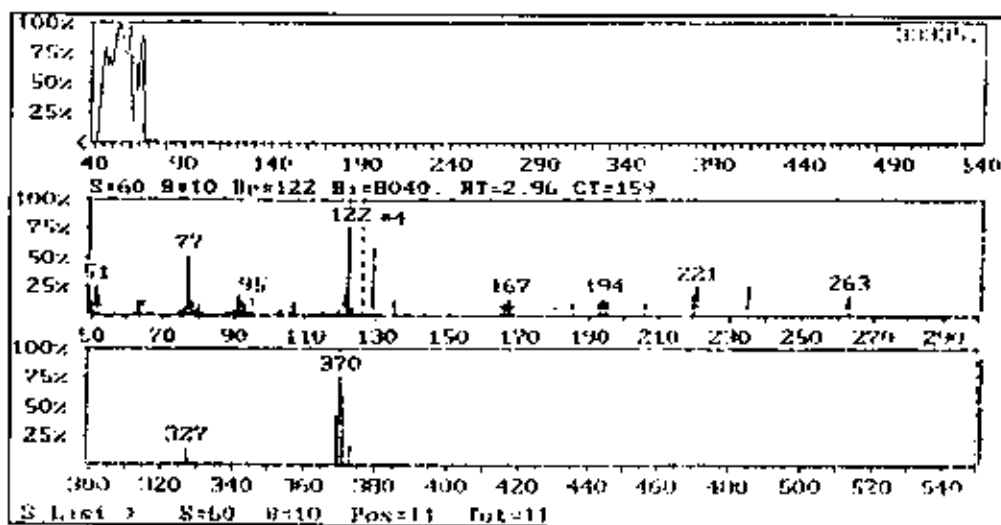


Figure (12): The mass fragmentation pattern of ligand IV.

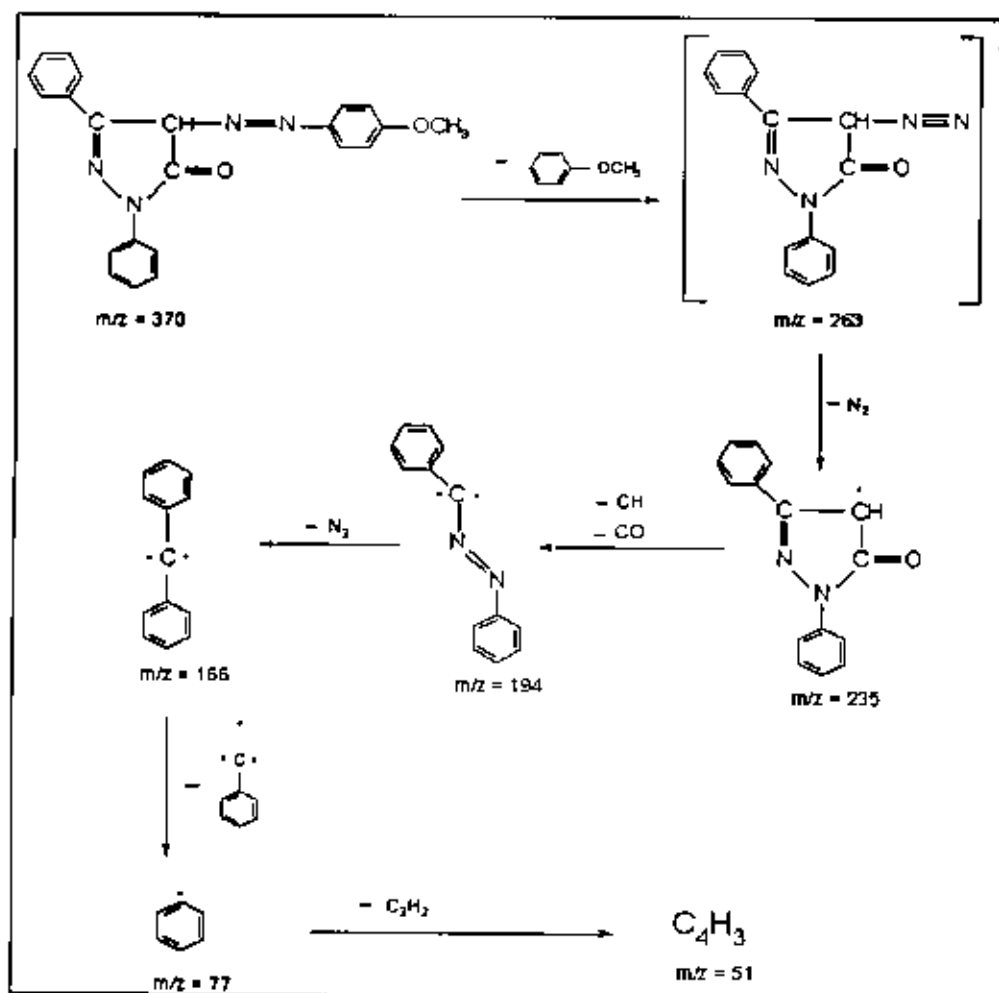


Figure (13): Schematic diagram illustrates the general mechanism of fragmentation of ligand IV.

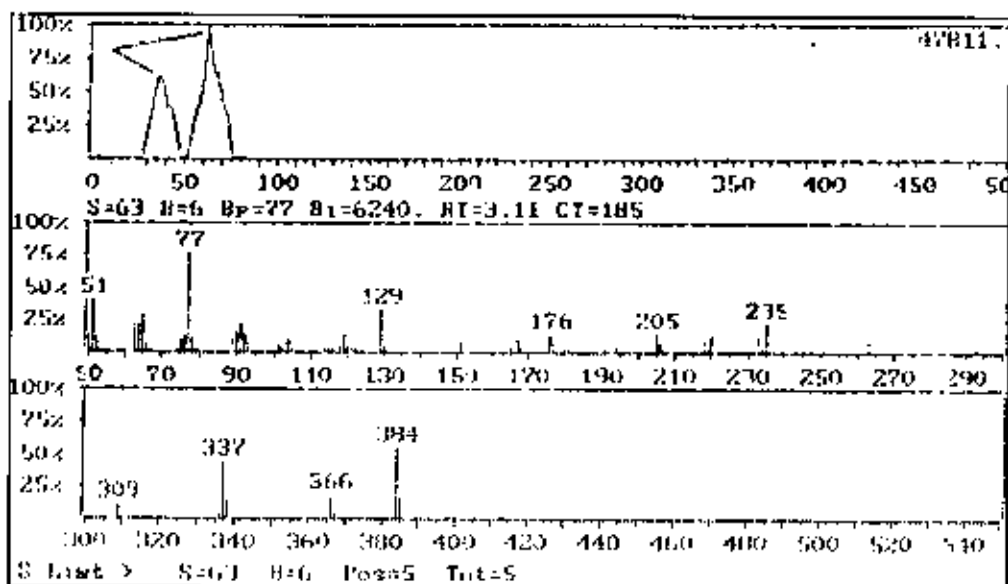


Figure (14): The mass fragmentation pattern of ligand V.

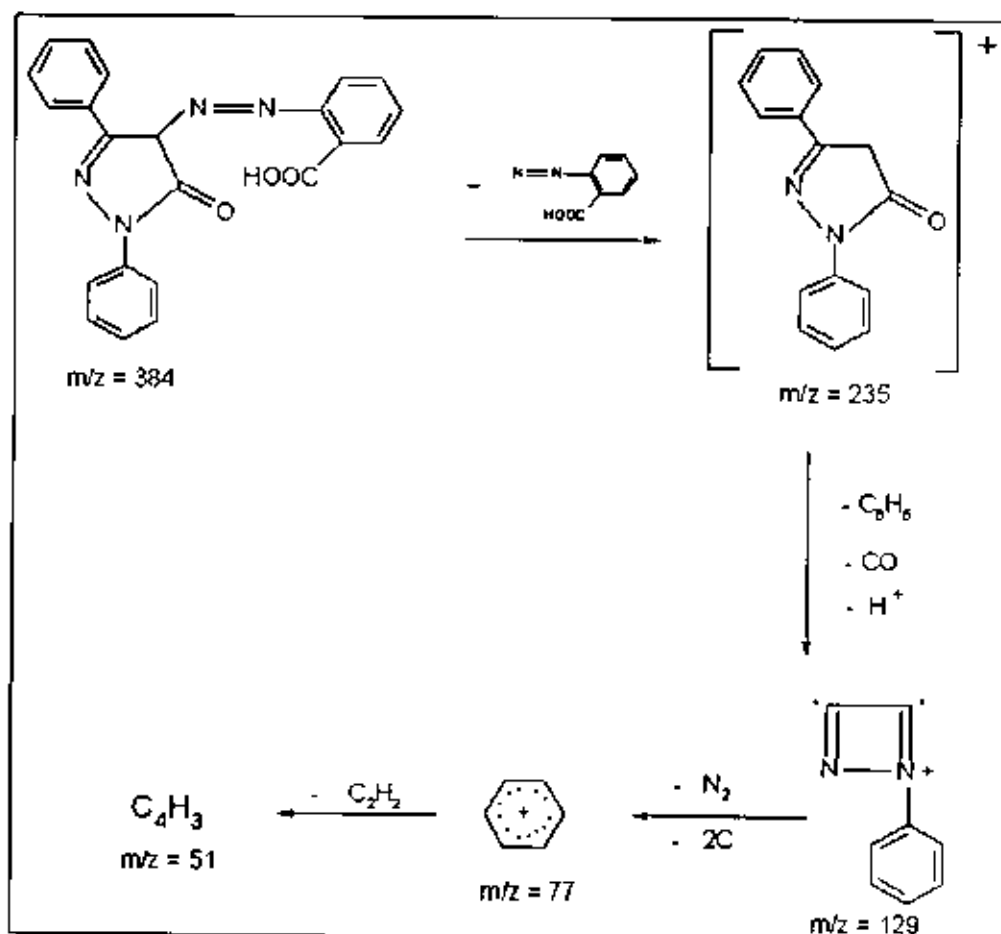


Figure (15): Schematic diagram illustrates the general mechanism of fragmentation of ligand V.

Referring to the figures (6-15), the mass spectral pattern of ligand I shows a peak of 339 (calcd. M.wt = 340). The fragmentation pattern of this ligand can be regarded as general scheme showing the main fragmentation paths involved. The differences in other ligands (II-V) result from the effect of electronegativities of the substituents attached to the aromatic ring.

For ligand II, the main peak is observed at 374 (caltd. M.wt = 374).

For ligand III, the main peak is observed at 354 (caltd. M.wt = 354).

For ligand IV, the main peak is observed at 370 (caltd. M.wt = 370).

For ligand V, the main peak is observed at 384 (caltd. M.wt = 384).

From the data obtained we concluded that the molecular weights are in good agreement with the calculated values.

III.1.4. Elemental analysis for the investigated ligands.

Table (3): Elemental analysis data of the investigated ligands (I-V)

Ligand	R	C% (Caltd) found	H% (Caltd) found	N% (Caltd) found	Cl% (Caltd) found
I	H	(74.12) 74.84	(4.71) 5.03	(16.47) 16.64	-----
II	p-Cl	(67.38) 67.24	(4.02) 4.52	(14.95) 15.17	(9.48) 9.64
III	p-CH ₃	(74.57) 73.47	(5.08) 5.37	(15.82) 15.85	-----
IV	p-OCH ₃	(71.35) 71.31	(4.86) 5.03	(15.13) 13.51	-----
V	o-COOH	(68.75) 68.08	(4.17) 4.54	(14.58) 14.91	-----

III.1.5. The absorption of ligand V in organic solvents of different polarities.

Using the equations mentioned previously, the following parameters $[(D-1)/(D+1)]$, $f(D)$ and $\phi(D)$ ^[86] were calculated for different solvents and are listed in table (4).

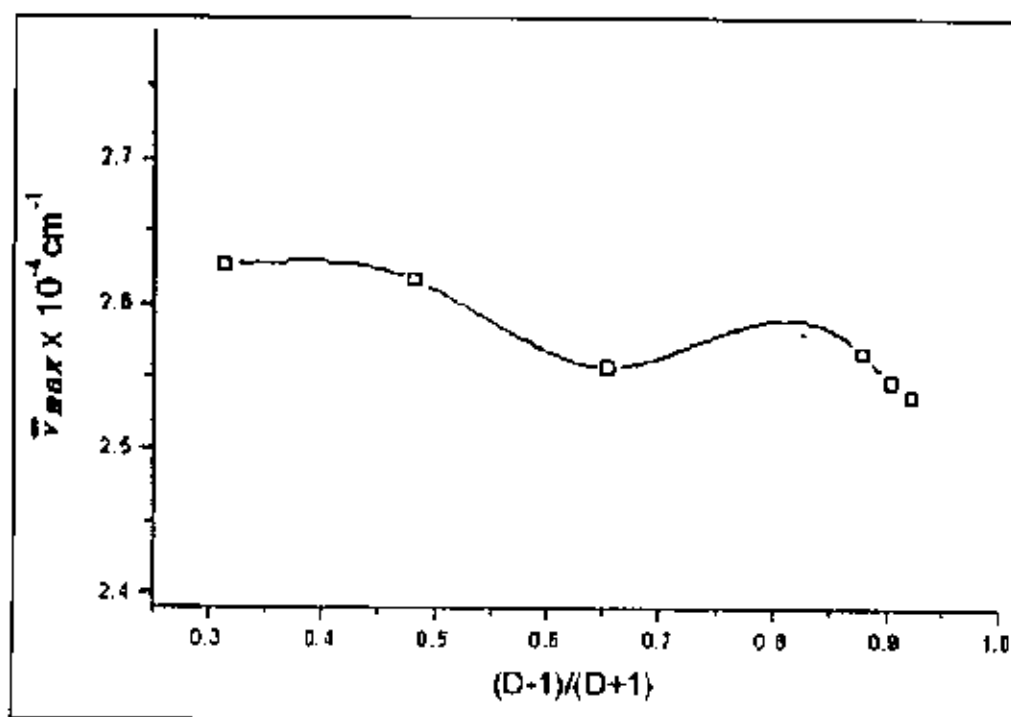
The plots of $(D-1)/(D+1)$, $f(D)$ and $\phi(D)$ against the wavenumber ν_{max} (in cm^{-1}) of the charge transfer (C.T.) band observed at λ_{max} are shown in figures (16-18).

The deviation in linearity in case of ligand V indicates that the dielectric constant is not the only parameter governing the solvent shift. This may be attributed to solvation which appears to be more important than the dielectric constant of the solvent.

Solvation, however, may also be partly due to certain chemical properties including the formation of hydrogen bonding between the solute and the solvent molecule^[87]. The change in the strength of solute-solvent hydrogen bonding and the solvation energy on going from the ground to excited state depends on the properties of both solute and solvents^[88]. These changes contribute to the band shift, whether to higher or lower energy and the observed shift is the resultant effect of these different factors. This phenomenon can be used in structure elucidation for ligands.

Table (4) : Some solvent parameters.

solvent	D	(D-1)/(D+1)	f(D)	ϕ (D)
Ethanol	25.00	0.923	0.941	0.889
methanol	32.70	0.941	0.955	0.913
isopropanol	18.60	0.898	0.922	0.854
1,4 - dioxane	3.30	0.500	0.571	0.400
cyclohexane	2.00	0.333	0.400	0.250
chloroform	5.10	0.672	0.732	0.577

**Figure (16)** : Relation between the maximum absorption of C.T. band of ligand V and $(D-1)/(D+1)$ of solvents of different polarities (ethanol, methanol, isopropanol, dioxane, cyclohexane and chloroform).

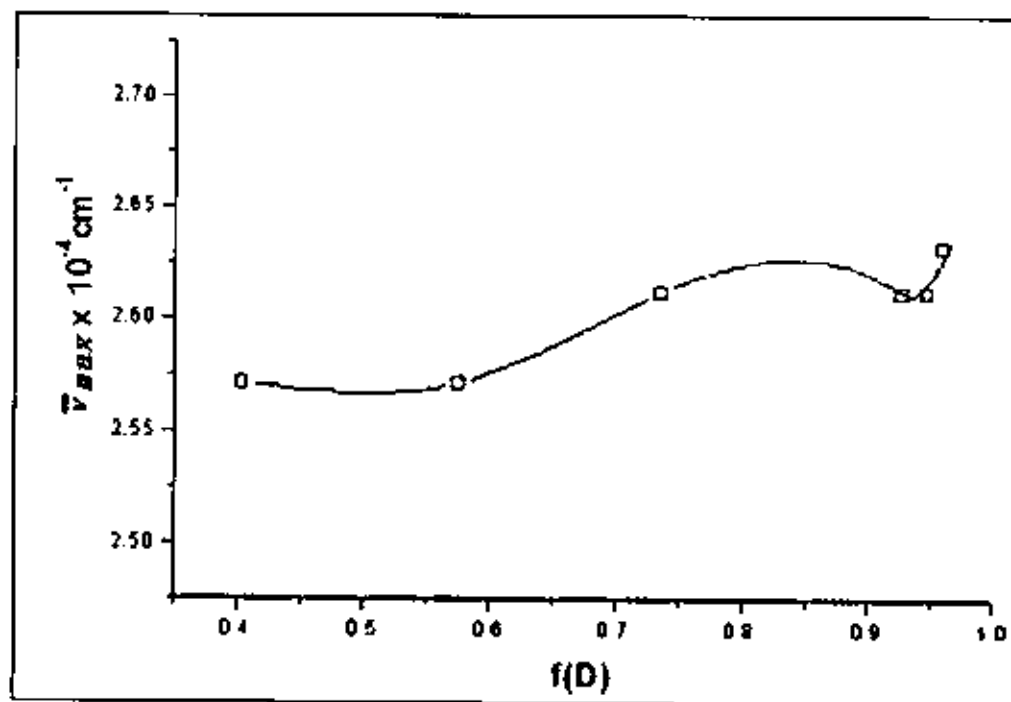


Figure (17) : Relation between the maximum absorption of C.T. band of ligand V and $f(D)$ of solvents of different polarities (ethanol, methanol, isopropanol, dioxane, cyclohexane and chloroform).

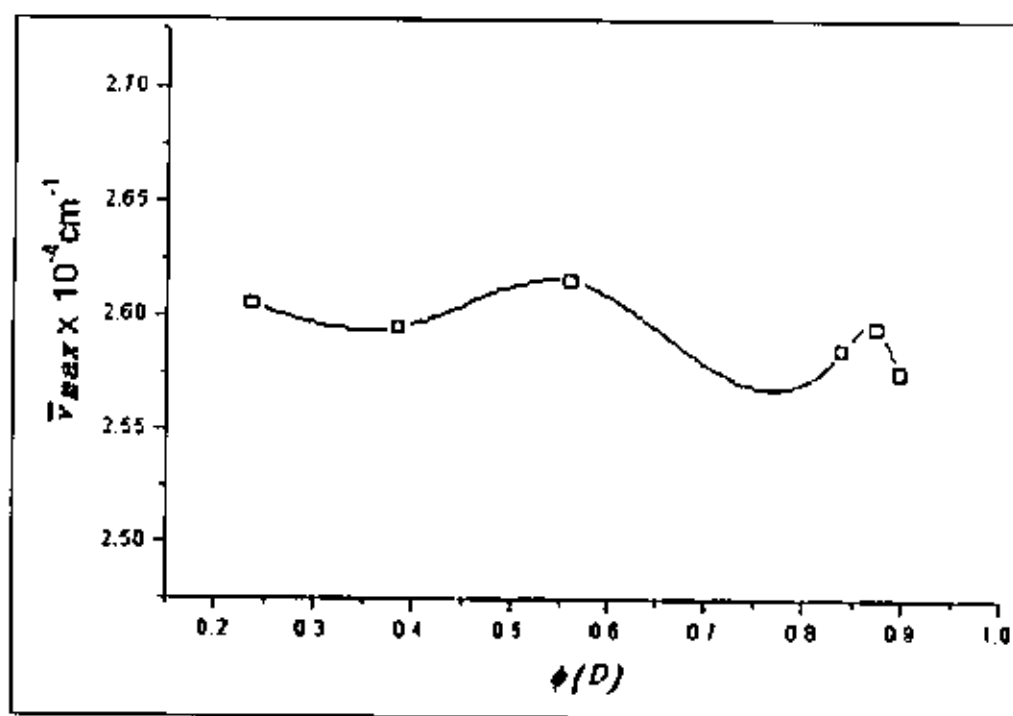


Figure (18) : Relation between the maximum absorption of C.T. band of the investigated ligand V and $\phi(D)$ of solvents of different polarities (ethanol, methanol, isopropanol, dioxane, cyclohexane and chloroform).

III.2. Stoichiometry and structure of the solid complexes.

The solid complexes of the metal ions (Mn^{2+} , Co^{2+} , Ni^{2+} , Cu^{2+} and Zn^{2+}) with the investigated ligands (I-V) were prepared as described in the experimental section. The resulting complexes were subjected to elemental analysis for (C, H, N, Cl) and metal content^[69], infrared spectral studies (IR), magnetic susceptibility, thermogravimetric analysis (TG), differential thermal analysis (DTA) and electron spin resonance (ESR).

The solid chelates of the bivalent metal ions (Mn^{2+} , Co^{2+} , Ni^{2+} , Cu^{2+} and Zn^{2+}) with 1,3-diphenyl-4-arylazo-5-pyrazolones were prepared as previously described under the experimental part. The resulting chelates were subjected to elemental analysis for C, H, N, Cl and metal content, infrared spectral studies (IR), molar conductance, nuclear magnetic resonance (1H NMR), thermogravimetric analysis (TG), differential thermal analysis (DTA). The results of elemental analysis which listed in tables (12-16) are in good agreement with those required by the proposed formula where in all cases 2:2 and 2:3 (M:L) solid complexes were isolated^[44] for ligands I-IV, for ligand V 1:1 and 1:2 complexes were isolated. The infrared spectra of the free ligands and solid complexes are recorded as KBr discs. In order to comment on the structure of the solid chelates using the IR spectra, first the IR spectra of free ligands must be discussed to assign the important bands in their spectra.

III.2.1. Infrared spectra of the solid complexes.

The infrared spectra of the solid complexes display interesting changes which may give a reasonable idea about the structure of these complexes.

The main IR bands of the solid complexes are given in tables (5-9), and the spectra in figures (19-28).

Comparison of the IR spectra of the metal complexes, figures (19-28), with those of the free ligands, figure (4), shows that the $\nu_{N=N}$ are shifted to the lower wavenumber on complex formation indicating that it is center of chelation.

The $\nu_{C=O}$ are disappeared indicating that it is a center of chelation as it losses its double bond character (-C-O-M-) this is confirmed by the appearance of a new band corresponding to ν_{C-O} in the range 1211-1296 cm^{-1} for all of the investigated complexes.

The OH stretching frequency appears in the spectra of all of the complexes under study as a sharp band appears in the range 3494-3244 cm^{-1} which is ascribed to chelated OH^- ion which is neutralizes the charge on the metal ion.

The spectra of metal complexes exhibit bands in the ranges (482-590) and (410-505) cm^{-1} which may assigned to (M←N) and (M←O) stretching frequencies^[89], respectively. In other words, these bands are possibly due to the formation of coordination bonds between the donor atoms (O and N) and the central metal ion.

However, if these changes are interpreted in relation to elemental analysis, tables (12-16), and the results of thermogravimetric analysis, the picture of the solid chelates may be classified.

%T

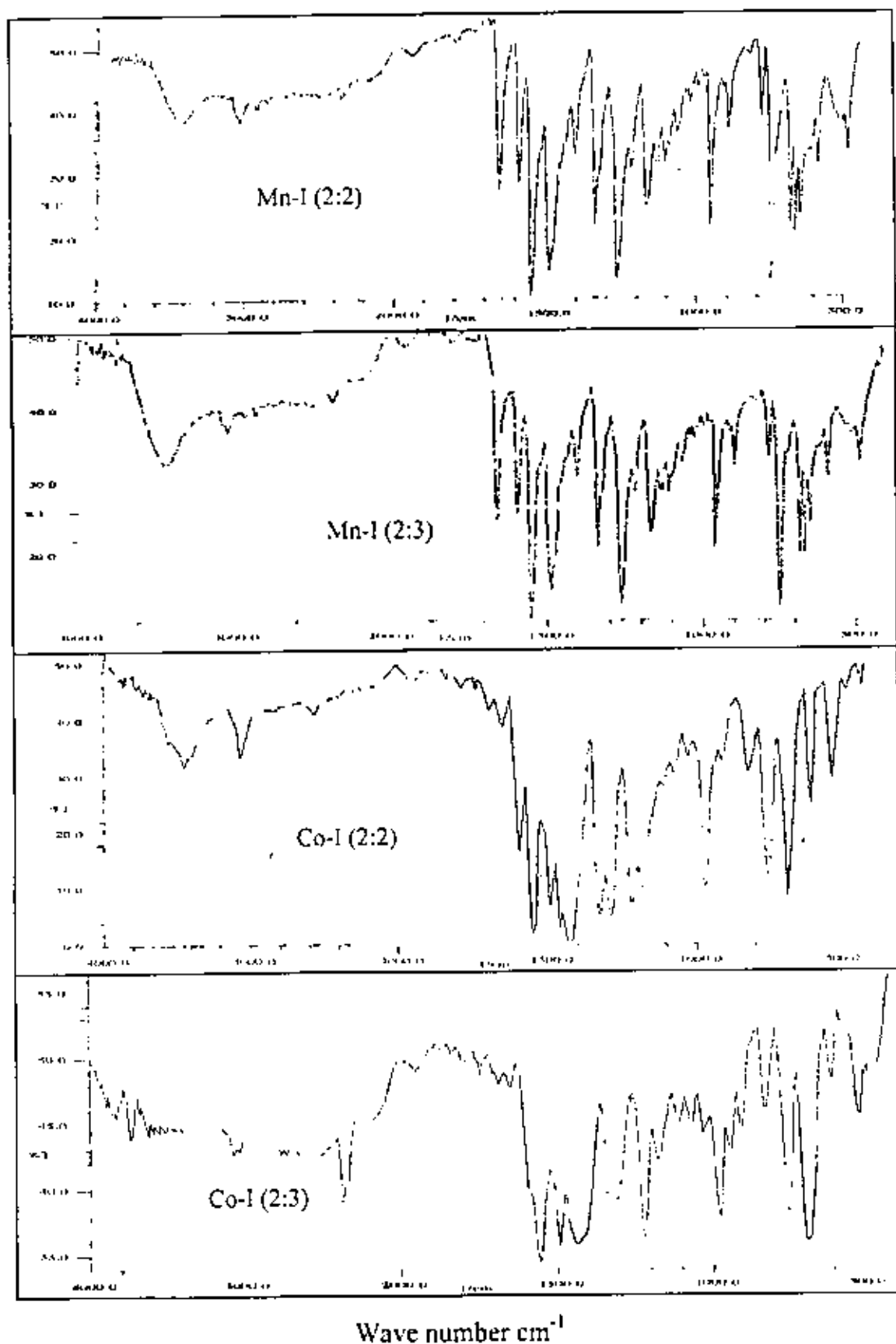


Figure (19): Infrared spectra of the complexes of ligand I with the metal ions Mn²⁺ and Co²⁺.

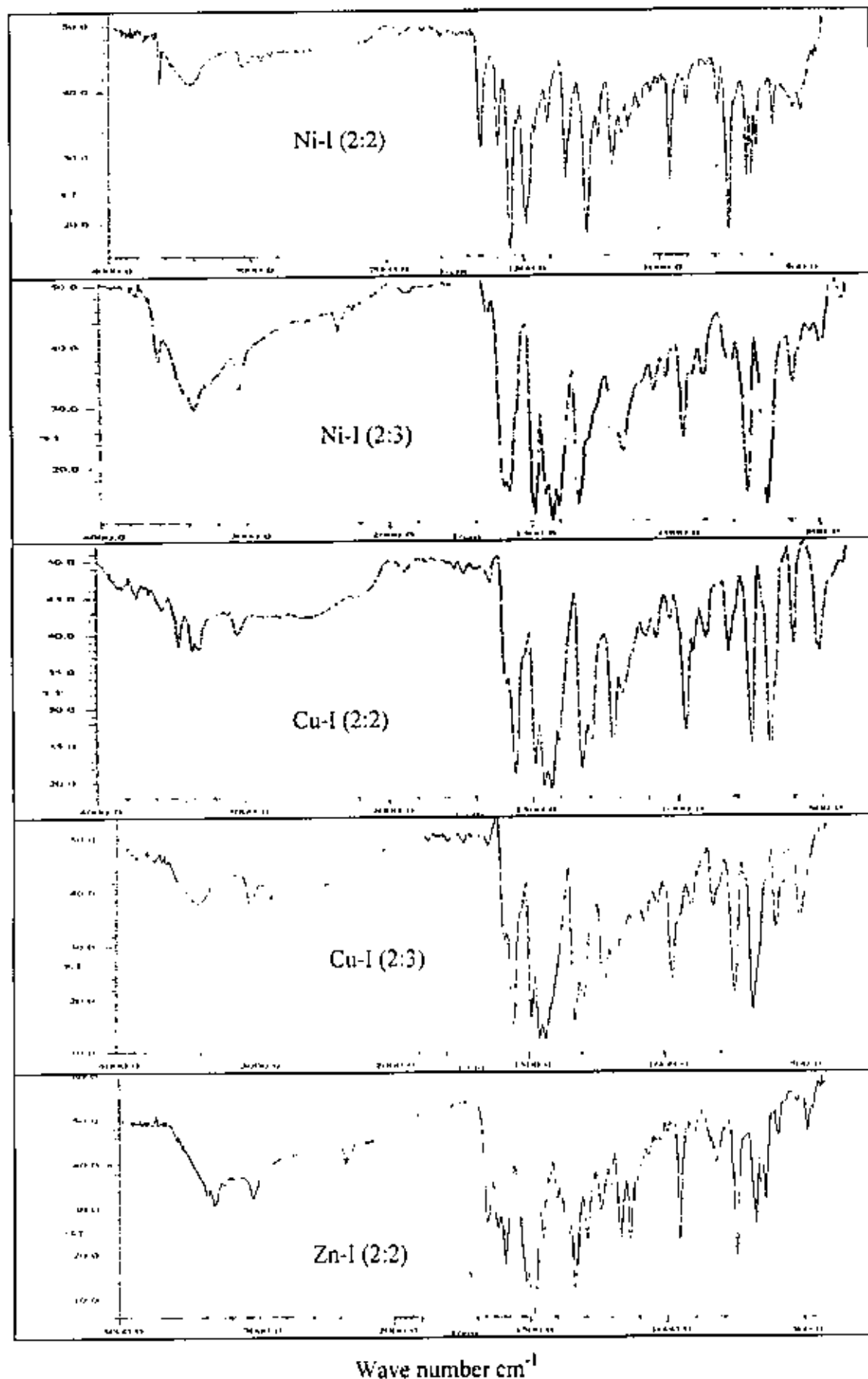


Figure (20): Infrared spectra of the complexes of ligand I with the metal ions Ni^{2+} , Cu^{2+} and Zn^{2+} .

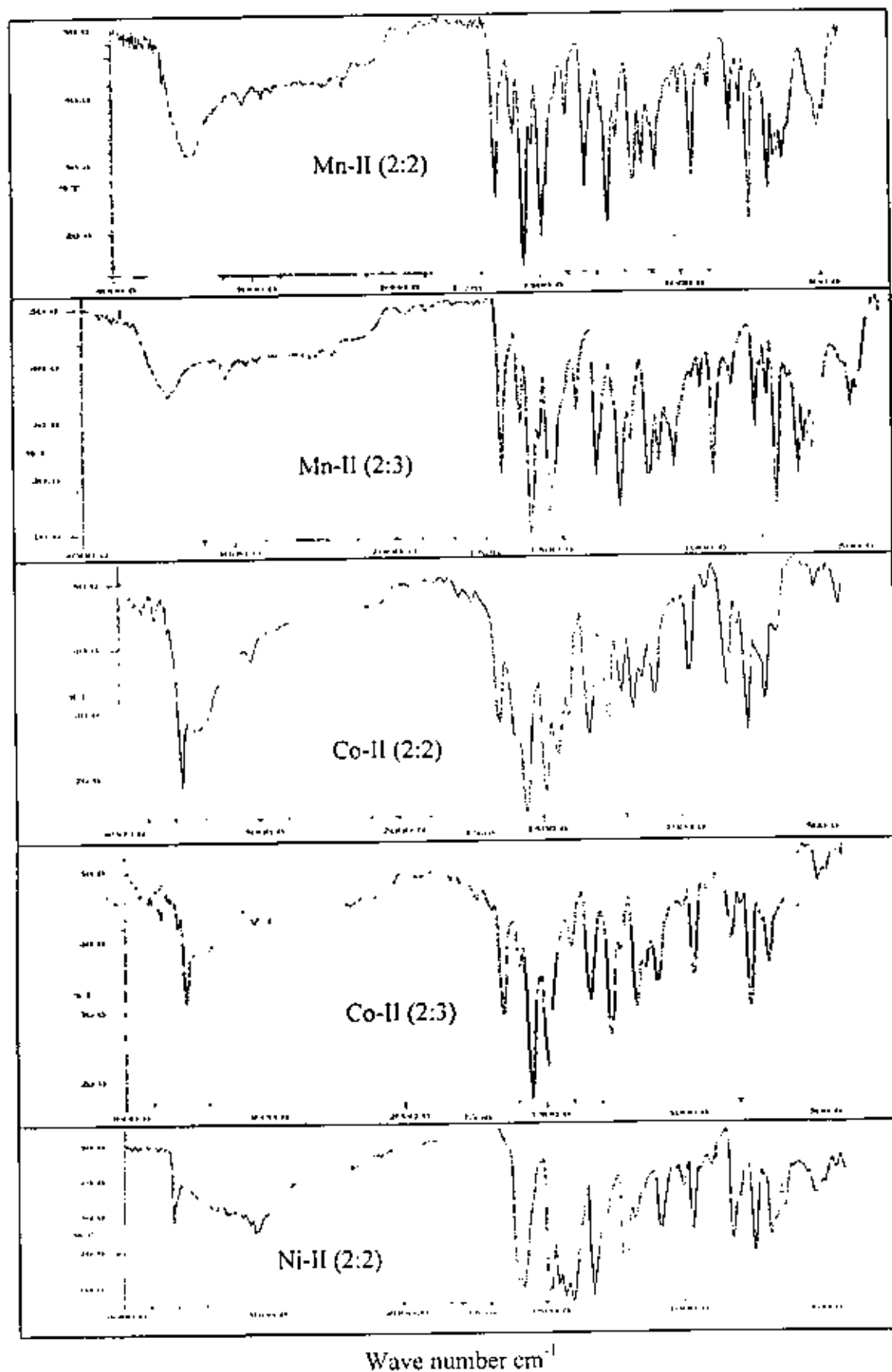


Figure (21): Infrared spectra of the complexes of ligand II with the metal ions Mn^{2+} , Co^{2+} and Ni^{2+} .

%T

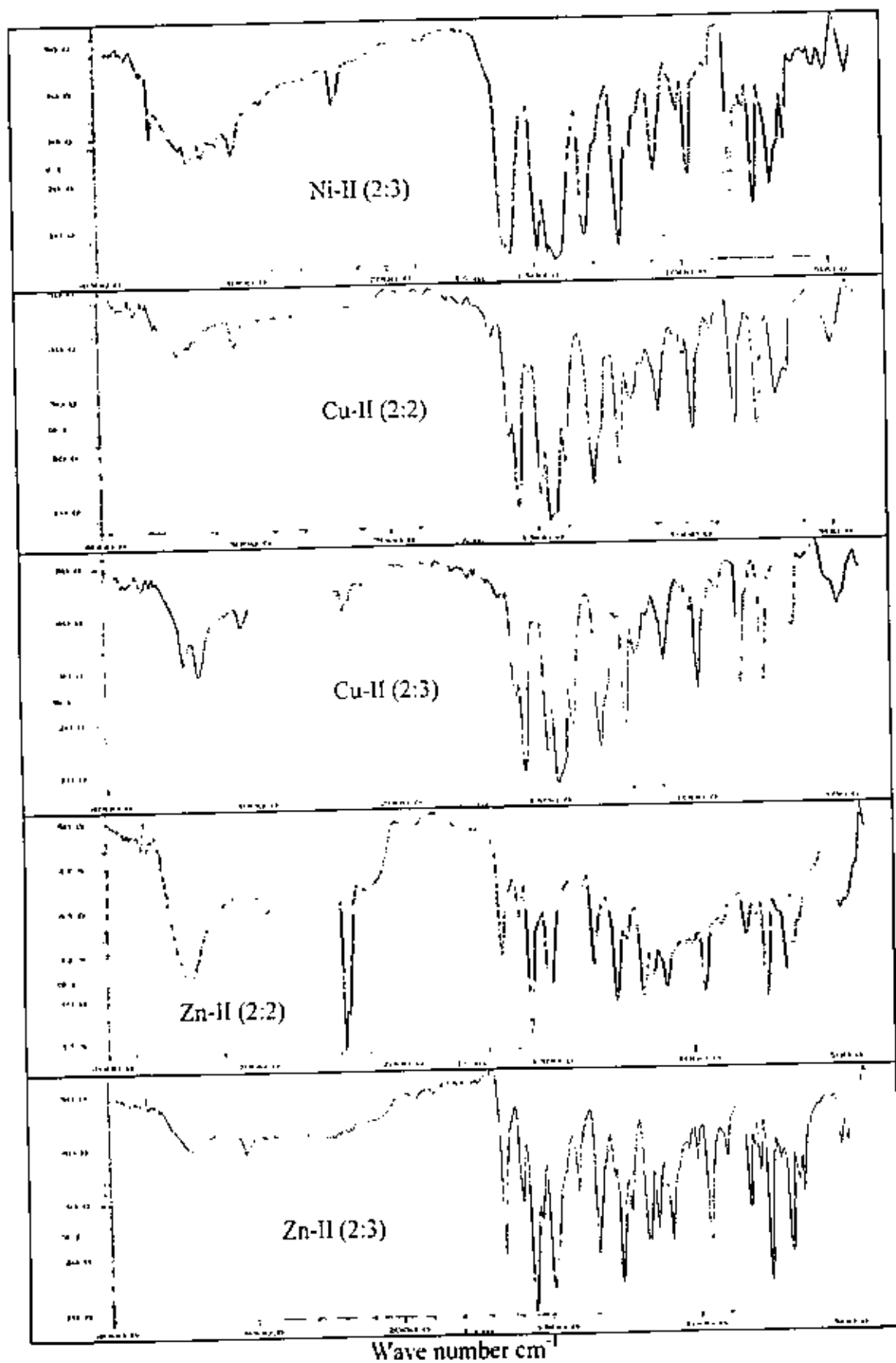


Figure (22): Infrared spectra of the complexes of ligand II with the metal ions Ni^{2+} , Cu^{2+} and Zn^{2+} .

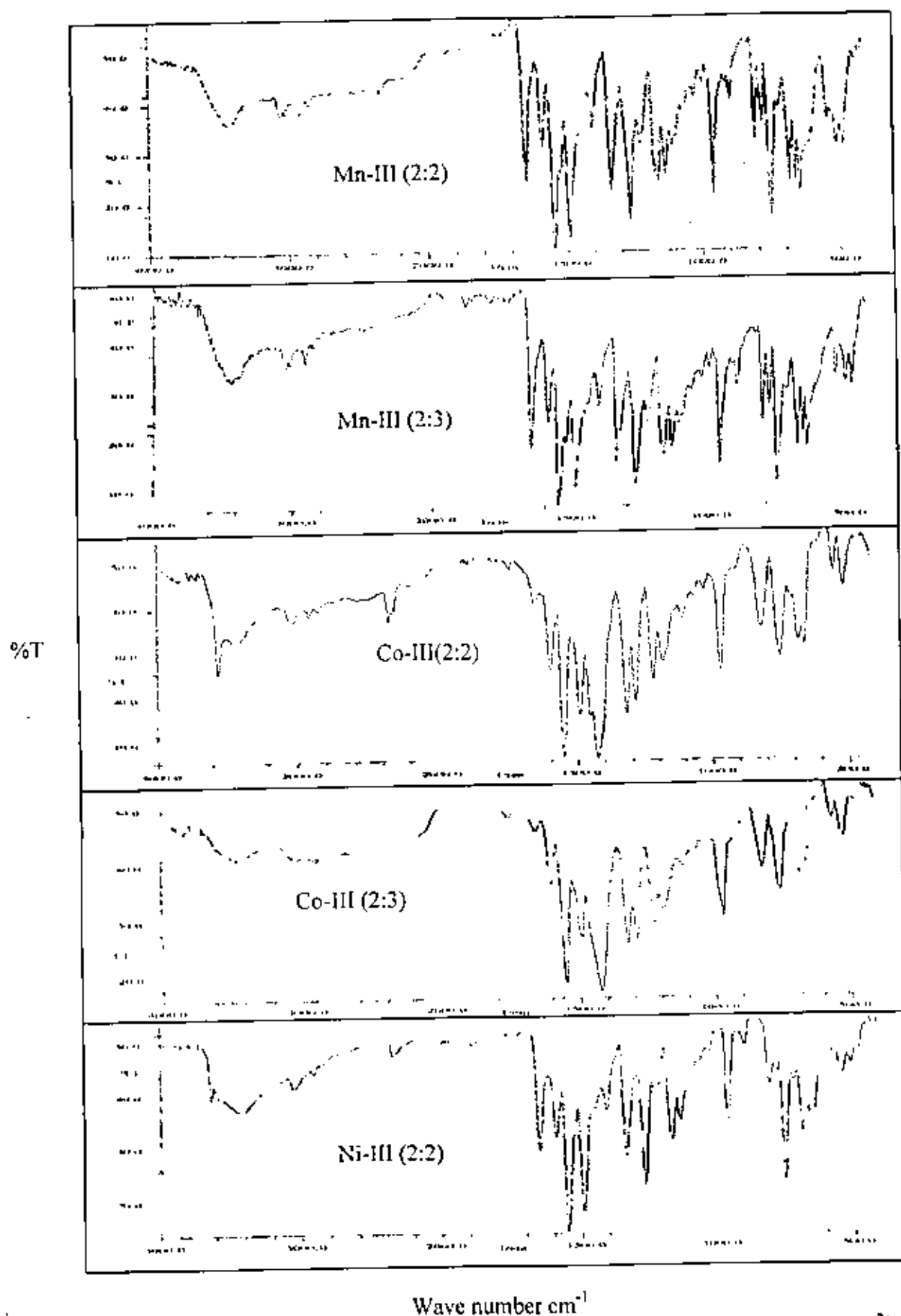


Figure (23): Infrared spectra of the complexes of ligand III with the metal ions Mn^{2+} , Co^{2+} and Ni^{2+} .

%T

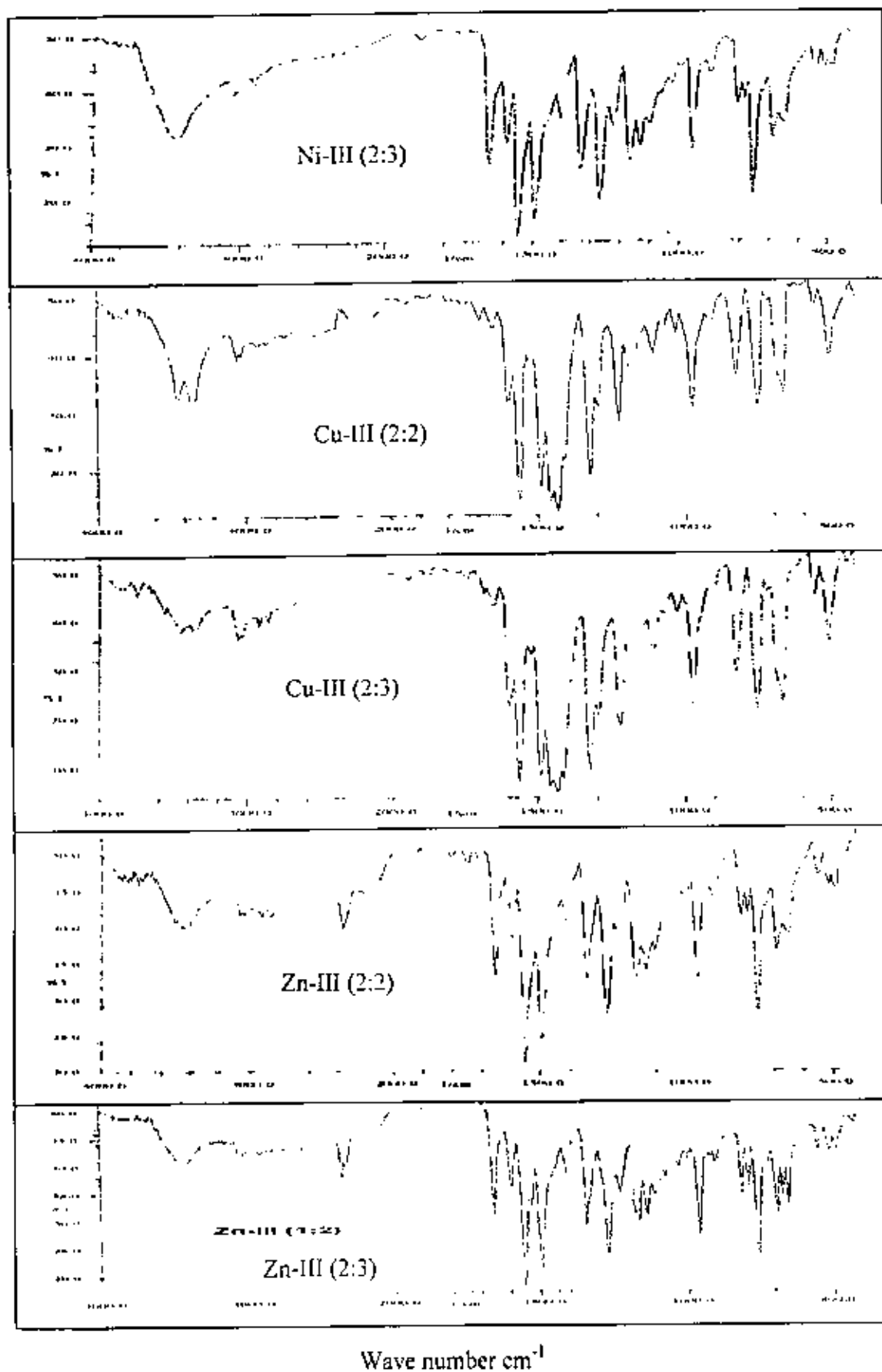
Wave number cm^{-1}

Figure (24): Infrared spectra of the complexes of ligand III with the metal ions Ni^{2+} , Cu^{2+} and Zn^{2+} .

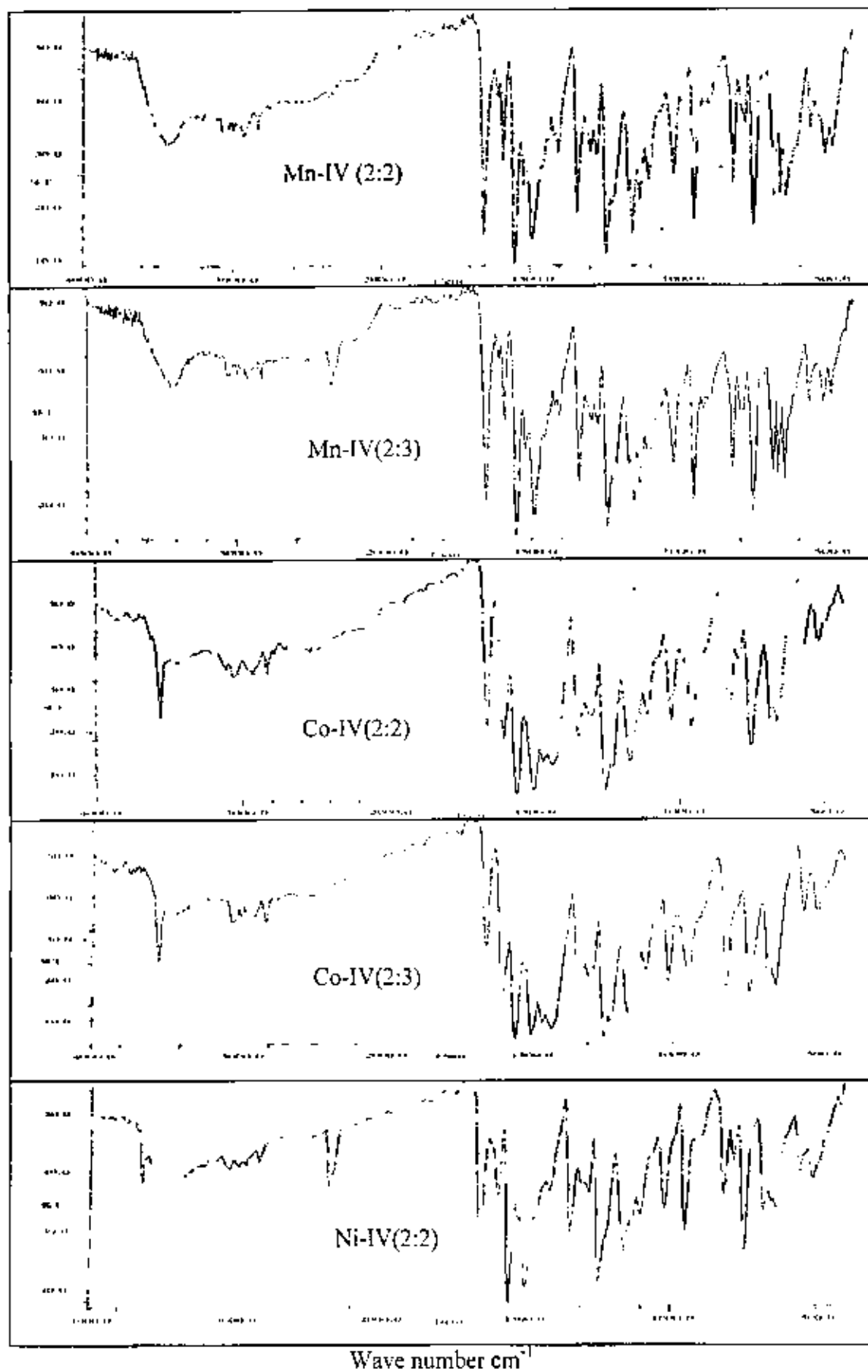


Figure (25): Infrared spectra of the complexes of ligand IV with the metal ions Mn^{2+} , Co^{2+} and Ni^{2+} .

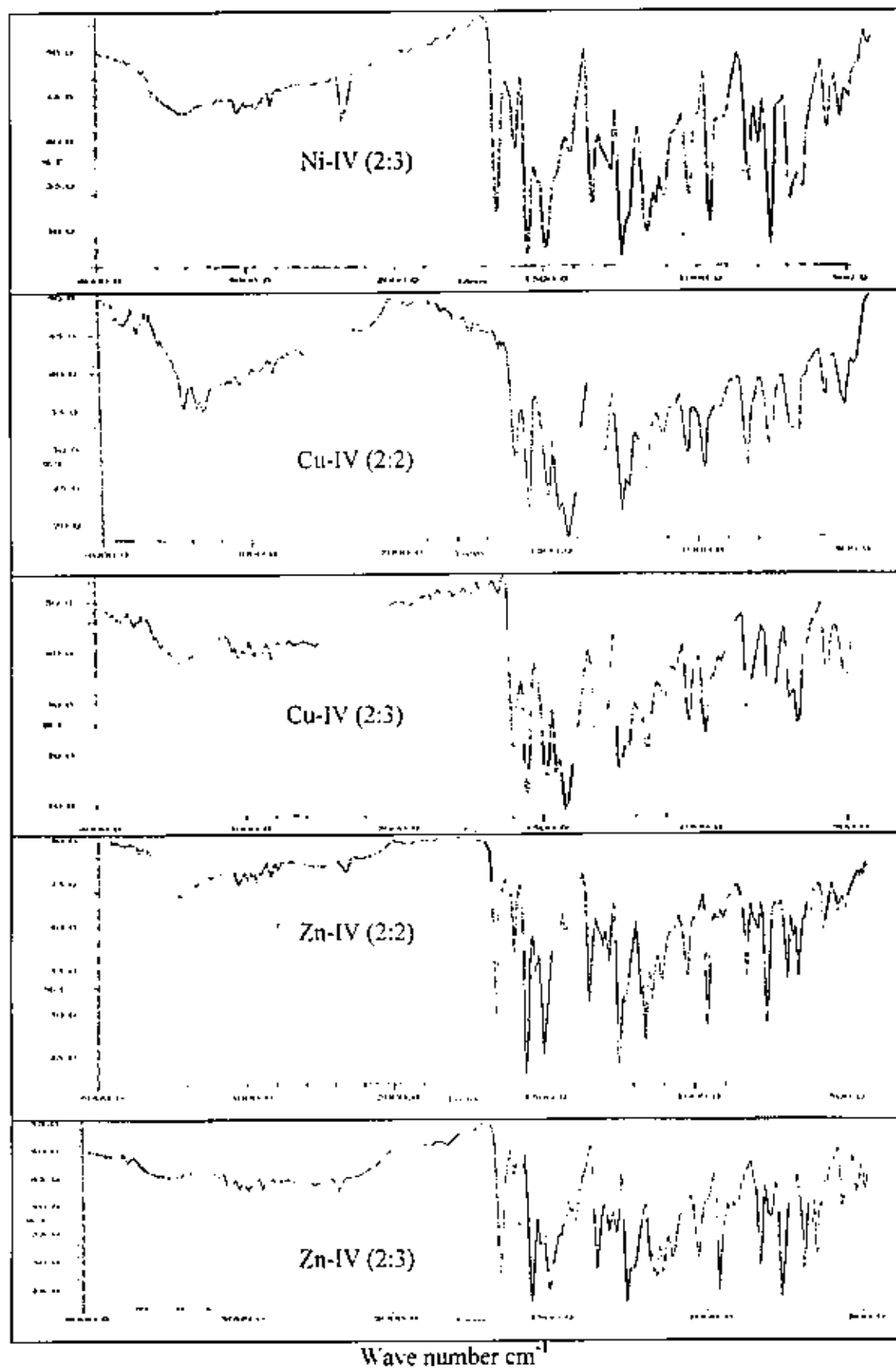


Figure (26): Infrared spectra of the complexes of ligand IV with the metal ions Ni^{2+} , Cu^{2+} and Zn^{2+} .

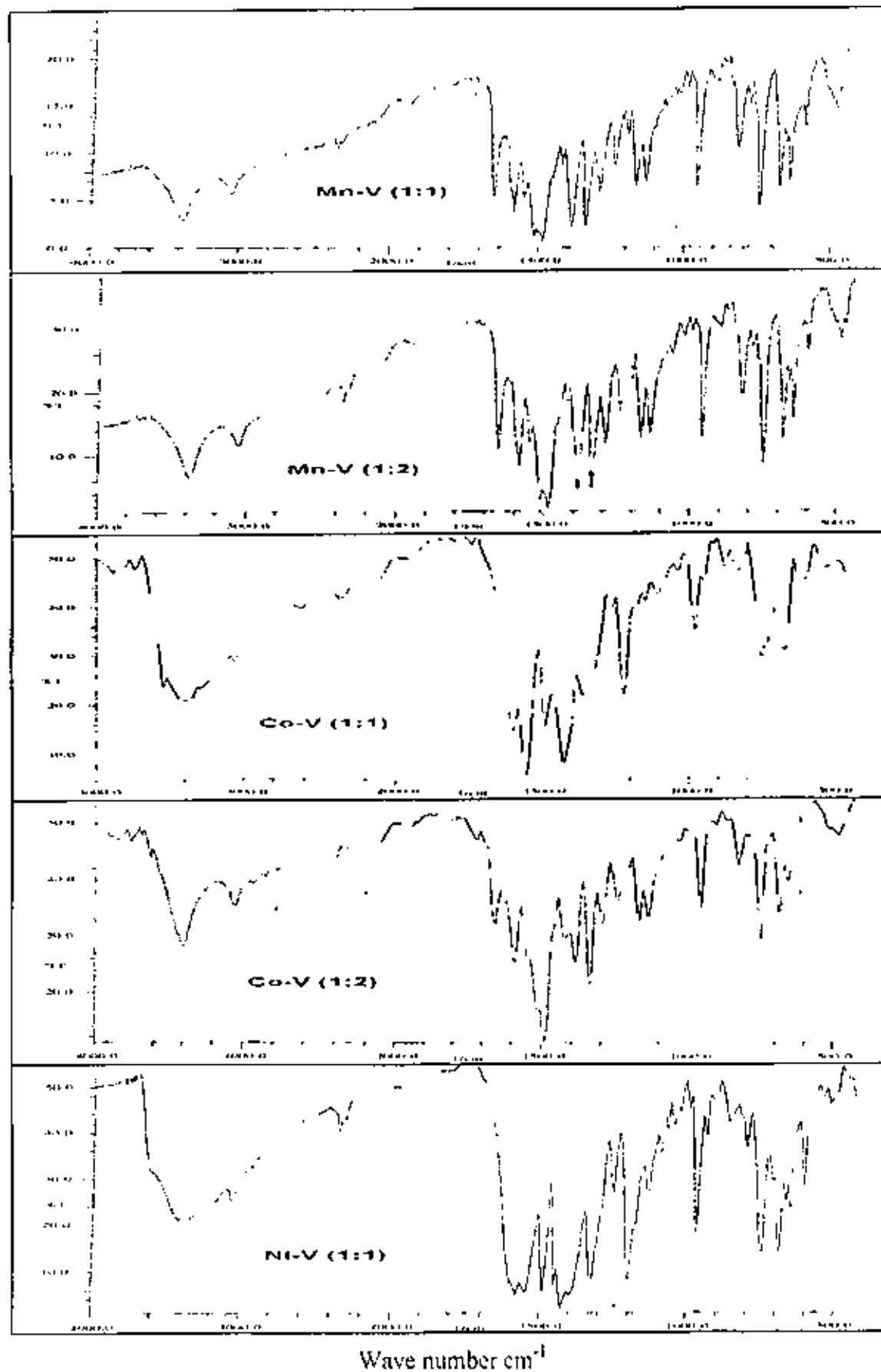


Figure (27): Infrared spectra of the complexes of ligand V with the metal ions Mn²⁺, Co²⁺ and Ni²⁺.

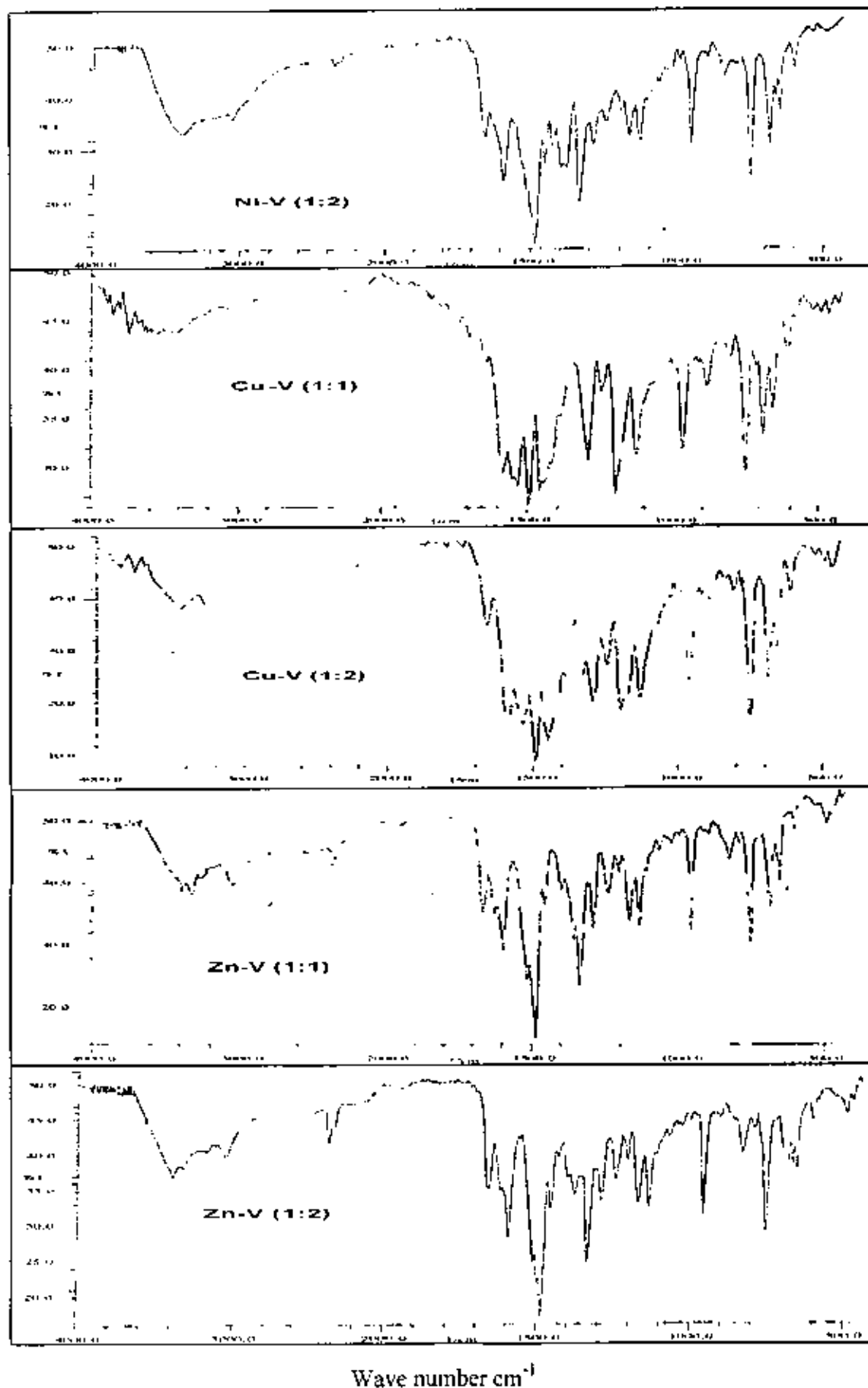


Figure (28): Infrared spectra of the complexes of ligand V with the metal ions Ni^{2+} , Cu^{2+} and Zn^{2+} .

Table (5): The most significant bands in IR spectra of the complexes of ligand I with the metal ions (Mn^{2+} , Co^{2+} , Ni^{2+} , Cu^{2+} and Zn^{2+}).

Complex	Band Assignment						
	ν_{OH}	$\nu_{C=N}$	$\nu_{C=C}$	$\nu_{N=N}$	$\nu_{C=O}$	ν_{M-N}	ν_{M-O}
Mn-I (2:2)	3413	1596	1550	1488	1265	590	489
Mn-I (2:3)	3444	1596	1550	1488	1265	590	489
Co-I (2:2)	3448	1593	1593-1550	1492	1218	520	416
Co-I (2:3)	3494	1554	1554	1492	1218	513	474
Ni-I (2:2)	3425	1658	1596-1550	1488	1265	510	424
Ni-I (2:3)	3363	1658	1600-1581	1488	1211	528	416
Cu-I (2:2)	3355	1654	1558	1488	1222	567	428
Cu-I (2:3)	3440	1654	1593-1558	1488	1218	509	424
Zn-I (2:2)	3386	1666	1596	1485	1242	532	424

Table (6): The most significant bands in IR spectra of the complexes of ligand II with the metal ions (Mn^{2+} , Co^{2+} , Ni^{2+} , Cu^{2+} and Zn^{2+}).

Complex	Band Assignment						
	ν_{OH}	$\nu_{C=N}$	$\nu_{C=C}$	$\nu_{N=N}$	$\nu_{C=O}$	ν_{M-N}	ν_{M-O}
Mn-II (2:2)	3433	1589	1554	1488	1261	505	420
Mn-II (2:3)	3398	1589	1554	1488	1261	505	443
Co-II (2:2)	3436	1651	1554	1488	1261	509	474
Co-II (2:3)	3436	1589	1554	1488	1261	505	416
Ni-II (2:2)	3340	1581	1488	1454	1215	532	424
Ni-II (2:3)	3348	1581	1488	1454	1211	536	420
Cu-II (2:2)	3344	1647	1593-1566	1458	1222	617	416
Cu-II (2:3)	3363	1647	1593-1566	1458	1222	493	416
Zn-II (2:2)	3433	1651	1589	1454	1261	478	410
Zn-II (2:3)	3417	1651	1589	1454	1261	505	482

Table (7): The most significant bands in IR spectra of the complexes of ligand III with the metals (Mn^{2+} , Co^{2+} , Ni^{2+} , Cu^{2+} and Zn^{2+}).

Complex	Band Assignment						
	ν_{OH}	$\nu_{C=N}$	$\nu_{C=C}$	$\nu_{N=N}$	$\nu_{C=O}$	ν_{M-N}	ν_{M-O}
Mn-III (2:2)	3421	1593	1554	1488	1269	509	443
Mn-III (2:3)	3375	1593	1554	1488	1272	509	439
Co-III (2:2)	3444	1596	1550	1488	1288	520	416
Co-III (2:3)	3448	1596	1550	1488	1288	520	466
Ni-III (2:2)	3436	1651	1593-1550	1488	1269	516	428
Ni-III (2:3)	3440	1651	1593-1550	1488	1269	513	428
Cu-III (2:2)	3352	1647	1596-1562	1488	1296	559	416
Cu-III (2:3)	3355	1651	1596-1562	1488	1296	509	416
Zn-III (2:2)	3440	1651	1593-1550	1488	1269	543	486
Zn-III (2:3)	3433	1651	1593-1554	1488	1269	547	489

Table (8): The most significant bands in IR spectra of the complexes of ligand IV with the metal ions (Mn^{2+} , Co^{2+} , Ni^{2+} , Cu^{2+} and Zn^{2+}).

Complex	Band Assignment						
	ν_{OH}	$\nu_{C=N}$	$\nu_{C=C}$	$\nu_{N=N}$	$\nu_{C=O}$	ν_{M-N}	ν_{M-O}
Mn-IV (2:2)	3444	1693	1550-1523	1492	1245	520	412
Mn-IV (2:3)	3398	1593	1550-1523	1492	1245	516	412
Co-IV (2:2)	3440	1596	1596-1550	1492	1245	516	420
Co-IV (2:3)	3421	1596	1596-1550	1492	1245	520	424
Ni-IV (2:2)	3425	1654	1589-1550	1492	1245	516	428
Ni-IV (2:3)	3386	1654	1589-1550	1492	1245	516	424
Cu-IV (2:2)	3244	1647	1596-1554	1492	1249	567	470
Cu-IV (2:3)	3440	1647	1554-1488	1454	1249	567	505
Zn-IV (2:2)	3433	1654	1593-1550	1492	1254	567	470
Zn-IV (2:3)	3390	1654	1593-1550	1492	1245	520	493

Table (9): The most significant bands in IR spectra of the complexes of ligand V with the metal ions (Mn^{2+} , Co^{2+} , Ni^{2+} , Cu^{2+} and Zn^{2+}).

Complex	Band Assignment						
	ν_{OH}	$\nu_{C=N}$	$\nu_{C=C}$	$\nu_{N=N}$	ν_{C-O}	ν_{M-N}	ν_{M-O}
Mn-V (1:1)	3379	1585	1485	1427	1296	489	420
Mn-V (1:2)	3375	1585	1485	1427	1296	489	420
Co-V (1:1)	3394	1600	1554	1488	1222	532	451
Co-V (1:2)	3390	1589	1488	1423	1296	482	420
Ni-V (1:1)	3379	1596	1581	1450	1253	520	432
Ni-V (1:2)	3394	1658	1593	1485	1249	520	447
Cu-V (1:1)	3390	1643	1585	1435	1249	524	428
Cu-V (1:2)	3425	1658	1585	1435	1245	520	424
Zn-V (1:1)	3325	1627	1596	1485	1242	470	451
Zn-V (1:2)	3386	1662	1596	1485	1245	489	439

III.2.2. ¹H NMR spectra of the complexes

Figures (29-30) illustrate ¹H NMR spectra of Zn complexes with the investigated ligands (I-V), ¹H NMR spectral data of Zn complexes with the investigated ligands (I-V) are illustrated in tables (10-11).

For the complex [Zn-I (2:2)] the signal observed at 16.6 ppm is assigned to the proton of the chelated OH group. The signals observed within the range (8.19-6.71) ppm are assigned to the protons of the aromatic (-CH) groups. The signal observed at 3.32 ppm is assigned to H₂O protons of the solvent. The signal observed at 2.5 ppm is assigned to the protons of DMSO.

For the complex [Zn-II (2:2)] the signals observed at (8.00-7.48) ppm are assigned to the aromatic (CH) protons. The upfield shift of these signals may be due to complexation. The signal observed at 3.35 ppm is assigned to the H₂O protons of the solvents. The signal observed at 2.51 ppm is assigned to the proton of DMSO.

For the complex [Zn-II (2:3)] the signal observed at 13.6 ppm is assigned to the proton of NH group. The signals observed within the range (8.14-7.27) ppm are assigned to the aromatic (CH) proton. The upfield shift of these signals may be due to complexation. The signal observed at 3.30 ppm is assigned to the H₂O protons of the solvent. The signal observed at 3.50 ppm is assigned to the protons of the DMSO.

For the complex [Zn-III (2:2)] the signal observed at 13.8 ppm is assigned to the proton of NH group. The signals observed within the range (8.18-7.13) ppm are assigned to the aromatic (CH) protons. The downfield shift of these signals may be due to complexation. The signal observed at 3.35 ppm is assigned to the H₂O protons of the solvent. The

signal observed at 2.52 ppm is assigned to the protons of the DMSO. The signal observed at 2.34 ppm is assigned to the protons of the $-\text{CH}_3$ group.

For the complex [Zn-III (2:3)] the signal observed at 13.8 ppm is assigned to the proton of NH group. The signals within the range (8.20-7.28) ppm are assigned to the aromatic (CH) protons; the upfield shift of these signals may be due to the complexation. The signal observed at 3.35 ppm is assigned to the solvent H_2O protons. The signal observed at 2.51 ppm is assigned to the protons of DMSO. The signal observed at 2.33 ppm is assigned to the protons of the $-\text{CH}_3$ group.

For the ligand [Zn-IV (2:2)] the signal observed at 13.1 ppm is assigned to the proton of NH group. The signals observed within the range 8.14-7.01 ppm are assigned to the aromatic (C-H) protons. The upfield shift of these signals may be attributed to complexation. The signals observed at 3.37 ppm is assigned to the protons of the solvent. The signal observed at 2.52 ppm is assigned to the protons of the DMSO. The signal observed at 3.77 ppm is assigned to the protons of the OCH_3 group.

For the complex [Zn-IV (2:3)] the signal observed at 13.8 ppm is assigned to the proton of NH group. The signals observed within the range (8.18-7.03) ppm are assigned to the aromatic (CH) protons. The signal observed at 3.33 ppm is assigned to the protons of the solvent. The signal observed at 2.51 ppm is assigned to the protons of DMSO. The signal observed at 3.79 ppm is assigned to the protons of OCH_3 group.

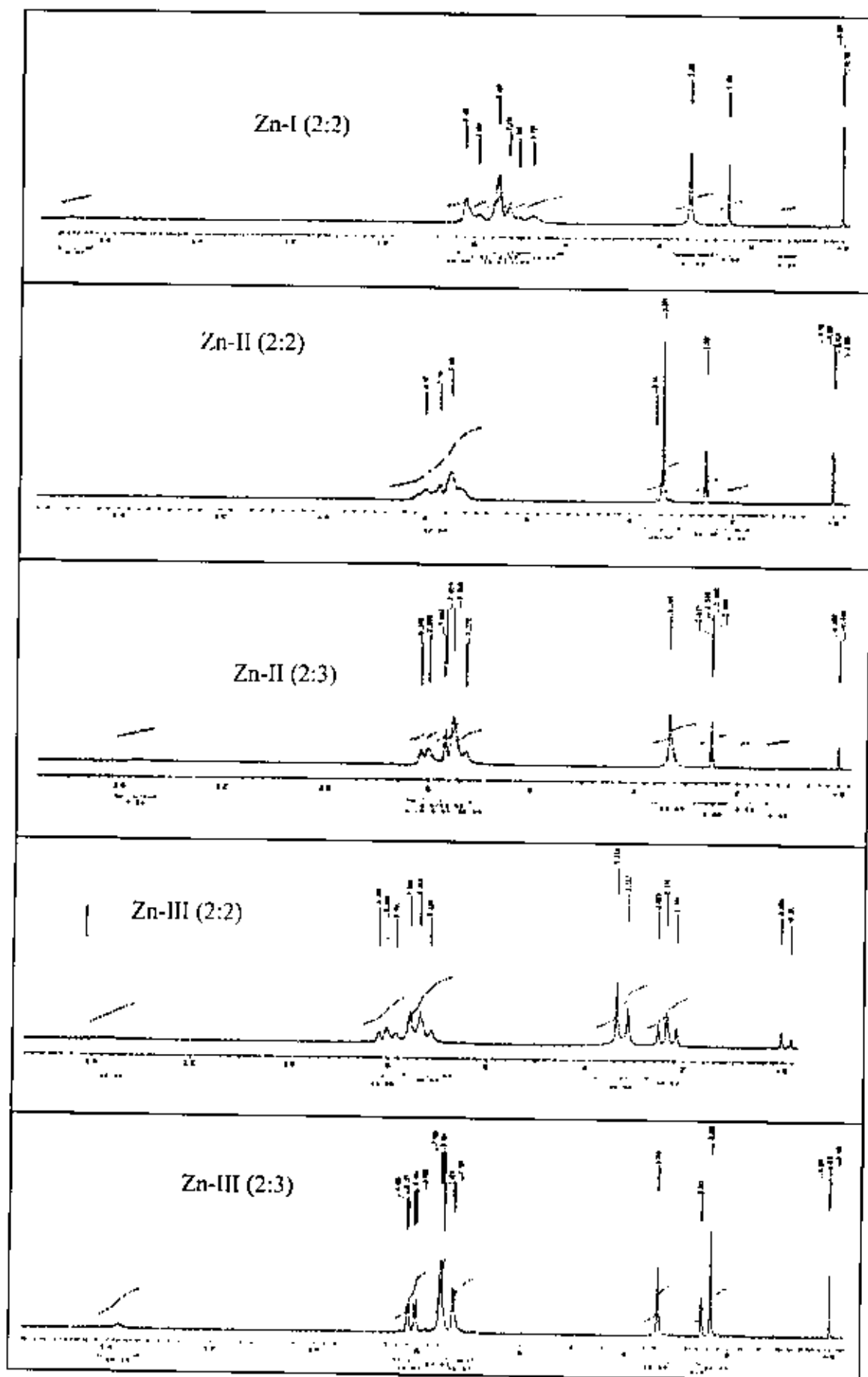


Figure (29): ^1H NMR spectra of the complexes of Zn with ligands I, II and III.

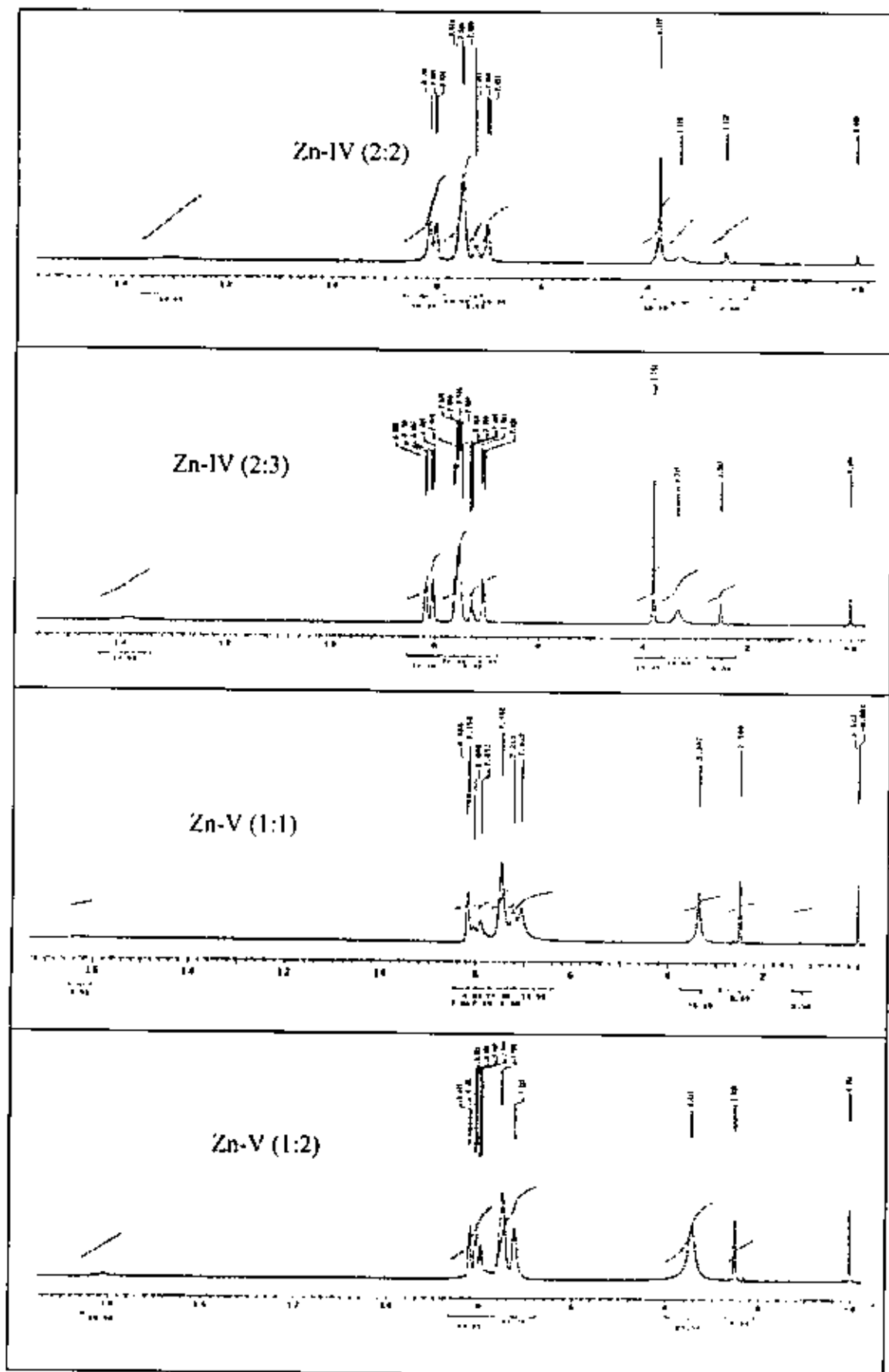


Figure (30): ^1H NMR spectra of the complexes of Zn with ligands IV and V.

Table (10): ^1H NMR spectral data of Zn complexes with the investigated ligands (I-III).

complex M:L	Chemical shift	Assignment
Zn-I (2:2)	16.6	OH bridge
	8.19-6.71	Aromatic C-H protons
	3.32	H ₂ O solvent protons
	2.5	DMSO protons
Zn-II (2:2)	8.00-7.48	Aromatic C-H protons
	3.35	H ₂ O solvents protons
	2.51	DMSO protons
Zn-II (2:3)	13.6	NH hydrazone
	8.14-7.27	Aromatic protons
	3.30	H ₂ O solvent protons
	2.50	DMSO protons
Zn-III (2:2)	13.8	NH hydrazone
	8.18-7.13	Aromatic protons
	3.35	H ₂ O solvent protons
	2.52	DMSO protons
	2.34	CH ₃ protons
Zn-III (2:3)	13.8	NH proton
	8.20-7.28	Aromatic protons
	3.35	H ₂ O protons
	2.51	DMSO protons
	2.33	CH ₃ protons

Table (11): ^1H NMR spectral data of Zn complexes with the investigated ligands (IV and V).

complex M:L	Chemical shift	Assignment
Zn-IV (2:2)	13.1	NH proton
	8.14-7.01	Aromatic protons
	3.77	OCH ₃ protons
	3.37	H ₂ O solvents protons
	2.52	DMSO protons
Zn-IV (2:3)	13.8	NH proton
	8.18-7.03	Aromatic protons
	3.79	OCH ₃ protons
	3.33	H ₂ O solvent protons
	2.51	DMSO protons
Zn-V (1:1)	16.4	OH proton
	8.18-7.05	Aromatic protons
	3.37	H ₂ O solvent protons
	2.50	DMSO protons
Zn-V (1:2)	16.2	NH proton
	8.21-7.23	Aromatic protons
	3.43	H ₂ O solvent protons
	2.51	DMSO protons

For the complex [Zn-V (1:1)] the signal observed at 16.4 ppm is assigned to the chelated (OH) group. The downfield shift of these signals may be due to complexation results from increasing the electron cloud of the metal ion. The signals observed within the range (8.18-7.05) ppm are assigned to the protons of the aromatic (CH) groups. The upfield shift of these signals may be due to complexation. The signal observed at 3.37 ppm is assigned to the H₂O protons of the solvent. The signal observed at 2.50 is assigned to the proton of the DMSO.

For the complex [Zn-V (1:2)] the signal observed at 16.2 ppm is assigned to the proton of the NH group. The downfield shift of this signal may be due to complexation results from increasing the electron cloud of the metal ion. The signals observed within the range 8.21-7.23 ppm are assigned to the protons of the aromatic (CH) groups. The signal observed at 3.43 ppm is assigned to the H₂O protons of the solvent. The signal observed at 2.51 ppm is assigned to the protons of DMSO.

III.2.3. Elemental analysis for the complexes.

Table (12): Elemental analysis, molar conductance (Λ_m) and μ_{eff} for the complexes of the divalent metal ions (Mn^{2+} , Co^{2+} , Ni^{2+} , Cu^{2+} and Zn^{2+}) with ligand I.

Complex	C% (Calcd) found	H% (Calcd) found	N% (Calcd) found	M% (Calcd) found	Λ_m	μ_{eff}
Mn-I (2:2)	(61.17)	(4.12)	(13.59)	(6.66)	6.66	5.13
	61.87	3.89	14.54	6.21		
Mn-I (2:3)	(65.91)	(4.01)	(14.64)	(4.78)	4.78	4.75
	66.03	4.01	15.55	4.23		
Co-I (2:2)	(60.58)	(4.08)	(13.46)	(7.08)	7.08	3.99
	58.78	4.76	14.08	7.12		
Co-I (2:3)	(65.46)	(3.98)	(14.54)	(5.10)	5.10	2.79
	65.99	3.88	16.08	5.08		
Ni-I (2:2)	(60.58)	(4.08)	(13.47)	(7.06)	7.06	3.89
	60.14	4.14	14.08	7.01		
Ni-I (2:3)	(65.48)	(3.98)	(14.55)	(5.03)	5.03	2.67
	66.26	4.20	14.59	5.22		
Cu-I (2:2)	(59.92)	(4.04)	(13.31)	(7.55)	7.55	1.31
	60.93	4.41	13.96	7.63		
Cu-I (2:3)	(64.94)	(3.95)	(14.43)	(5.37)	5.37	1.26
	65.13	4.08	14.53	6.02		
Zn-I (2:2)	(59.66)	(4.02)	(13.2)	(7.73)	7.73	0.91
	58.99	4.47	13.36	7.54		
Zn-I (2:3)	(64.73)	(3.93)	(14.38)	(5.51)	5.51	0.54
	64.76	4.07	14.50	5.59		

Table (13): Elemental analysis, molar conductance (Λ_m) and μ_{eff} for the complexes of the divalent metal ions (Mn^{2+} , Co^{2+} , Ni^{2+} , Cu^{2+} and Zn^{2+}) with ligand II.

Complex	C% (Calcd) found	H% (Calcd) found	N% (Calcd) found	Cl% (calcd) found	M% (Calcd) found	(Λ_m)	μ_{eff}
Mn-II (2:2)	(56.44) 56.35	(3.36) 3.55	(12.55) 12.88	(7.83) 8.41	(6.15) 6.78	49.16	5.80
Mn-II (2:3)	(60.46) 60.99	(3.43) 3.20	(13.43) 15.44	(8.51) 7.83	(4.39) 4.54	13.44	4.06
Co-II (2:2)	(56.00) 56.92	(3.33) 3.38	(12.44) 12.62	(7.77) 8.03	(6.54) 6.69	44.25	3.42
Co-II (2:3)	(60.05) 58.69	(3.41) 3.34	(13.35) 13.18	(8.46) 8.36	(4.68) 5.21	15.22	3.81
Ni-II (2:2)	(56.03) 56.10	(3.29) 3.43	(12.45) 13.05	(7.78) 8.00	(6.52) 7.03	35.18	2.70
Ni-II (2:3)	(60.10) 61.08	(3.41) 3.55	(13.35) 12.91	(8.40) 8.43	(4.66) 4.59	9.11	2.28
Cu-II (2:2)	(55.04) 54.85	(3.52) 3.37	(12.30) 11.91	(7.70) 7.31	(6.98) 7.25	25.13	1.75
Cu-II (2:3)	(59.64) 58.26	(3.39) 3.46	(13.25) 12.85	(8.29) 9.04	(5.00) 5.02	17.25	1.76
Zn-II (2:2)	(55.21) 58.83	(3.28) 3.96	(12.27) 13.48	(7.66) 7.37	(7.16) 7.55	37.35	0.73
Zn-II (2:3)	(59.46) 65.55	(3.38) 3.13	(13.21) 13.67	(8.37) 8.15	(5.14) 4.93	11.50	0.97

Table (14): Elemental analysis, molar conductance (Λ_m) and μ_{eff} for the complexes of the divalent metal ions (Mn^{2+} , Co^{2+} , Ni^{2+} , Cu^{2+} and Zn^{2+}) with ligand III.

Complex	C% (Calcd) found	H% (Calcd) found	N% (Calcd) found	M% (Calcd) found	(Λ_m)	μ_{eff}
Mn-III (2:2)	(61.98) 60.16	(4.46) 4.45	(13.14) 13.23	(6.44) 6.35	32.77	5.06
Mn-III (2:3)	(69.23) 68.93	(4.54) 4.45	(14.68) 14.55	(4.80) 4.66	13.62	5.93
Co-III (2:2)	(61.40) 60.59	(4.41) 4.47	(13.02) 13.63	(6.85) 7.11	13.18	2.98
Co-III (2:3)	(66.17) 66.78	(4.34) 4.98	(12.95) 12.20	(4.58) 5.06	7.70	2.90
Ni-III (2:2)	(63.66) 64.21	(4.58) 5.04	(13.50) 13.79	(7.07) 7.33	13.14	3.40
Ni-III (2:3)	(66.19) 67.30	(4.34) 4.44	(14.04) 14.53	(4.90) 4.65	6.67	2.91
Cu-III (2:2)	(60.75) 60.84	(4.37) 4.50	(12.88) 12.50	(7.30) 7.94	14.06	1.55
Cu-III (2:3)	(65.19) 65.19	(4.31) 4.15	(13.93) 13.23	(5.26) 5.54	8.25	1.29
Zn-III (2:2)	(60.49) 59.27	(4.35) 3.96	(12.83) 12.35	(7.49) 6.99	14.42	0.59
Zn-III (2:3)	(65.46) 66.64	(4.29) 4.38	(13.88) 13.74	(5.40) 5.51	8.47	0.57

Table (15): Elemental analysis, molar conductance (Λ_m) and μ_{eff} for the complexes of the divalent metal ions (Mn^{2+} , Co^{2+} , Ni^{2+} , Cu^{2+} and Zn^{2+}) with ligand IV.

Complex	C% (Calcd) found	H% (Calcd) found	N% (Calcd) found	M% (Calcd) Found	(Λ_m)	μ_{eff}
Mn-IV (2:2)	(59.73) 58.44	(4.29) 4.36	(12.67) 12.69	(6.21) 6.52	38.15	5.91
Mn-IV (2:3)	(64.03) 64.02	(4.20) 4.28	(13.58) 13.35	(4.44) 4.33	10.40	5.07
Co-IV (2:2)	(59.20) 58.57	(4.26) 4.41	(12.55) 11.62	(6.60) 6.45	32.20	3.62
Co-IV (2:3)	(63.62) 64.49	(4.17) 4.98	(13.39) 13.45	(4.73) 4.79	9.30	2.55
Ni-IV (2:2)	(59.23) 59.65	(4.26) 4.14	(12.56) 12.38	(6.58) 6.83	35.70	2.88
Ni-IV (2:3)	(64.64) 65.63	(4.17) 4.28	(13.50) 13.98	(4.71) 4.23	7.58	3.29
Cu-IV (2:2)	(58.02) 57.79	(4.17) 4.25	(12.30) 12.96	(6.97) 6.58	29.13	1.59
Cu-IV (2:3)	(63.15) 63.59	(4.14) 4.60	(13.39) 13.72	(5.09) 5.05	7.16	1.31
Zn-IV (2:2)	(58.35) 59.82	(4.20) 4.99	(12.37) 12.81	(7.91) 7.34	9.17	0.005
Zn-IV (2:3)	(62.96) 63.62	(4.13) 4.57	(13.35) 13.82	(5.19) 4.91	8.59	0.79

Table (16): Elemental analysis, molar conductance (Λ_m) and μ_{eff} for the complexes of the divalent metal ions (Mn^{2+} , Co^{2+} , Ni^{2+} , Cu^{2+} and Zn^{2+}) with ligand V.

Complex	C% (Calcd) found	H% (Calcd) found	N% (Calcd) found	M% (Calcd) Found	(Λ_m)	μ_{eff}
Mn-V (1:1)	(55.39) 56.29	(3.73) 3.84	(12.30) 12.97	(12.07) 11.79	38.17	6.17
Mn-V (1:2)	(64.31) 63.86	(3.65) 3.99	(13.64) 13.54	(6.69) 6.15	14.24	6.61
Co-V (1:1)	(54.91) 54.74	(3.70) 3.11	(12.20) 12.10	(12.84) 12.16	25.58	4.18
Co-V (1:2)	(64.00) 64.04	(3.63) 3.44	(13.57) 13.32	(7.14) 7.33	8.16	4.35
Ni-V (1:1)	(54.93) 54.99	(4.14) 4.61	(12.20) 12.10	(12.70) 12.52	45.78	2.31
Ni-V (1:2)	(64.02) 63.86	(3.63) 4.21	(13.58) 13.91	(7.11) 6.81	12.44	2.07
Cu-V (1:1)	(54.36) 54.22	(3.88) 3.37	(12.08) 12.63	(13.70) 13.31	29.92	1.30
Cu-V (1:2)	(63.65) 63.51	(3.61) 3.66	(13.50) 13.70	(7.65) 7.89	7.35	1.24
Zn-V (1:1)	(54.14) 55.04	(3.65) 3.78	(12.03) 12.41	(14.04) 14.89	24.15	0.75
Zn-V (1:2)	(63.50) 62.26	(3.60) 4.00	(13.47) 13.48	(7.86) 7.93	10.24	0.59

III.2.4. Thermogravimetric analysis (TG).

These methods of analysis open up new possibilities for the investigation of metal complexes^[90,91]. The aim of this study is to obtain information concerning the thermal stability of the divalent transition metal-azopyrazolone complexes, establish whether the water molecules are inner or outersphere if present and suggest a general scheme for the thermal decomposition of these complexes. The thermogram follows the decrease in sample weight with the linear increase in temperatures.

In the present investigation, heating rates were suitably controlled at $10^{\circ}\text{C min}^{-1}$ and the weight loss followed up to 800°C . From TG curves obtained, figures (31-40), the weight loss for each complex were calculated within the temperature range at which the loss occurs. The found and calculated (based on the suggested stoichiometry) mass losses are collected in table (17).

Inspection of the TG curves for complexes, the initial weight loss occurring at temperature range ($126\text{-}223^{\circ}\text{C}$).

The TG curves show the decomposition of the organic moiety of the chelates and this continues till a constant weight is obtained where the metal oxide (MO) residues are formed as the final product for complexes.

TG analysis of the complexes of the divalent metal ions (Mn^{2+} , Co^{2+} , Ni^{2+} , Cu^{2+} and Zn^{2+}) with the investigated ligands (I-IV) 2:2 and 2:3, 1:1 and 1:2 for ligand V are performed and are shown in table (17). The weight loss being measured from ambient temperature up to 800°C at rate of $10^{\circ}\text{C min}^{-1}$. The weight loss for each chelate obtained from the thermographs was used to calculate the decomposed ion of the organic material present, since no hygroscopic water was observed up to the $120\text{-}223^{\circ}\text{C}$ range.

For the [Mn-I (2:2)] chelate, four phenyl molecules, eight nitrogen atoms and hydroxyl group are expelled within the temperature range 150-378°C corresponding to a loss of 53.51% (caltd. 53.04%). In the temperature range 378-459 a weight loss of 30.23% (caltd. 29.73%) is observed corresponding to the loss of two phenyl, six carbon atoms, two hydrogen atoms and one OH group. At the end of the thermogram, the metal contents were calculated from the residual weight of 6.78% (caltd. 8.60%) which is in good agreement with the calculated values obtained by determination of the metal content after decomposition of the chelate applying the method described by McDonald^[69] and with the results of elemental analysis table (12).

For the [Mn-I (2:3)] chelate, three phenyl molecules, four nitrogen atoms, and two carbon atoms are expelled within the temperature range 223-319°C corresponding to a loss of 27.26% (caltd. 27.11%). In the temperature range 319-557°C a weight loss of 62.22% (caltd. 61.64%) is observed corresponding to the loss of six phenyl, eight nitrogen, seven carbon, hydroxyl group, two oxygen atoms. At the end of the thermogram the metal contents were calculated from the residual weight of 11.04% (caltd. 12.36%) which is in good agreement with the calculated values obtained by determination of the metal content after decomposition of the chelate applying the method described by McDonald^[69] and with the result of elemental analysis table (12).

For the [Ni-II (2:2)] chelate, four nitrogen atoms are expelled within the temperature range 126-242°C corresponding to a loss of 5.92% (caltd. 6.21%). In the temperature range 242-365°C a weight loss of 21.91% (caltd. 22.43%) is observed corresponding to the loss of two phenyl, four carbon atoms and two hydrogen atoms. In the temperature range 365-553°C a weight loss of 56.70% (caltd. 54.75%) is observed

corresponding to the loss of four nitrogen atoms, four phenyl molecules, two chloro atoms, two carbon atoms and two hydroxyl groups. At the end of the thermogram the metal contents were calculated from residual weight of 15.85% (caltd. 16.61%) which is in good agreement with the calculated values obtained by determination of the metal content after decomposition of the chelate applying the method described by McDonald and with the result of elemental analysis table (13).

For the [Ni-II (2:3)] chelate, three carbon atoms are expelled within the temperature range 165-357°C corresponding to a loss of 2.61% (caltd. 2.86%). In the temperature range 357-465°C a weight loss of 17.74% (caltd. 17.13%) is observed corresponding to the loss of two phenyl molecules, two nitrogen atoms and one chloro atom. In the temperature range 465-642°C a weight loss of 50.15% (caltd. 50.95%) is observed corresponding to the six phenyl, two chloro, two carbon atoms and six nitrogen. At the end of the thermogram the metal contents were calculated from the residual weight of 12.44% (caltd. 11.64%) which is in good agreement with the calculated values obtained by determination of the metal content after decomposition of the chelate applying the method described by McDonald^[69] and with the result of elemental analysis table (13).

For the [Co-III (2:2)] chelate, two methyl group, two phenyl and four nitrogen atoms are expelled within the temperature range 200-362°C corresponding to a loss of 26.40% (caltd. 27.67%). In the temperature range 362-435°C a weight loss of 15.60% (caltd. 14.65%) is observed corresponding to the loss of two hydroxyl group, four nitrogen atoms and three carbon atoms. In the temperature range 435-519°C a weight loss of 39.25% (caltd. 40.00%) is observed corresponding to the loss of four phenyl, and three carbon atoms. At the end of the thermogram the metal

contents were calculated from the residual weight of 16.87% (caltd. 17.42%) which is in good agreement with the calculated values obtained by determination of the metal content after decomposition of the chelate applying the method described by McDonald^[69] and with the result of elemental analysis table (14).

For the [Co-III (2:3)] chelate, three methyl group, four phenyl and four nitrogen atoms are expelled within the temperature range 200-357°C corresponding to a loss of 34.82% (caltd. 34.17%). In the temperature range 357-508°C a weight loss of 59.21% (caltd. 58.56%) is observed corresponding to the loss of seven phenyl, four nitrogen and nine carbon atoms. At the end of the thermogram the metal contents were calculated from the residual weight of 5.83% (caltd. 6.26%) which is in good agreement with the calculated values obtained by determination of the metal content after decomposition of the chelate applying the method described by McDonald^[69] and with the result of elemental analysis table (14).

For the [Cu-IV (2:2)] chelate, two phenyl, two methoxy, four nitrogen, two carbon atoms and two hydroxyl groups are expelled within the temperature range 135-393°C corresponding to a loss of 36.22% (caltd. 36.62%). In the temperature range 393-464°C a weight loss of 14.93% (caltd. 14.65%) is observed corresponding to the loss of one phenyl and four nitrogen atoms. In the temperature range 464-557°C a weight loss of 29.44% (caltd. 29.52%) is observed corresponding to the loss of three phenyl, and three carbon atoms. At the end of the thermogram the metal contents were calculated from the residual weight of 17.55% (calcd. 17.64%) which is in good agreement with the calculated values obtained by determination of the metal content after

decomposition of the chelate applying the method described by McDonald^[69] and with the result of elemental analysis (15).

For the [Cu-IV (2:3)] chelate, two methoxy groups are expelled within the temperature range 137-230°C corresponding to a loss of 4.87% (caltd. 4.94%). In the temperature range 230-340°C a weight loss of 18.11% (caltd. 17.94%) is observed corresponding to the loss of two phenyl, four nitrogen atoms and one hydroxyl group. In the temperature range 340-483°C a weight loss of 66.31% (caltd. 64.19%) is observed corresponding to the loss of seven phenyl groups, eight nitrogen, nine carbon atoms, one oxygen and one methoxy group. At the end of the thermogram the metal contents were calculated from the residual weight of 10.62% (caltd. 12.67%) which is in good agreement with the calculated values obtained by determination of the metal content after decomposition of the chelate applying the method described by McDonald^[69] and with the result of elemental analysis table (15).

For the [Zn-V (1:1)] chelate, one phenyl group, two nitrogen atoms and one hydrogen atom are expelled within the temperature range 196-342°C corresponding to a loss of 23.87% (caltd. 22.58%). In the temperature range 342-457°C a weight loss of 28.63% (caltd. 28.79%) is observed corresponding to the loss of one phenyl, one carbon atom and one carboxylic group. In the temperature range 457-715°C a weight loss of 34.91% (caltd. 34.59%) is observed corresponding to the loss of one phenyl group, two nitrogen atoms, two carbon atoms and two oxygen atoms. At the end of the thermogram the metal contents were calculated from the residual weight of 17.56% (caltd. 17.48%) which is in good agreement with the calculated values obtained by determination of the metal content after decomposition of the chelate applying the method

described by McDonald^[69] and with the result of elemental analysis table (16).

For the [Zn-V (1:2)] chelate, two carbon atoms are expelled within the temperature range 192-261°C corresponding to a loss of 2.75% (calcd. 2.88%). In the temperature range 261-357°C a weight loss of 24.88% (calcd. 23.33%) is observed corresponding to the loss of two phenyl groups, two nitrogen atoms, one carbon atom and one hydrogen atom. In the temperature range 357-457°C a weight loss of 30.65% (calcd. 31.15%) is observed corresponding to the loss of three phenyl, and two nitrogen atoms. In the temperature range 457-642°C a weight loss of 29.86% (calcd. 29.58%) is observed corresponding to the loss of one phenyl, four nitrogen atoms, two carbon atoms and two carboxyl group. At the end of the thermogram the metal content were calculated from the residual weight of 9.7% (calcd. 9.78%) which is in good agreement with the calculated values obtained by determination of the metal content after decomposition of the chelate applying the method described by McDonald^[69] and with the result of elemental analysis table (16).

III.2.5. Differential thermal analysis (DTA).

The differential thermal analysis curves (DTA) are characterized by the presence of a large and sharp exothermic peak on the DTA curves at the temperature range (426-549), figures (31-40). For [Mn-I (2:2)] and [Mn-I (2:3)] are 437 and 438. For [Ni-II (2:2)] and [Ni-II (2:3)] are 461 and 526. For [Co-III (2:2)] and [Co-III (2:3)] are 500 and 426. For [Cu-IV (2:2)] and [Cu-IV (2:3)] are 476 and 443. For [Zn-V (1:1)] and [Zn-V (1:2)] are 549 and 542, respectively. At these temperatures the chelates are no longer stable and a phase change is liable to occur due to the change in crystal structure of the complexes. i.e. crystallographic phase transition. Rising the temperature than these temperatures results in the decomposition and combustion begins leaving a final residue of the metal oxide.

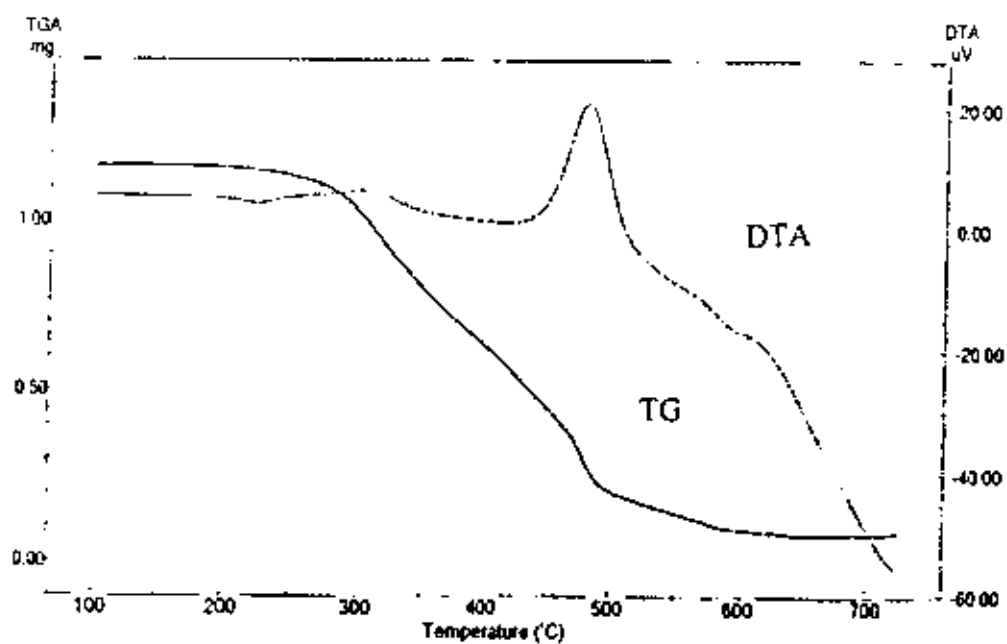


Figure (31): TG of the complex [Mn-I (2:2)]

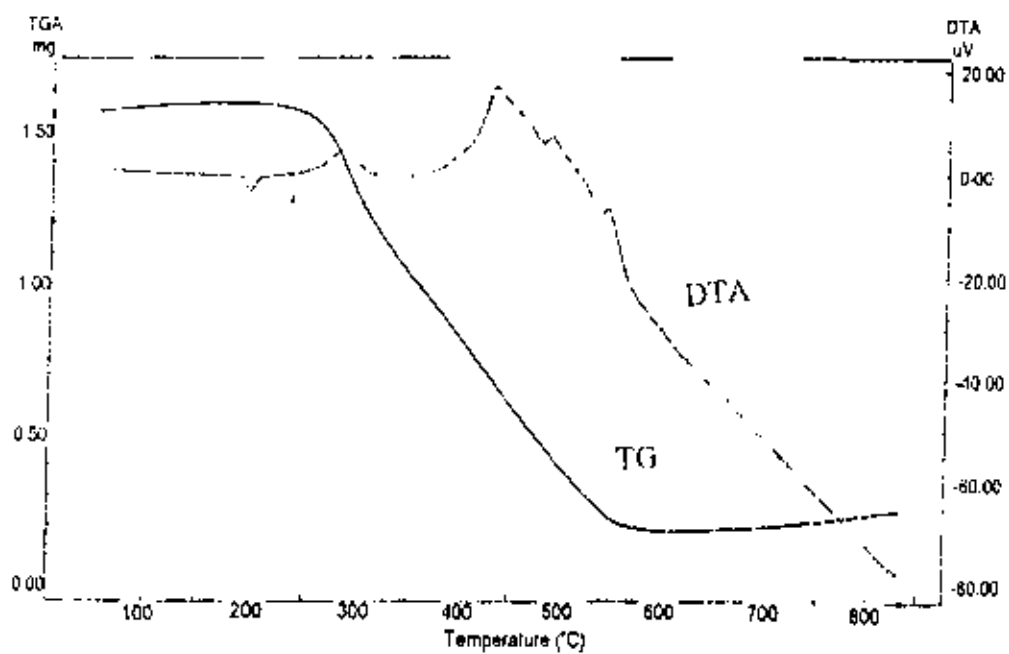


Figure (32): TG of the complex [Mn-I (2:3)].

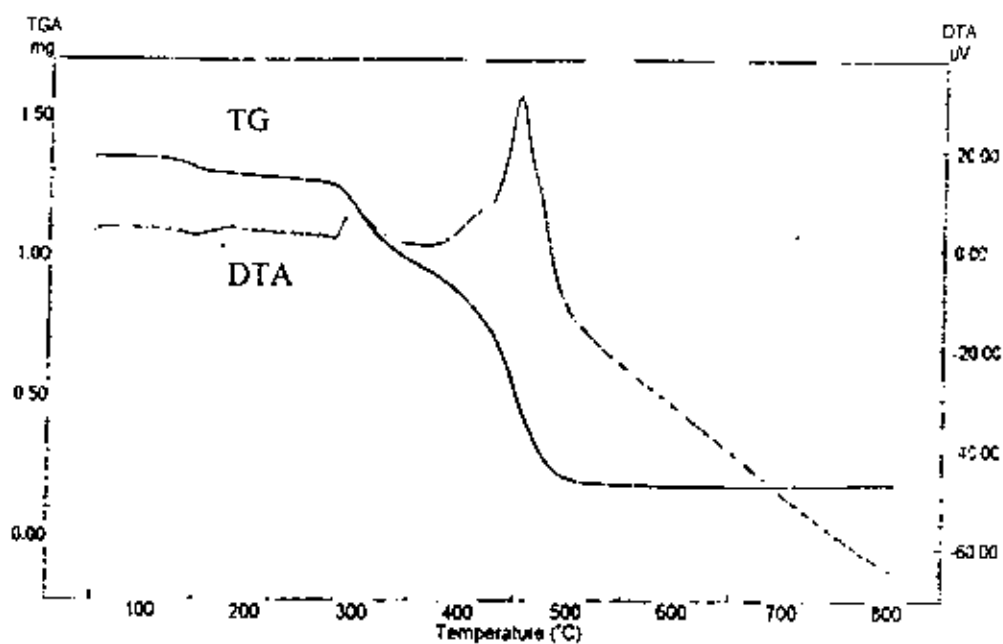


Figure (33): TG of the complex [Ni-II (2:2)].

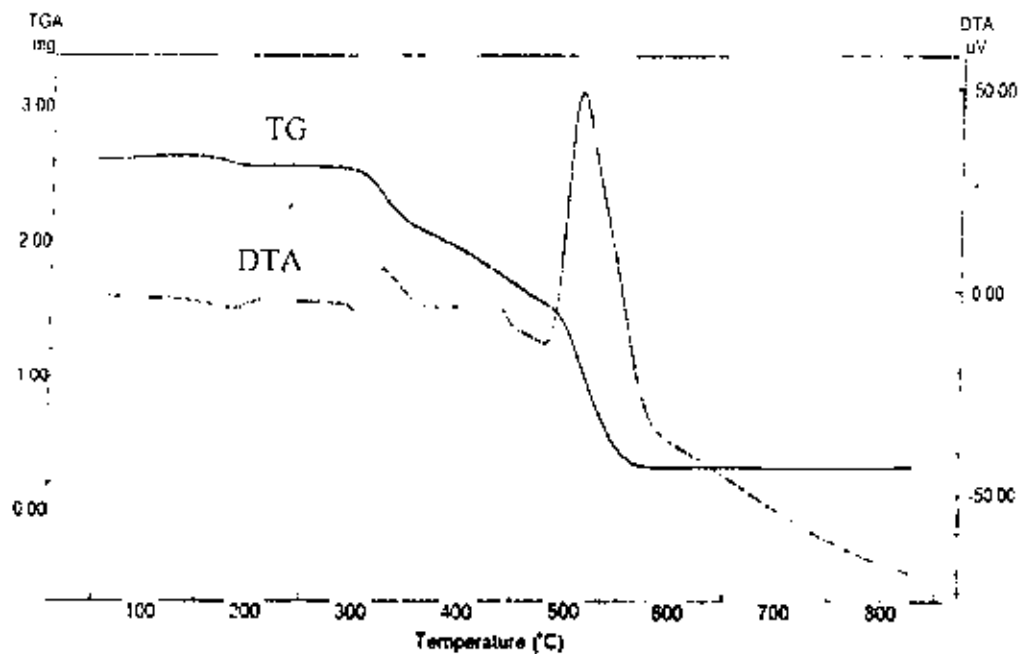


Figure (34): TG of the complex [Ni-II (2:3)].

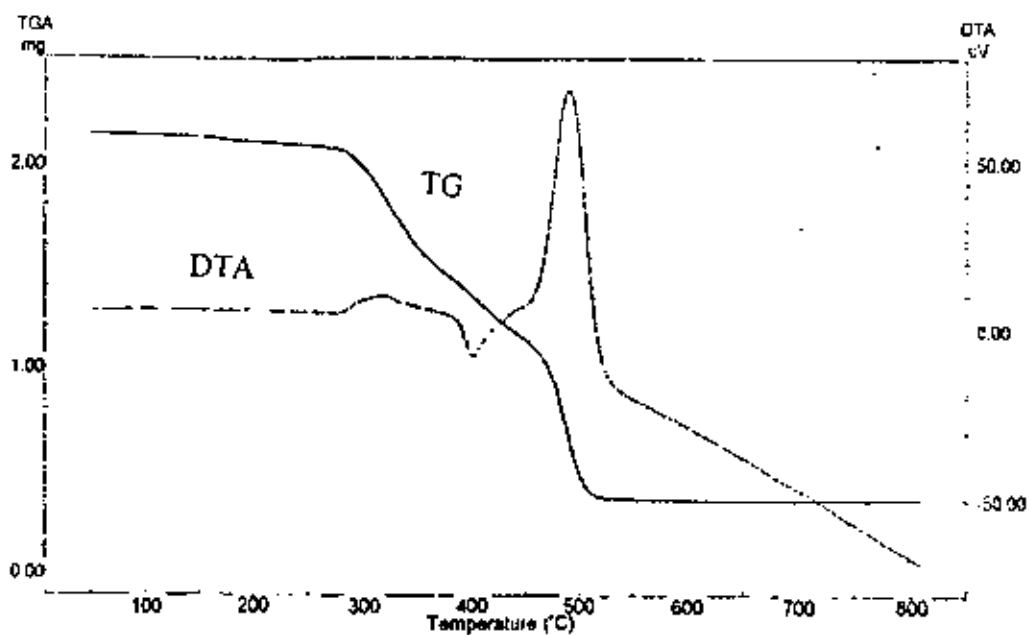


Figure (35): TG of the complex [Co-III (2:2)].

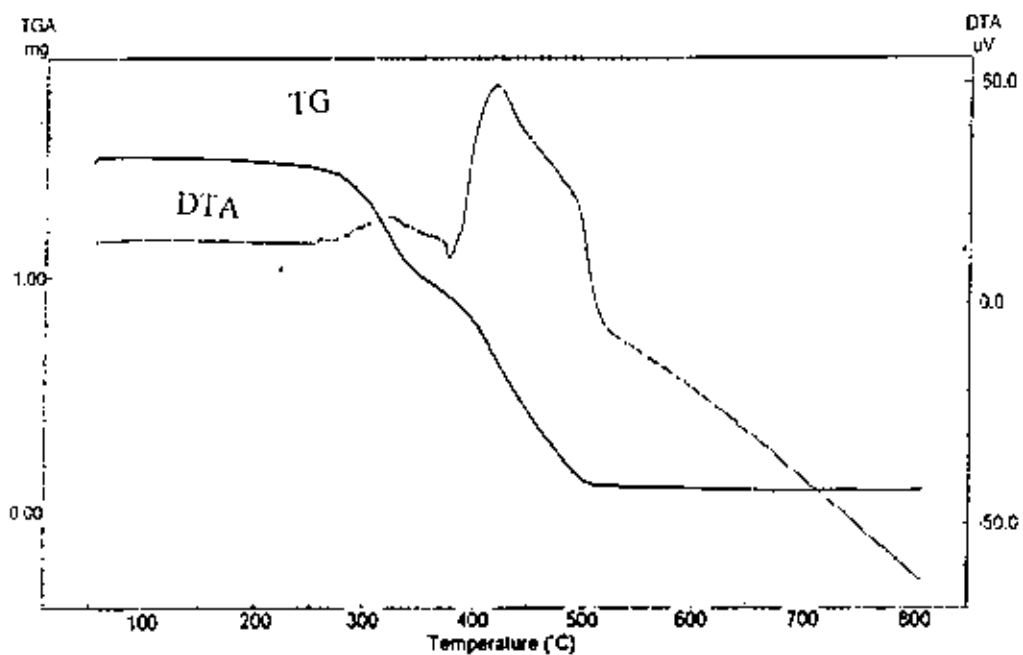


Figure (36): TG of the complex [Co-III (2:3)].

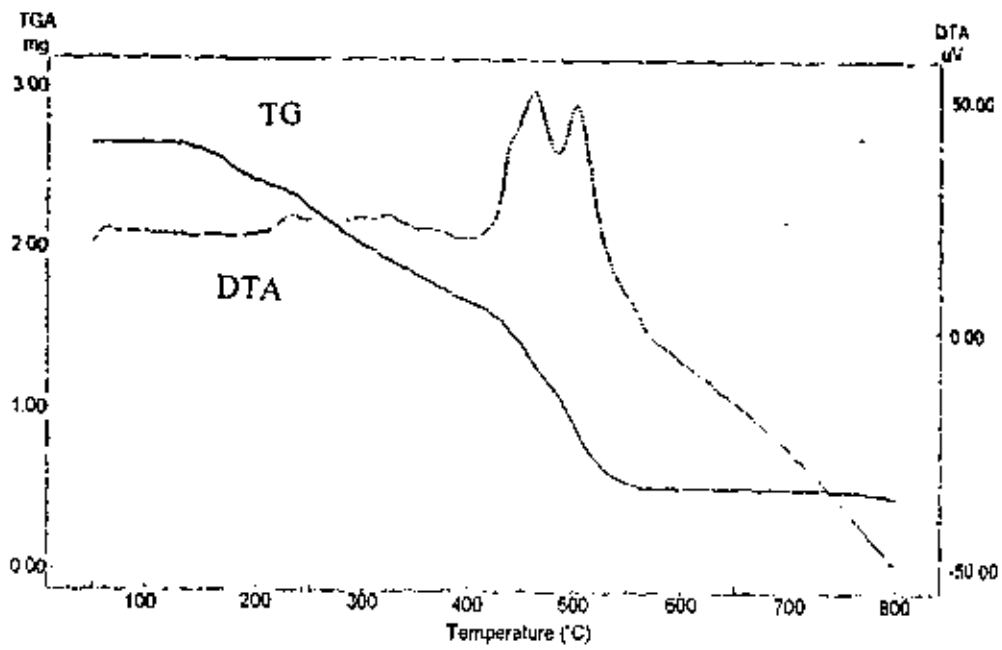


Figure (37): TG of the complex [Cu-IV (2:2)].

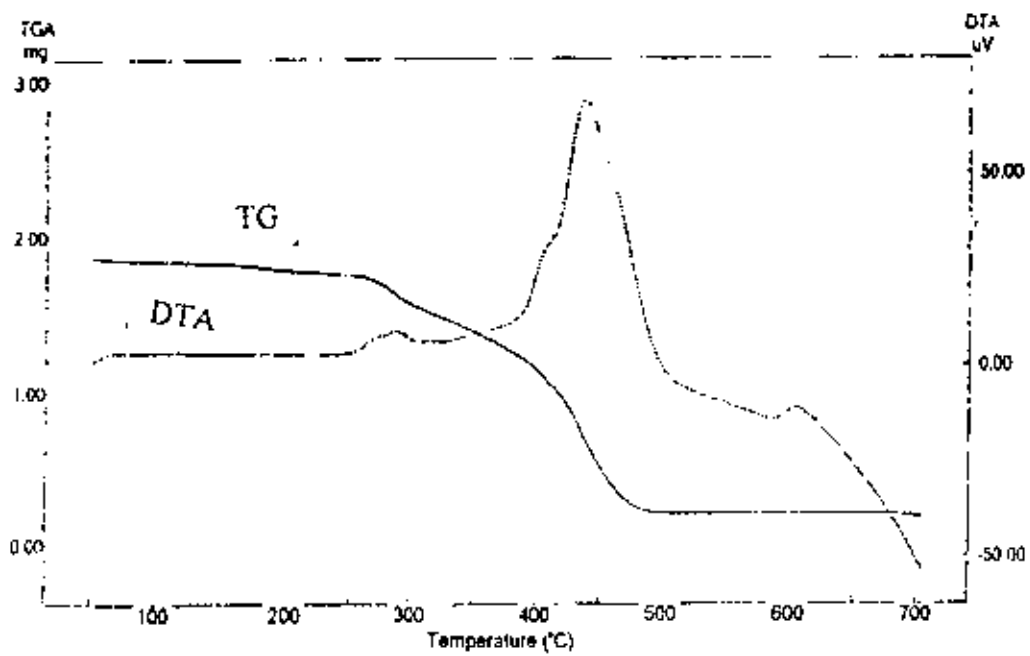


Figure (38): TG of the complex [Cu-IV (2:3)].

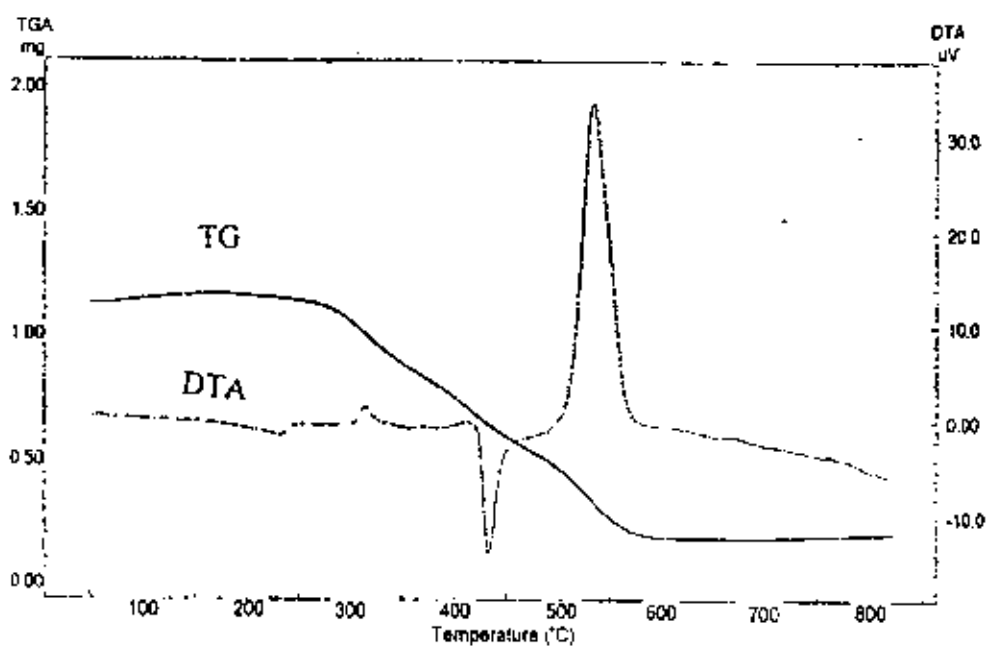


Figure (39): TG of the complex [Zn-V (1:1)].

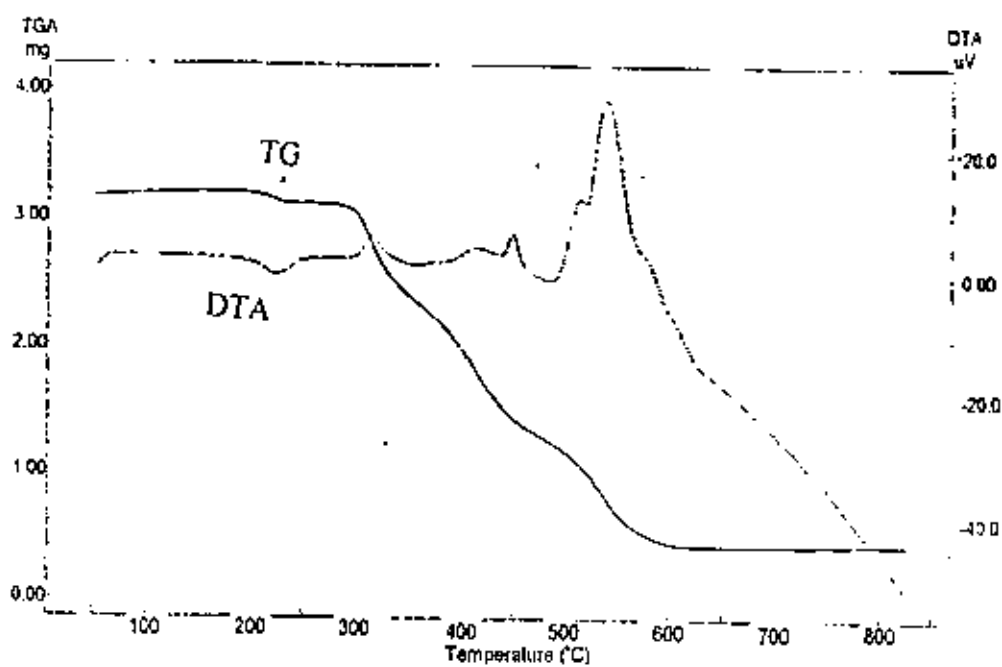


Figure (40): TG of the complex [Zn-V (1:2)].

Table (17): Molecular weight, temperatures of decomposition, loss percent and the corresponding groups in thermogravimetry (TG).

Complex (ligand-metal)	M.wt	Temp (°C)	Calcd loss%	Found loss%	Assignment
Mn-I (2:2)	823.86	150-378 378-459 459-800	53.04 29.73 8.60	53.51 30.23 6.78	4C ₆ H ₅ , 8N, OH 2C ₆ H ₄ , 6C, 2 H, OH MnO
Mn-I (2:3)	1146.86	223-319 319-557 557-800	27.11 61.64 12.36	27.26 62.66 11.04	3C ₆ H ₅ , 4N, 2C 6C ₆ H ₅ , 8N, 7C, OH, 2O 2MnO
Ni-II (2:2)	900.4	126-242 242-365 365-553 553-800	6.21 22.43 54.75 16.61	5.92 21.91 56.70 15.85	4N 2C ₆ H ₄ , 4C, 2 H 4C ₆ H ₅ , 2Cl, 2OH, 4N, 2C, OH 2NiO
Ni-II (2:3)	1257.9	165-357 357-465 465-642 642-800	2.86 17.13 50.95 11.64	2.61 17.74 50.15 12.44	3C 2C ₆ H ₄ , 2N, Cl 6C ₆ H ₅ , 2Cl, 2C, 6N 2NiO
Co-III (2:2)	859.86	200-362 362-435 435-519 519-800	27.67 14.65 40.00 17.42	26.4 15.6 39.25 16.87	2CH ₃ , 2C ₆ H ₄ , 4N 2OH, 4N, 3C 4C ₆ H ₅ , 3C 2CoO
Co-III (2:3)	1196.86	200-357 357-508 508-800	34.17 58.56 6.26	34.51 59.23 5.83	3CH ₃ , 4C ₆ H ₄ , 4N 5C ₆ H ₅ , 2C ₆ H ₄ , 4N, 9C CoO
Cu-IV (2:2)	901	135-393 393-464 464-557 557-800	36.62 14.65 29.52 17.64	36.22 14.93 29.44 17.55	2OH, 4N, 2C ₆ H ₅ , 2OCH ₃ , 2C C ₆ H ₄ , 4N 2C ₆ H ₅ , C ₆ H ₄ , 3C 2CuO
Cu-IV (2:3)	1254	137-230 230-340 340-483 483-800	4.94 17.94 64.19 12.67	4.87 18.11 66.31 10.62	2OCH ₃ 2C ₆ H ₄ , 4N, OH 6C ₆ H ₅ , C ₆ H ₄ , 8N, 9C, OCH ₃ , O 2CuO
Zn-V (1:1)	465.38	196-342 342-457 457-715 715-800	22.56 28.79 34.59 17.48	23.87 28.63 34.91 17.56	C ₆ H ₄ , 2N, H C ₆ H ₅ , COOH, C C ₆ H ₅ , 2C, 2N, 2O ZnO
Zn-V (1:2)	831.38	192-261 261-357 357-457 457-642 642-800	2.88 23.33 31.15 29.58 9.78	2.75 24.88 30.65 29.86 9.70	2C C ₆ H ₅ , 2N, C, H, C ₆ H ₄ 3C ₆ H ₅ , 2N C ₆ H ₄ , 4N, 2COOH, 2C ZnO

III.2.6. Molar conductivity measurements.

The molar conductivities of the solid complexes were measured for the solutions of the complexes of 2:2 and 2:3 for ligands (I-IV), and of 1:1 and 1:2 for ligand V are in the range 7.16-49.26 $\text{ohm}^{-1} \text{cm}^2 \text{mol}^{-1}$. These values were measurably small for the ionic complexes of the divalent metal ions. These low conductivity values may be attributed to the absence of chloride ions rather than ionic association to the metal ions during complex formation. This directly supports the fact that all of the investigated complexes are non-ionic in nature. The conductivity values for all of the investigated complexes are listed in tables (12-16).

III.2.7. Magnetic susceptibility measurements.

The magnetic moment (μ) of a transition metal can give important information about the number of unpaired electrons in the metal ion, and in some special cases help to indicate the structure of the complex. The general equation for the magnetic moments of the first row transition metal ions is given by the relation:

$$\mu_{(S+L)} = \sqrt{4S(S+1) + L(L+1)} \quad (\text{B.M.})$$

where S is the total of the spin quantum numbers and L is the resultant of the orbital angular momentum quantum number of all the electrons in the molecules and $\mu_{(S+L)}$ is the magnetic moment given in the unit of Bohr magnetons. In a large number of complexes of first row transition elements the orbital contributions is quenched by the electric field of the surrounding atoms and one can consider only spin contributions and hence

$$\mu_s = \sqrt{4S(S+1)}$$

or in terms of the number of unpaired electrons, n , where $n = S/2$ we have:

$$\mu_s = \sqrt{n(n+2)} \quad (\text{B.M.})$$

Experimentally determined the values of μ are in some cases higher than those calculated using the spin only approximation. Such is the case of Co^{2+} complexes, in which case orbital contribution can not be neglected.

The calculated magnetic moments of (2:2) and (2:3) (M:L) complexes of the investigated ligands (I-IV) and of (1:1) and (1:2) for ligand (V) with Mn^{2+} metal ion are in the range 4.6-5.91 B.M. indicating the presence of 5 unpaired electrons in d-orbital ($\mu_{\text{eff}} = 5.91$). The decrease in μ_{eff} of the complexes is due to spin-spin coupling of the two metal ions present in the same complex molecule. Tables (12-16)

For Co^{2+} , (2:2) and (2:3) (M:L) complexes with the investigated ligands (I-IV) and (1:1) and (1:2) for ligand (V), the calculated magnetic moments of the complexes are in the range 2.55-3.21 B.M. indicating the presence of three unpaired electrons per metal ion. Tables (12-16)

Ni^{2+} (2:2) and (2:3) (M:L), (1:1) and (1:2) for ligand (V) complexes show μ_{eff} in the range 2.07-3.98 B.M. denoting two unpaired electrons and showing paramagnetic properties for all of the investigated ligands (I-V). Tables (12-16).

For Cu^{2+} complexes (2:2) and (2:3) (M:L) of ligands (I-IV), and (1:1) and (1:2) complexes of ligand V the calculated magnetic moments of the complexes are in the range 1.24-1.76 B.M. indicating the presence of one unpaired electron per metal ion in its d-orbital. Table (12-16).

For Zn^{2+} (2:2) and (2:3) (M:L) of ligands (I-IV), (1:1) and (1:2) of ligand (V) complexes, the calculated magnetic moments are in the range 0.54-0.97 B.M. indicating the absence of unpaired electrons and Zn^{2+} complexes was a diamagnetic properties. Table (12-16).

All of the metal ions (Mn^{2+} , Co^{2+} , Ni^{2+} and Cu^{2+}) complexes show paramagnetism, which means that the ligands have little effects on the metal ions field i.e. the ligands exhibit a weak field effect.

Zn^{2+} complexes show diamagnetic behavior since the d-orbitals are completely filled and Zn^{2+} considered as non-transition metal ion.

III.2.8. Electronic spin resonance (ESR).

The X-band ESR spectra of Cu^{2+} - azopyrazolone complexes at room temperature generally show one or two broad signals depending on the nature of the ligands used and the type of the complexes formed. ESR spectra of Cu^{2+} complexes with the investigated ligands (I, IV and V) are illustrated in figures (41-46).

The g values (g_{\perp} and g_{\parallel}) which reflect the geometry of the Cu^{2+} - environments are given in table (18).

Generally, the complexes are not magnetically dilute, therefore, exchanges^[92] and for dipolar forces are expected to operate in such a case, the g anisotropy is likely to be reduced. The absence of hyperfine is taken as evidence of exchange as is the fact that

$$G = g_{\parallel} - 2/g_{(\perp-2)}$$

is lower than four^[93] which could be attributed to tetrahedral symmetry around the Cu^{2+} ions. Moreover, the apparent broadening of the ESR signals may be due to an interaction between Cu^{2+} ions which are probably present in nonequivalent lattice position, the positive shift of g values from that of the free electron (2.0023) indicates a high covalent character of the bonding between the Cu^{2+} ions and the azopyrazolone ligands^[94].

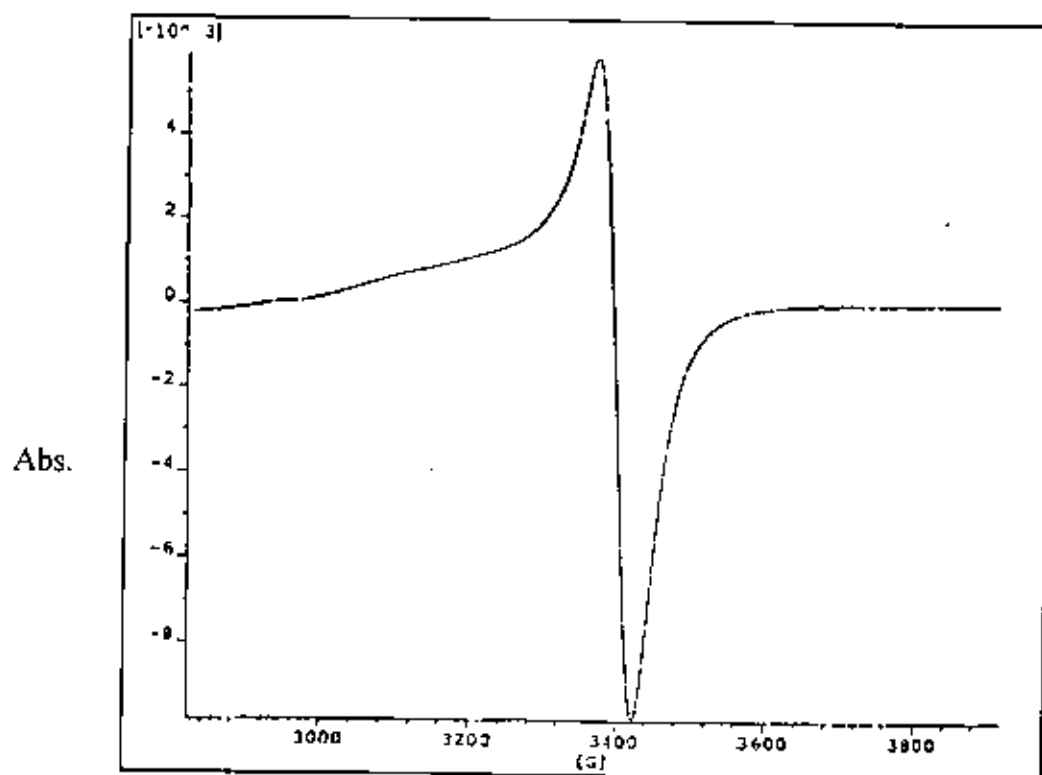


Figure (41): ESR spectrum of the complex [Cu-I (2:2)].

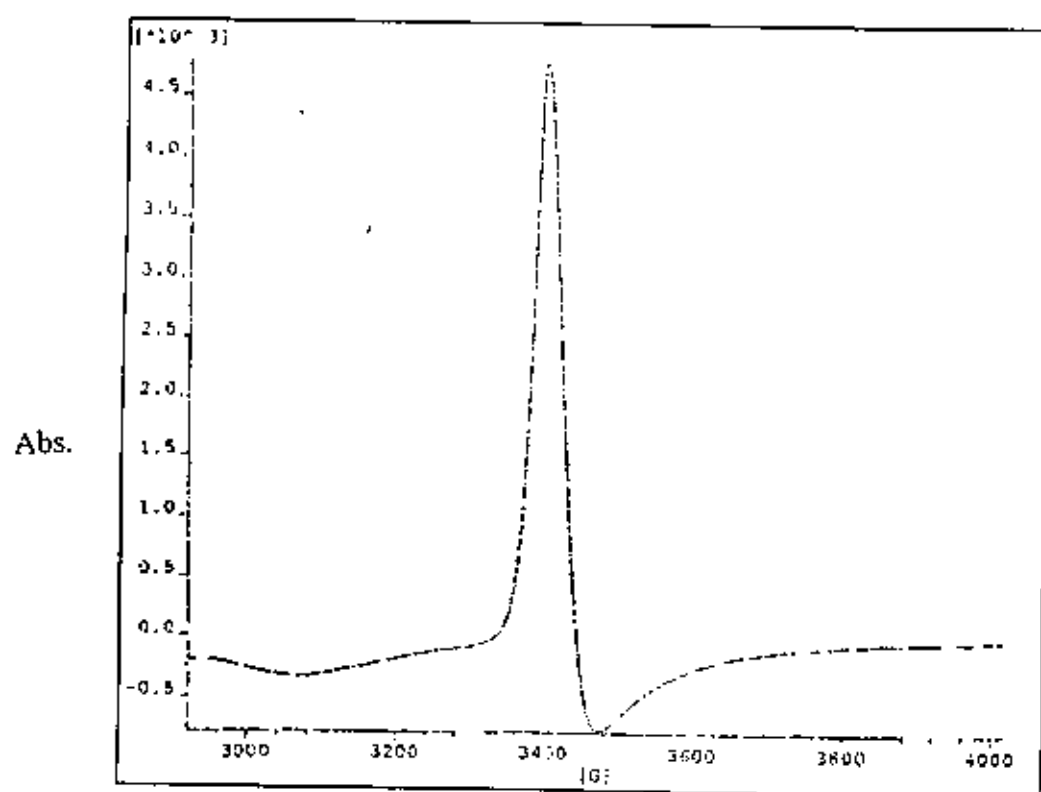


Figure (42): ESR spectrum of the complex [Cu-I (2:3)].

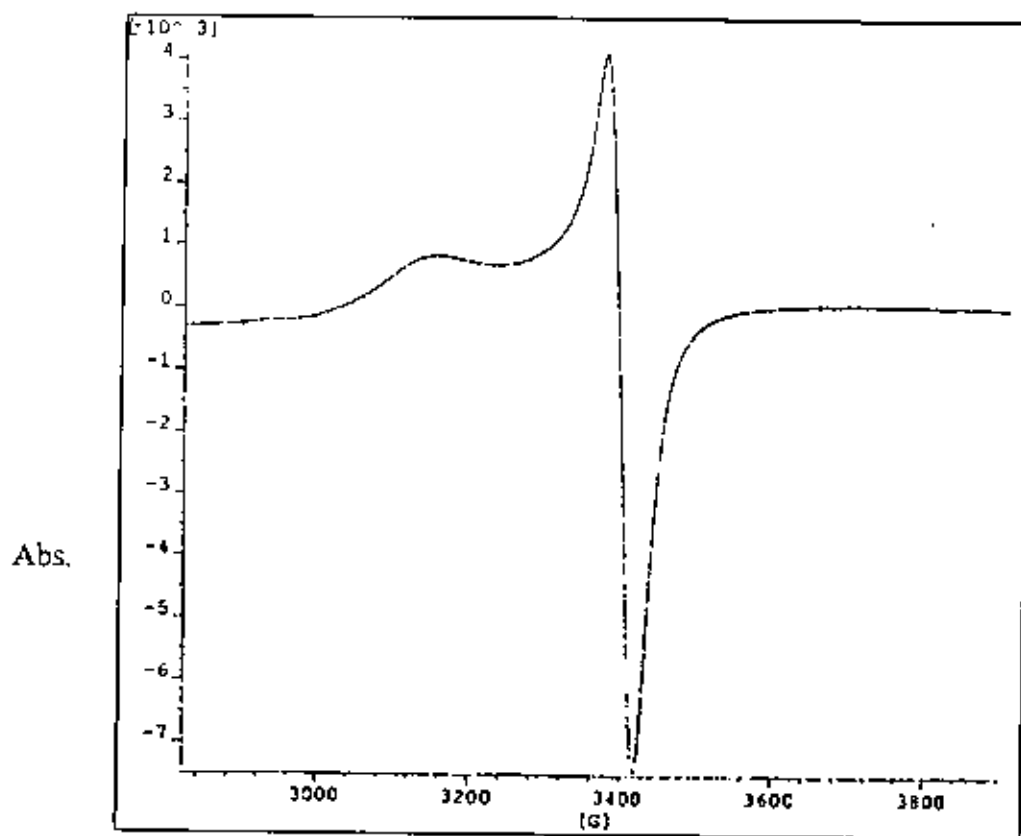


Figure (43): ESR spectrum of the complex [Cu-IV (2:2)].

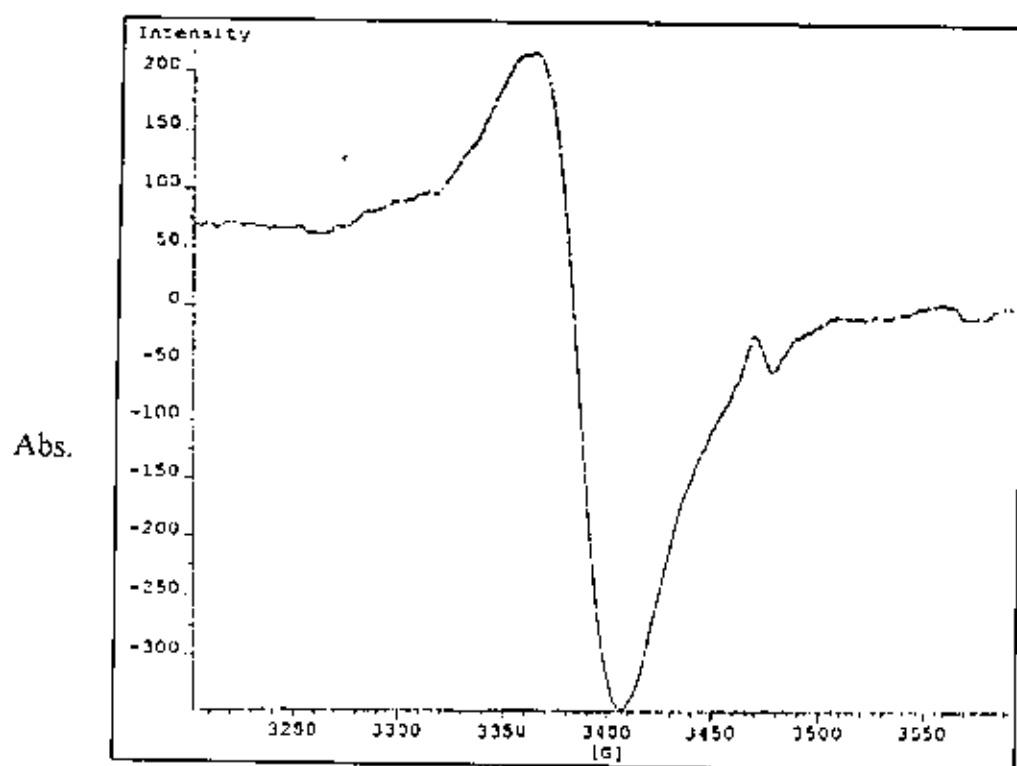


Figure (44): ESR spectrum of the complex [Cu-IV (2:3)].

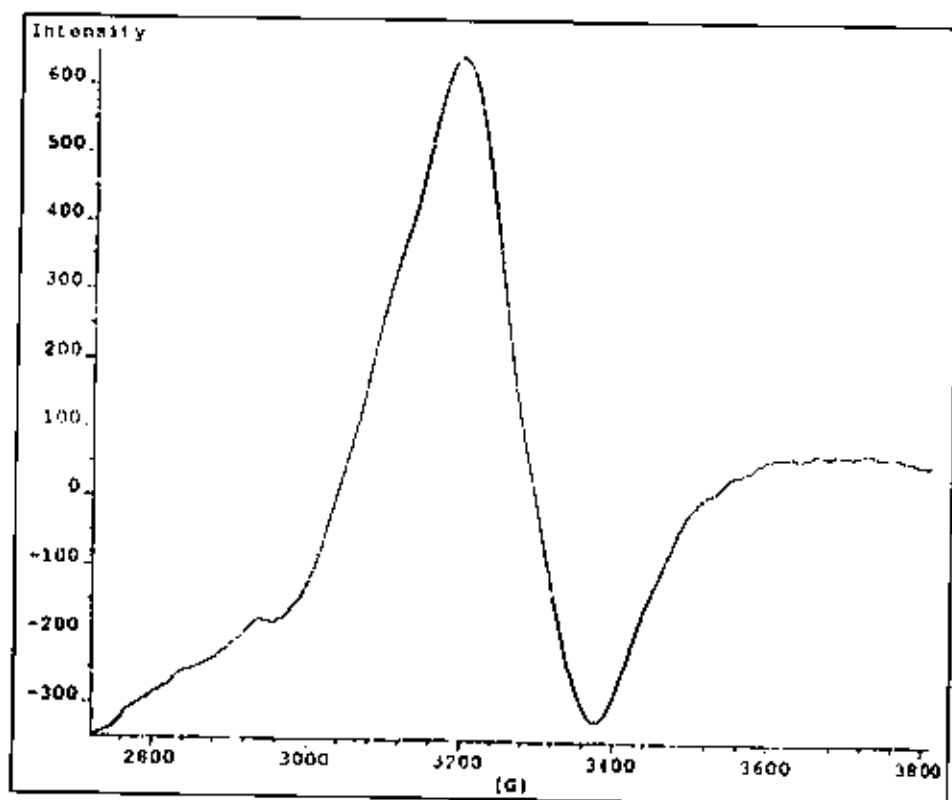


Figure (45): ESR spectrum of the complex [Cu-V (1:1)].

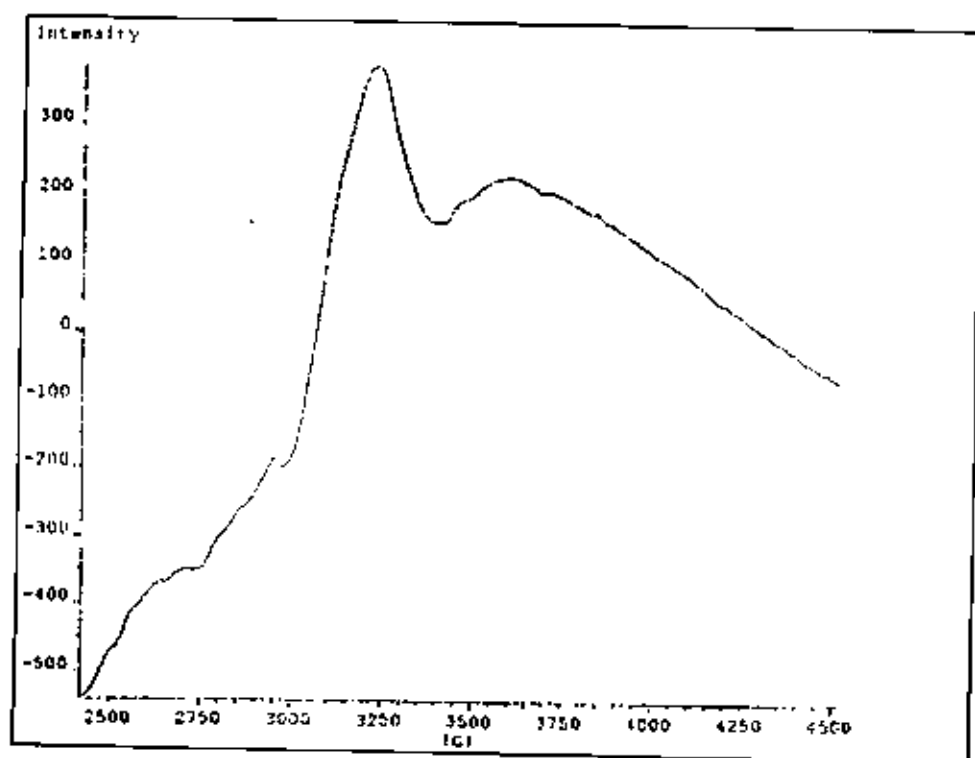


Figure (46): ESR spectrum of the complex [Cu-V (1:2)].

Table (18): ESR spectral data of Cu^{2+} complexes with ligands I, IV and V.

Complex	$g_z = g_{\parallel}$	$g_x = g_{\perp}$
Cu-I (2:2)	2.0559
Cu-I (2:3)	2.03806
Cu-IV (2:2)	2.05616	2.06776
Cu-IV (2:3)	2.06037	2.07141
Cu-V (1:1)	2.12941	2.18337
Cu-V (1:2)	2.11293	2.17279

III.2.9. General structures of the complexes.

Based on the results of elemental analysis, IR, ^1H NMR, thermal analysis, Electron spin resonance (ESR) and magnetic moments calculations. For ligand V, 1:1 and 1:2 complexes are isolated; their structures may be formulated as seen in figures (47). The proposed stereochemical structures for the investigated metal complexes suggest tetrahedral geometry for 1:1 complexes and suggest octahedral geometry for 1:2 complexes and all of the formed complexes are without coordinated water molecules.

The proposed stereochemical structure for the investigated metal complexes suggest tetrahedral geometry with respect to Mn, Co, Ni, Cu and Zn with the investigated ligands (I-IV) 2:2 and 2:3, and are illustrated in figure (48).

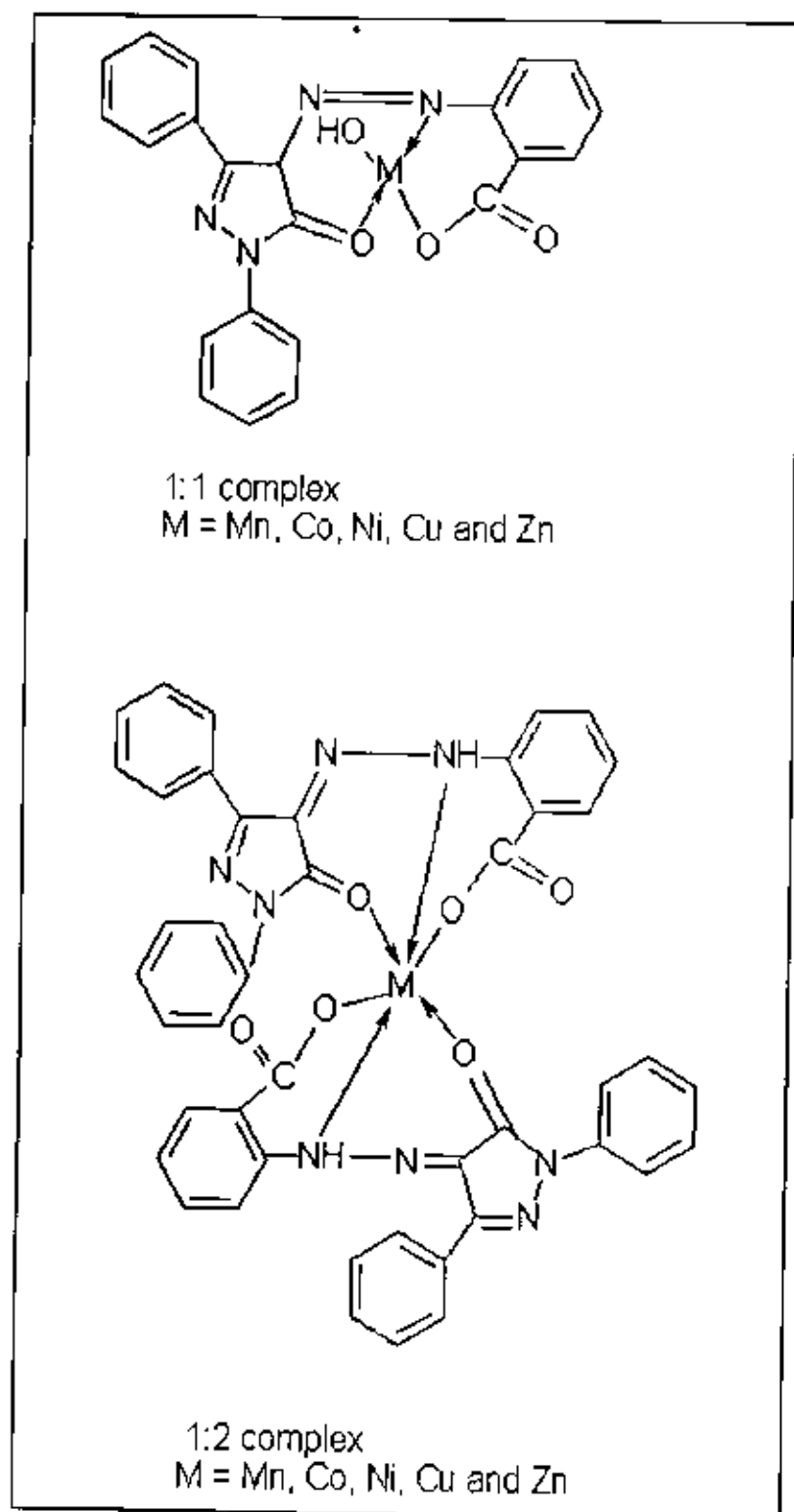
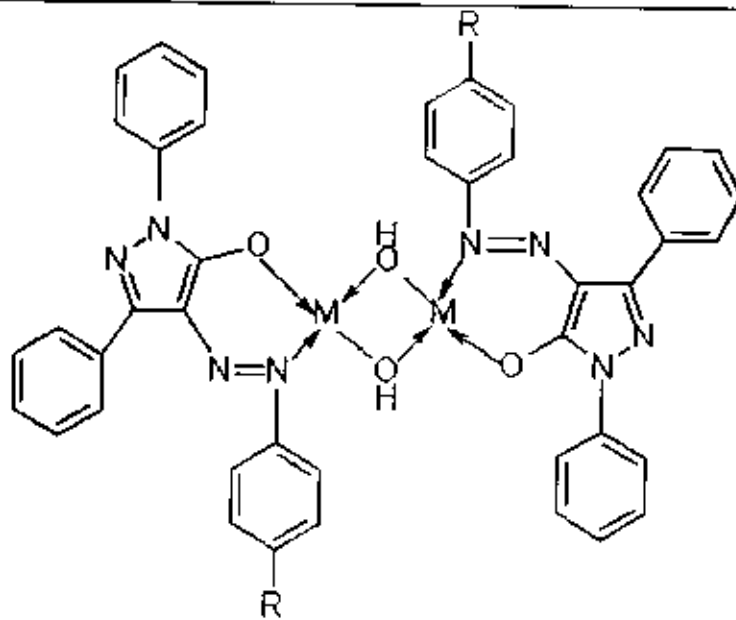
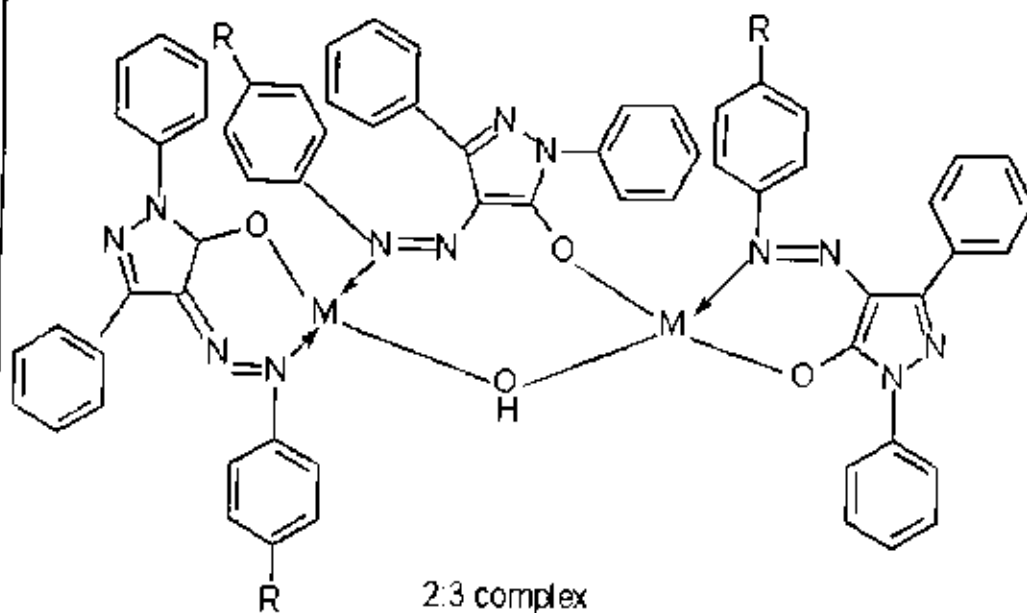


Figure (47): Structures of 1:1 and 1:2 complexes of ligand V.



2:2 complex
 R = H, Cl, CH₃, OCH₃



2:3 complex
 R = H, Cl, CH₃, OCH₃

Figure (48): Structures of 2:2 and 2:3 complexes of ligands (I-IV).

SUMMARY

Summary

The present thesis comprises three chapters:

- 1- **Chapter I** includes the literature survey. The previous studies available in the literature have been reviewed with emphasis on those concerned with the chemistry of the transition metals, including formation of the transition metal complexes with various ligands. A literature survey is also given with regard to the structure, interpretation of color changes, absorption spectra, complex formation, ability of pyrazolone derivatives and their uses. Also a literature survey on the divalent metal ions of Mn, Co, Ni, Cu, and Zn is given.
- 2- **Chapter II** includes the experimental part, involving materials, preparations of various compounds and solutions, instruments used and working procedures. It also includes all detailed methods of calculations. The elemental analysis are also given for the prepared compounds.
- 3- **Chapter III** includes the results and discussion:
 - a. The electronic absorption spectra of the investigated ligand (V) was investigated in some organic solvents of different polarities. The solvent effect on absorption bands was studied. The plots of dielectric constant D , $(D-1)/(D+1)$, \sqrt{D} and $\phi(D)$ against ν of the band observed in the C.T. band are not linear relations.

- b. The mass spectra of all ligands (I-V) were studied to get further insight as the nature and different fragmentations which are characteristic for every compound. The mass spectra of each compound showed the molecular ion M^+ at m/z value corresponding to its molecular weight.
- c. The infrared spectra, 1H NMR and elemental analysis were also obtained and studied for the investigated ligands (I-V).
- d. The solid complexes of the transition metal ions with the investigated ligands (I-V) were prepared and the precipitated complexes were chemically analyzed. The results of analysis suggested chemical composition for each of the solid complexes obtained. IR, 1H NMR, thermal analysis, magnetic susceptibility, mass spectra, electron spin resonance (ESR) and molar conductance confirmed the compositions and structure of the separated solid complexes. The results show 2:2 and 2:3 (M:L) complexes for ligand (I-IV), 1:1 and 1:2 (M:L) complexes for ligand V.

The complexes were formed through coordination with the oxygen of the pyrazolone ring, N of the azo-hydrazo group and covalent bond with the oxygen of the hydroxyl group.

REFERENCES

References

1. I. L. Finar, "Organic Chemistry: The Fundamental Principles", 6th Edition, Longman-London, p845, (1973).
2. K. Schofield, M. R. Grimmett, B. R. T. Keene, "Hetero Aromatic Nitrogen Compounds The Azoles", Cambridge University Press-Cambridge, p43, (1984).
3. M. T. El-Haty, F. A. Adam, N. A. Abdalla, Pak. J. Sci. Ind. Res. 31(6), 398, (1988).
4. G. Hinsche, E. Uhlemann, K. Koehler, R. Kiremse, Z. Chem, 26(6), 216, (1986).
5. P. Indrasenan, G. Rajendran, Synth. React. Inorg. Met.-Org. Chem., 22(6), 715, (1992).
6. E. T. Karaseva, L. F. Polomoshnova, L. V. Teplukhina, Zh. Neorg. Khim, 34(11), 2861, (1989).
7. B. kuncheria, P. Indrasenan, Indian J. Chem., 27A(11), 1005, (1988).
8. R. C. Mauraya, D. D. Mishra, Transition Met. Chem., 12(6), 551, (1987).
9. R. C. Mauraya, D. D. Mishra, M. Pandey, P. Shukla, Natl. Acad. Sci. Lett., 14(9), 383, (1991).
10. E. C. Okafor, P. U. Adiukwu, B. A. Uzoukwu, Synth. React. Inorg. Met.-Org. Chem. 23(1), 97, (1993).

11. A. A. Solovskii, N. F. Chebotareva, V. F. Mironov, *Zh. Neorg. Khim.*, 34(11), 2966, (1989).
12. A. I. Vogel, "Quantitative Inorganic Analysis Including Elementary Instrumental Analysis", 2nd Edition, Longman-London, (1962).
13. M. Wisniewski, L. Pacak, *Pol. J. Chem.*, 65(11), 2073, (1991).
14. J. E. Albery, J. Hukki, P. Laitinev, J. Myry, *Arzneim. Forsch.*, 17, 214, (1967).
15. O. Danek, S. Nouzova, *Collect. Czech. Chem. Commun.*, 33(2), 425, (1968).
16. M. R. Patel, R. A. Pallare, C. V. Delwala, *Indian J. Microbiol.*, 6(3), 35, (1966).
17. F. A. Adam, M. T. El-Haty, A. H., N. A. Abdalla, *Bull. Soc. Chim. Fr.*, 4, 605, (1988).
18. S. M. Fahmy, A. H. Badran, M. H. Elnagdi, *J. Chem. Technol. Biotechnol.*, 30(7), 390, (1980).
19. D. R. Gupta, R. K. Arora, *Acta. Chim. Hung.*, 118(1), 79, (1985).
20. V. S. Jolly, L. F. Polomoshnova, L. V. Teplukhina, *Zh. Neorg. Khim.*, 34(11), 2861, (1989).
21. A. C. Ojha, R. Jain, *Pol. J. Chem.*, 56(10), 1553, (1982).
22. R. A. Parent., *J. Soc. Dyes color*, 92(10), 371, (1976).

23. G. S. Saharia, H. R. Sharma, *J. Indian Chem. Soc.*, 51, 345, (1974).
24. C. P. Singh, A. C. Ohja, *J. Indian Chem. Soc.*, 57, 1172, (1980).
25. A. Tantawy, F. Goda, A. M. Abdelal, *Chim. Pharm. J.*, 47(1), 37, (1995).
26. M. T. El-Haty, *Asian J. Chem.*, 3(2), 189, (1991).
27. L. G. Kuzmina, L. P. Grigoreva, Y. T. Struchkov, Z. I. Ezhkova, B. E. Zaitsev, V. A. Zaitseva, P. P. Pronkin, *Khim. Gelerotskil. Soedin*, 6, 816, (1985).
28. G. A. El-Inany, K. A. R. Salib, S. B. El-Maraghy, S. L. Stefan, *Egypt. J. Chem.*, 27(3), 357, (1985).
29. R. M. Mohamed, A. H. Refait, U. S. Kamal, *Bull. Soc. Chim. Fr.*, 3(2), 164, (1984).
30. F. A. Snavely, H. Y. Claude, *J. Am. Chem. Soc.*, 33(2), 513. (1968).
31. I. S. Shpileva, N. A. Klyuev, F. L. Kolodkin, R. A. Khmel'nitskii, I. I. Levkoev, *Dokl. Akad. Nauk SSSR*, 217(2), 365, (1974).
32. F. A. Amer, L. P. Strand, G. W. Francis, *Org. Mass Spectrum*, 12(9), 557, (1977).
33. I. S. Shpileva, N. A. Klyuev, F. L. Kolodkin, R. A. Khmel'nitskii, I. I. Levkoev, *Zh. Org. Khim.*, 12(12), 249, (1976).

34. S. H. Etaiw, F. A. Anwer, F. M. Issa, *Revue Roum. Chim.*, 23(1), 79, (1978).
35. G. A. El-Inany, S. A. El-Wahab, Y. M. Issa, *Egypt J. Chem.*, 25(2), 101, (1982).
36. P. Nikolov, F. Fratev, S. Stoyanov, O. E. Polanskii, *Z. Naturforsch.*, 36A(2), 191, (1981).
37. N. R. Shah, J. R. Shah, *Acta Cienc. Indica. Chem.*, 7(1), 17, (1981).
38. N. R. Shah, J. R. Shah, *Acta Cienc. Indica. Chem.*, 12(1), 41, (1986).
39. M. S. Rizk, H. M. Abdel-Fattah, I. M. Abbass, Y. M. Issa, *J. Indian Chem. Soc.*, 71, 93, (1994).
40. F. A. Snavely, D. K. Bruce, *J. Am. Chem. Soc.*, 81, 4199, (1968).
41. M. T. El-Haty, N. A. Abdella, *J. Electrochem. Soc. India*, 40(4), 173, (1991).
42. M. T. El-Haty, F. A. Adam, *Bull. Soc. Chim. Fr.*, 5(1), 129, (1983).
43. L. I. Ali, S. L. Stefan, *Pak. J. Sci. Ind. Res.*, 37(6), 235, (1994).
44. M. S. Masuod, A. R. Yousef, M. A. Mustafa, *Transition met. Chem.*, 13(4) 253, (1988).

45. M. S. Ryabov, E. V. Nikiforov, B. V. Zaitsev, I. A. Naumova, Zh. Neorg. Khim., 25(7), 1878, (1990).
46. F. A. Snavely, J. E. Scott, D. Richmand, J. J. Farrel, J. Coord. Chem., 6(3), 167, (1977).
47. R. R. Shukla, S. Chandra, C. A. Srivastava, G. Narain, Indian J. Chem., 23A, 445, (1984).
48. H. S. Verrma, R. C. Saxena, K. C. Mathur, J. Indian Chem. Soc., 58, 1193, (1981).
49. R. R. Shukla, C.A. Srivastava, J. Indian Chem. Soc., 28, 937, (1981).
50. M. R. Mahmoud, F. A. Adam, K. Yousef, M. T. El-Haty, Bull. Soc. Chim. Belg., 92(1), 13, (1983).
51. K. C. Mathur, G. S. Saharia, H. R. Sharma, R. C. Saxena, Chem. Era., 18(10), 255, (1982).
52. S. A. abdel-Latif, Synth. React. Inorg. Met. -Org. Chem., 31(8), 1355, (2001).
53. H. B. Hassib, S.A. Abdel-Latif, Spectrochimica Acta., 59A, 2425, (2003).
54. S. A. Abdel-Latif, H. B. Hassib, J. Therm. Anal. Chem., 68, 983, (2002).

55. L. Guang-Fei, L. Lang, J. Dian-Zeng, W. Shu-Hua, X. Guan-Cheng, Y. Kar-Bei, *Huaxue xuebao (Huaxue xuebao)*, 62,7, 697 (2004).
56. M. Abd El-Moaz, *Publications of Helwan university, Egypt*, (2005).
57. C. Bătiu, I. Panea, L. Ghizdavu, L. David, S. Ghizdavu Pellascio, *J. Therm. Anal. Chem.*, 79, 129, (2005).
58. M. F. Braña, Ana Gradillas, Angel G. Ovalles, Berta López, Nuria Accro. *Bio Org. Med. Chem.*, 9 (2006).
59. L. A. Fedorov, *Russion Chemical Reviews*. 57, 941 (1988).
60. J. Skoweranda, M. Bukowska-Strzyzewska, W. Strzyzewski, *J. Chem. Crystallog.*, 24, 517 (1994).
61. El-Bindary, El-Sonbati, El-Mosalamy, *Publications of Mansoura University, Egypt*. 57(12), 2359 (2001).
62. A. S. Fouda, *Publications of Mansoura University, Egypt*, 5 (2005).
63. A. T. Mubarak, *Publications of King Khalid University*, 1041 (2004).
64. A. Corsini and E. J. Billo, *Can. J. Chem.*, 47(24), 4655 (1969).
65. R. Sarin, K. N. Munshi, *J. Inorg. Nucl. Chem.*, 34, 581(1972).

66. S. A. Abdel-Latif, O. M. El-Roudi and M. G. K. Mohamed, J. Therm. Anal. Cal., 73, 939 (2003).
67. A. I. Vogel, "A Text Book of Practical Organic Chemistry", 4th Edition, Longman-London, (1978).
68. A. O. Fitton, R. K. Smalley, "Practical Heterocyclic Chemistry", Academic press-London and New York, p25, (1968).
69. A. M. Macdonald, P. Sirichanya, MicroChem. J., 14, 199, (1969).
70. J. D. Lee, "A New Concise Inorganic Chemistry", 4th Edition, Chapman and Hall Ltd-London, p663, (1991).
71. L. J. Bellamy, "The Infrared Spectra of Complex Molecules", Chapman and Hall-London, (1975).
72. W. Aschkinass, Ann., 55,401, (1995).
73. H. W. Thompson, J. Chem. Soc.,328, (1948).
74. N. B. Colthup, J. Opt. Soc. Am., 40, 397, (1950).
75. S. A. Francis, J. Chem. Phys., 18, 861, (1950).
76. J. J. Fox, A. E. Martin, Proc. Rot. Soc., 208, 234, (1940).
77. F. Dalton, R. D. Hill, G.D. Meokins, J. Chem. Soc., 927, (1960).
78. D. H. Wiffer, H. W. Thompson, J. Chem. Soc., 268, (1945).
79. H. Khalifa, S. H. Etaiw, Y. M. Issa, A. T. Haji-Husseini, Egypt. J. Chem., 18, 855, (1975).

80. G. A. El-Inany, K. A. R. Salib, S. B. El-Maraghy, S. L. Stefan, *Egypt J. Chem.*, 27, 357, (1985).
81. J. McMurry, "Organic Chemistry", 5th Edition, Brooks/Cole (USA), p441-500 (2000).
82. N. T. Abdel-Ghani, Y. M. Issa, S. A. Abdel-Latif, *Thermochimica Acta.*, 143, 37, (1989).
83. R. M. Issa, S. A. Abdel-Latif, H. A. Abdel-Salam, *Synth. React. Inorg. Met.-Org. Chem.* 31, 95, (2001).
84. J. R. Francisco, M. Valls, A. Vigili, *Mag. Reson. Chem.*, 26, 511, (1988).
85. F.A. Cotton, P. Legzdins, *Inorg. Chem.*, 7, 1777, (1968).
86. P. Suppan, *J. Chem. Soc., (A)* 3125, (1968).
87. G. C. Pimental, *J. Am. Chem. Soc.*, 79, 3323, (1957).
88. N. S. Bayliss, E. G. Mackae, *J. phys. Chem.*, 18, 292, (1950).
89. A. A., Emara, *Synth. React. Inorg. Met.-Org. Chem.*, 29, 87, (1999).
90. T. R. Felthouse, D. N. Hendrickson, *Inorg. Chem.*, 17, 2636, (1978).
91. S. M. Abu-El-Wafa, R. M. Issa, A. M. El-Dekin, *Indian J. Chem.*, 29A, 285, (1990).

92. B. J. Hathaway, A. A. G. Tomlison, *Coord. Chem. Rev.*, 20, 423, (1995).
93. B. J. Hathaway, A. A. G. Tomlison, *Coord. Chem. Rev.*, 5, 1, (1970).
94. I. Fidone, K. W. H. Stevens, *Proc. Phys. Soc.*, 73, 116, (1959).

الخلاصة

قدمت نبذة عن المراجع على كيمياء العناصر الانتقالية مع المركبات العضوية، كذلك قدمت نبذة من المراجع على عناصر المنجنيز والكوبالت والنيكل والنحاس والزنك مع بعض المركبات العضوية كما قدمت نبذة من المراجع عن بعض مركبات البيرازولون ومشتقاتها شملت استخدامها ككواشف في الكيمياء التحليلية وكذلك الفاعلية البيولوجية لهذه المركبات.

يشتمل الباب الثاني على المواد المستخدمة وطرق تحضير مركبات البيرازولون والمحاليل المختلفة وأيضا طرق القياس والأجهزة وكذلك نتائج التحليل الدقيقة الخاصة بالمركبات المحضرة.

يتضمن الباب الثالث النتائج ومناقشتها من حيث:

1- دراسة السلوك الطيفي للمركب (V) في المذيبات العضوية المختلفة القطبية وذلك في مجال الأشعة فوق البنفسجية والمرئية، وقد درست العلاقات الخاصة بثابت العزل الكهربائي (D)

$$F(D) = 2(D-1)/(2D+1) \quad , \quad \phi(D) = (D-1)/(D+2)$$

مع الرقم الموجي لحزمة الامتصاص الواقعة في مجال الأشعة المرئية في مدى طيف انتقال الشحنة وقد وجد أن العلاقات غير خطية .

2- تم دراسة أطيف الكتلة على الليجانادات (I-V) قيد البحث لإلقاء المزيد من الضوء على طبيعة أنواع التكسير أو التجزئة المميزة لكل من الليجانادات مطابقا لوزنه الجزيئي.

3- تم كذلك دراسة تركيبات الليجانادات المحضرة بواسطة الأشعة تحت الحمراء والرنين المغناطيسي والتحليل العنصري.

4- أمكن فصل المتراكبات الصلبة لكل من أيونات العناصر الانتقالية (المنجنيز، الكوبلت، النيكل، النحاس والزنك). وقد أجري تحليل كيميائي دقيق لهذه المتراكبات باستخدام التحليل العنصري الذي يشمل تحليل كل من العناصر (الكور، الهيدروجين، الكربون، النيتروجين).

بالإضافة إلى أطيف الامتصاص التذبذبي في مجال الأشعة تحت الحمراء وأطيف الرنين النووي المغناطيسي والتحليل الحراري الوزني والتحليل الحراري التفاضلي .
كذلك تم دراسة العزم المغناطيسي لمتراكبات العناصر الانتقالية المذكورة مع جميع الليجاندات.

5- تم كذلك دراسة الرنين المغزلي الاليكتروني (ESR) لبعض متراكبات النحاس.

6- تم دراسة الموصلية الكهربائية المولارية للتعرف على طبيعة المتراكبات المحضرة من حيث كونها متراكبات متعادلة أو متراكبات أيونية في المذيب DMF ، أثبتت الدراسة أن جميع المتراكبات وجدت في الصورة المتعادلة.



هيئة المناهج

قسم الكيمياء

مناهج البكالوريوس

دراسة على بعض مشتقات أصباغ البيرازوليون الأزوية
ومركباتها مع بعض أيتونات العناصر الانتقالية

لرئيسية المناهج

مقدمة من الطالبة

عواطف عبد السلام مسعود

** لجنة المناقشة:

1 - د. سمير أبو القاسم عبد اللطيف

(مشرفاً رئيسياً)

1 - د. حسن عمرو عويس

(مشرفاً مساعداً)

2 - د. زيدان جاسم خلف

(ممتحناً داخلياً)

3 - د. سالم خليفة الفرد

(ممتحناً خارجياً)

.....

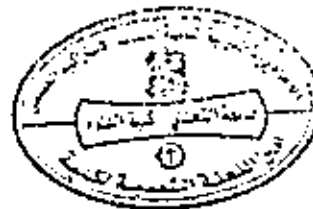
.....

.....

.....

.....

بمقام
د. أحمد فرج المنصور
أمين اللجنة الشعبية لكلية العلوم





جامعة التّحدي

كلية العلوم

قسم الكيمياء

دراسة على بعض مشتقات اصباغ البيرازولون الآزوية ومترابكباتها مع بعض أيونات العناصر الانتقالية

بعض مقدمه كجزء من متطلباته امتحان درجة الماجستير في الكيمياء

للطالبة/

مواطنه محمد الملام مسعود

تحت إشراف

د. حسن عمرون عويس محمد
أستاذ مساعد الكيمياء الفيزيائية
قسم الكيمياء - كلية العلوم
جامعة التّحدي

د. سمير أبو القاسم عبد اللطيف
أستاذ مساعد الكيمياء غير العضوية
قسم الكيمياء - كلية العلوم
جامعة عمر المختار

سرت - ليبيا

2008 - 2007